Hydrogeochemical Characteristics and Groundwater Flow Processes in Jiaozuo Area, a Semi-arid Piedmont Plain in North Henan Plain, China

中国河南平原北部の山麓平野における水文地球化学特性と地下水流動プロセス

A Dissertation Submitted to
the Graduate School of Life and Environmental Sciences,
the University of Tsukuba
in Partial Fulfillment of the Requirements
for the Degree of Doctor in Environmental Studies
(Doctoral Program in Sustainable Environmental Studies)

Junping LIU

Abstract

Groundwater plays a significant role in the eco-environment of arid/semi-arid regions and a thorough understanding of groundwater recharge is a prerequisite for the local groundwater management. Therefore, clarifying recharge sources and groundwater flow path in Jiaozuo area, a semi-arid inland piedmont plain in central China, is important for water resource protection in this deep water over-exploitation area.

The recharge process remains unrevealed in alluvial-proluvial fan area with a regional normal fault in the mountain front. To characterize the recharge regime, a case study is presented in a piedmont plain of North Henan Plain. In this study, 114 water samples were collected from rivers, springs and pumping wells in mountainous region and piedmont plain in 2013 (October) and 2014 (August). Local geological information of the aquifer system and hydrological conditions, together with hydrogeochemical isotopic tracer approach were used to investigate groundwater chemical evolution and their associated recharge processes.

This study shows that quality of deep groundwater in northern alluvial-proluvial fan and southern alluvial plain is distinct, in which isotopic compositions are more enriched in the deep groundwater of alluvial-proluvial fan than the alluvial plain. Local rainfall could not form the rapid recharge to piedmont aquifer in the short term owing to the large depth to the water table and its recharge is negligible. Meanwhile, no lateral or vertical upward recharge provides water to the basin aquifer due to the normal fault in the mountain boundary acts as a barrier.

In addition, shallow groundwater leakage in alluvial-proluvial fan area and confined deep groundwater in piedmont plain are the two main end sources of mixing deep groundwater in alluvial- proluvial fan. The infiltration of shallow groundwater is the greatest in the foothills and its contribution to the deep aquifer declines with increasing distance away from the fault. It is considered that shallow groundwater is the only recharge source of the deep aquifer in fan area and the mixing process reaches about 10 km away from the fault in Danhe River alluvial fan and less than 6

km in the Xishihe River proluvial fan. Due to the mixture in the deep aquifer, major ions leached from shallow aquifer of alluvial-proluvial fan are diluted and the hydrochemical pattern is changed from Ca·Mg-HCO_3·SO_4 to Ca·Mg-HCO_3. This study also shows impermeable layers would primarily influence the mixing process in proluvial fan area more than alluvial fan on this site, therefore groundwater recharge in proluvial fan exhibits a relatively much limited mixture scale and a specific groundwater flow pattern.

Considering the occurrence of deep water over-exploitation in piedmont plain and flow system being disturbed, the improvement of the deep groundwater environment should be based on the shallow groundwater intrusion behavior in alluvial-proluvial fan in Jiaozuo area, which may facilitate the penetration of persistent contaminants into deep confined aquifer of southern piedmont plain.

Keywords: Groundwater recharge, normal fault, stable isotope, hydrochemistry, two end member mixing analysis, piedmont plain, North Henan Plain

Table of Contents

List of Figures

Chapter 1: Introduction

I. Groundwater recharge in (semi-) arid regions

The definition of (semi-) arid regions used in this study was developed according to the ratio of mean annual precipitation to potential evapotranspiration (PET): semi-arid (0.2–0.5), arid (0.05–0.2), which is calculated by United Nations Educational, Scientific, and Cultural Organization (UNESCO, 1979). Semi- arid and arid regions are expanding and account for around 30% of global terrestrial surface area, as illustrated in Figure 1 (Scanlon and Keese, 2006). Surface water is highly unreliable and generally scarce in semi- arid region due to the contamination effect and limited rainfall recharge, which makes groundwater the primary source of water supply in this region. It is reported by the International Atomic Energy Agency (IAEA) that much of the groundwater being developed in (semi-) arid regions is fossil water and is not sustainable. Meanwhile, due to the population growth in semi- arid region surpasses that in more humid settings, water scarcity will become more critical in the future (Scanlon and Keese, 2006).

Groundwater recharge in semi- arid region is an essential component in the understanding of regional flow systems and groundwater resources management (Jacobus and Simmers, 2006). In some cases, a continuous growth in human supplying demand on natural water supplies has resulted in a critical status of groundwater recharge (Devlin and Sophocleos, 2005). The intensive groundwater abstraction may disturb the naturally steady flow system, even at a regional scale (Folch, A., et al., 2011). Therefore, accurate evaluation of groundwater recharge is required for sustainable management of groundwater to meet increasing human demands (Yuan et al., 2011).

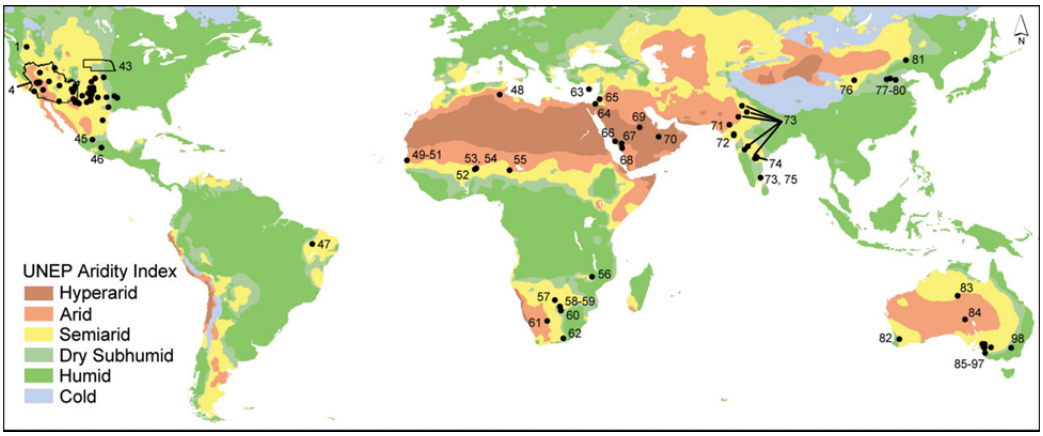

Figure 1: Global distribution of climatic zones (Scanlon and Keese, 2006).

II. Previous studies on groundwater recharge in (semi-) arid regions

Infiltration represents the water movement from surface into subsurface, which is equivalent to groundwater recharge based on the invariable climate and land use/land cover condition, while water moves to the water table. Meanwhile, recharge can be generally defined as an addition of water in the overlying unsaturated zone or surface water to an aquifer (Scanlon and Keese, 2006).

1. Studies on groundwater-surface water interaction in (semi-) arid regions

Direct recharge represents regional distributed recharge, such as rainfall infiltration or irrigation over large areas, while indirect recharge refers to concentrated recharge from surface topographic depressions, such as streams, lakes, and playas (Scanlon and Keese, 2006).

Groundwater isotopes combined with solute concentrations in water have been used for clarify the origin of groundwater and the interaction between groundwater and river water in arid and semi-arid regions (Tsujimura et al., 2007). Yuan et al. (2011) suggested that the runoff of the Beiyinshui River seeps in the streambed of upper reaches and then overflows seasonally in middle reach, meanwhile the recharge from middle reach to the aquifer is negligible. Chen et al. (2006) concluded that direct recharge from the Heihe River was the primary source of the shallow groundwater and that the mean residence time of groundwater recharge was 26 years in the Ejina Oasis. Dogramaci et al. (2012), based on the isotopic signature and concentrations of ions, clarified that intense rainfall events of >20 mm with limited evaporation prior to infiltration contribute most to recharge, and significant seepage from highly evaporated pools to groundwater is very limited (Figure 2). Moreover, Chen et al. (2006) identified nitrate contamination of groundwater in a wastewater irrigated field in North China Plain by use of multi tracers (^{18}O, ^{2}H and ^{15}N), confirmed that the nitrate present in contaminated groundwater originates from the wastewater irrigation. Nitrate was then used as a tracer to roughly estimate groundwater movement rates (Figure 3). In addition, Ma et al. (2009) investigated the limits to recharge from Tibetan plateau to Gobi desert, with multiple isotopic and hydrogeochemical tracers utilized. It is implied that rainfall has negligible impact on groundwater, and aquifer in

the desert is maintained by palaeowater, meanwhile the groundwater flow is relatively slow and water resources are non-renewable.

The previous studies suggest that groundwater recharge in semi-arid region is affected by site-specific conditions including the spatial and temporal heterogeneity in infiltration and evaporation (De Vries and Simmers, 2002; Gee and Hillel, 1988).

2. Studies on phreatic and deep groundwater recharge in (semi-) arid regions

In arid and semi-arid regions, the utilization of groundwater resources has increased dramatically, and substantial groundwater over-exploitation may trigger a series of water problems (Zhu et al., 2007), for instance, the exploitation of deep groundwater mostly causes long-term non-steady conditions, large-scale changes of flow patterns of the groundwater and hydraulic short circuits to phreatic aquifers, which may result in persistent contaminants penetrate deep aquifers (Seiler and Linder, 1995). For a sustainable development of groundwater, sources and main recharge mechanism of the phreatic and deep groundwater have been estimated.

Geological information of aquifers and hydrological conditions, combined with isotopic signature were used to investigate sources and associated recharge processes. Qian et al. (2006) revealed the recharge sources of deep groundwater and its circulation in the Ejina Basin. It is assumed that the deep groundwater in the riparian area was mainly recharged by the Heihe River water, while the deep aquifer in the Gurinai area is recharged by lateral inflow from the Badain Jaran Desert. Based on radiocarbon content, a hydrochemical investigation was conducted in the Minqin Basin to clarify the groundwater evolution and recharge (Zhu et al., 2007). It is reported that the deep groundwater is approximately 40 ka old, and was formed in a colder and wetter climatic condition, whereas the shallow groundwater is younger but generally older than 1 ka, which represents palaeowater mixed with a limited quality of modern recharge (Figure 4). In addition, Yuan et al. (2013) investigated upward recharge induced by the depression cone with the utilization of water table, chemical composition, stable isotopes and kinds of statistical analyses. It is concluded that shallow groundwater is recharged by deep groundwater in the center of depression cone, and the mixing process improves the quality of shallow groundwater (Figure 5).

3. Studies on mountain-front and mountain-block recharge

Mountain-front and mountain-block recharge have been defined as subsurface water entering adjacent basin aquifers, with its source in the mountain front or mountain block (Figure 6, Wilson and Guan, 2004).

Tectonic structure, particularly fault, which may form mountain-front recharge as a potential source of recharge to basins in semi-arid regions (Wilson and Guan, 2004), exerts an important role in groundwater flow process, and results in the recharge regime complex (Yuan et al., 2011). Significant studies were performed to clarify the relation between tectonic elements and potential groundwater recharge. It is reported that mountain-front recharge is affected by the fracture and upward flow recharges the overlying sedimentary aquifers in fault zones (Figure 7, Folch et al., 2011). Yuan et al. (2011) reported that fracture water ascending along a buried normal fault feed the unconfined aquifer in the alluvial fan/plain, meanwhile the hydrological efficiency of buried normal fault as preferential flow is also identified. And Bense and Person (2006) revealed the role of faults as preferential flow paths that vertically recharge aquifers at different depths over several hundred meters. At the same time it is demonstrated that basin-bounding faults act as a flow barrier to block mountain subsurface water recharging the basin aquifer (Chowdhury et al., 2008).

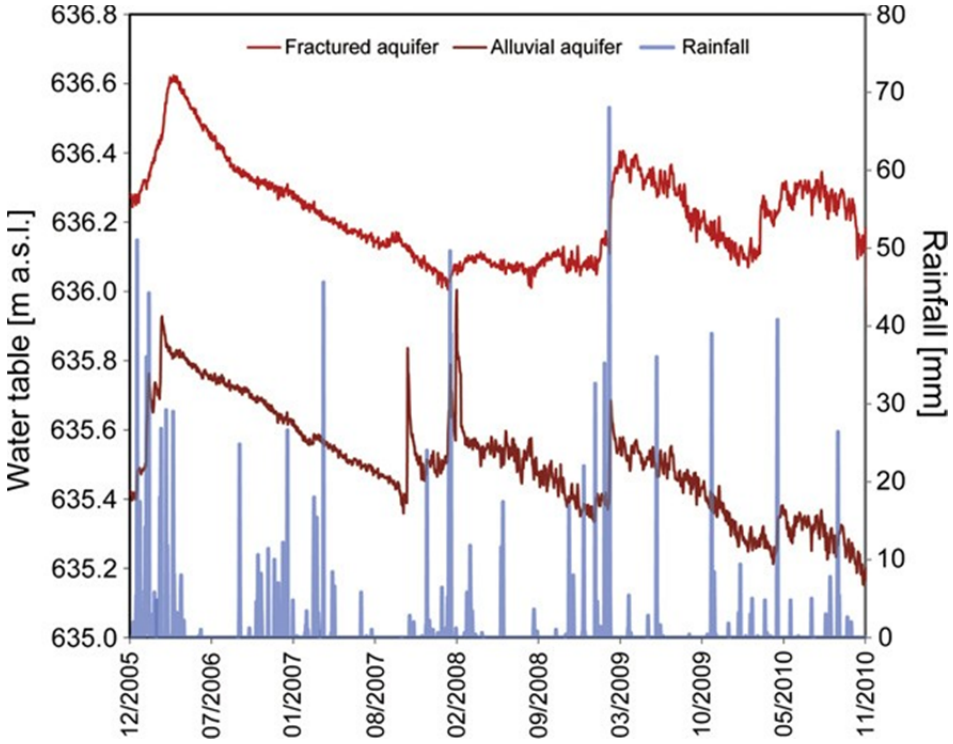

Figure 2: The response of two hydrographs installed in two bores located in a shallow alluvium aquifer (18 m deep) and in a deep fractured aquifer (40 m deep) about 5 km apart in the Hamersley Range (Dogramaci et al. 2012).

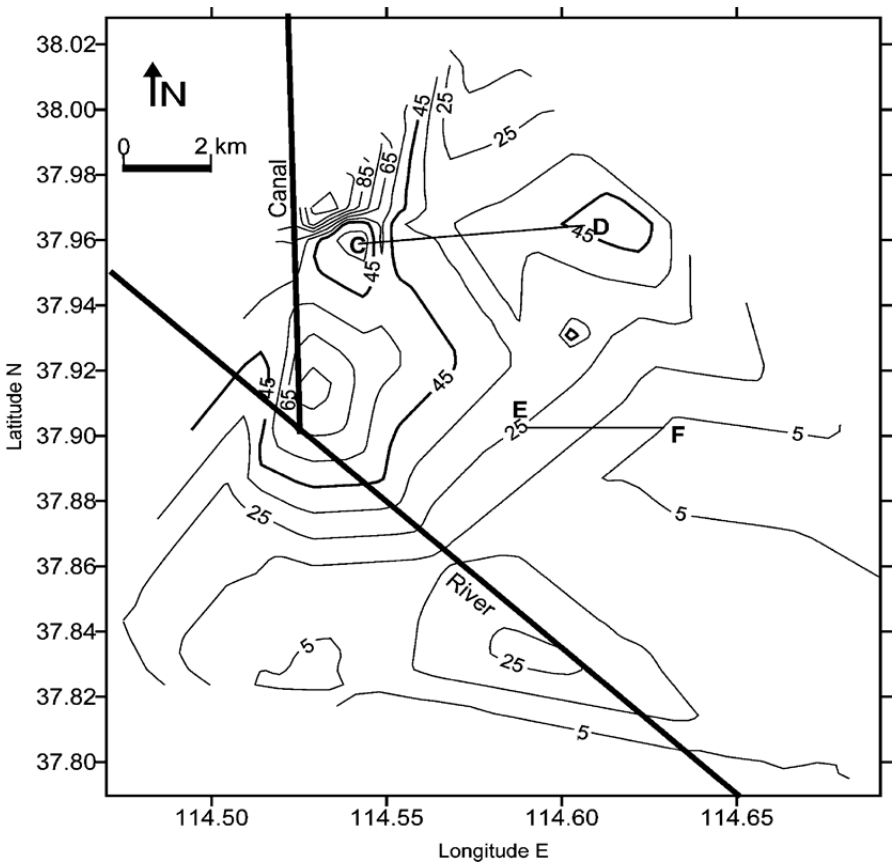

Figure 3: Contour of nitrate concentration (in NO_3^- mg/L) in groundwater. C-D and E-F are two cross sections for estimating horizontal transport rate (Chen et al. 2006).

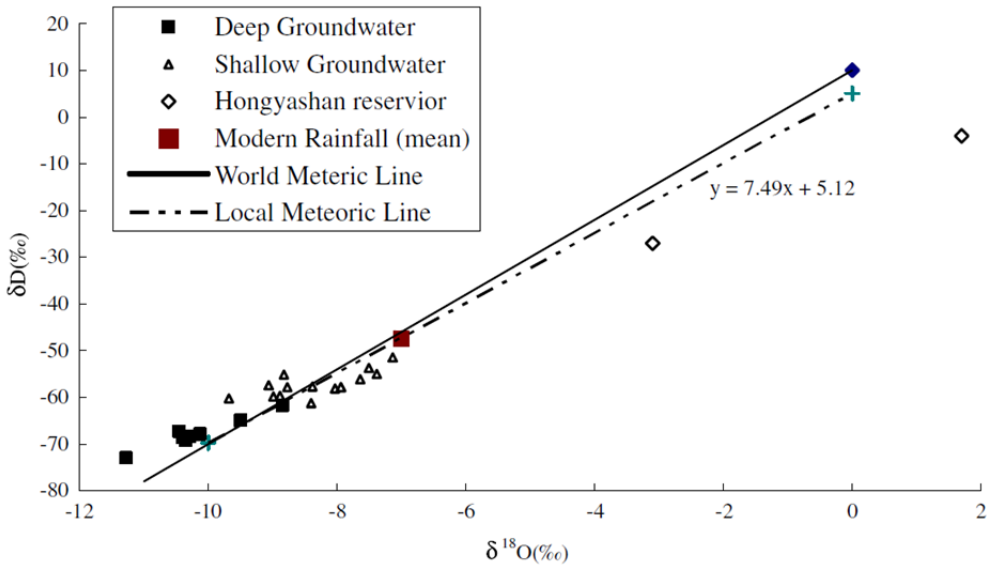

Figure 4: Plot of $\delta^{18}O$ and δD for groundwater from Minqin Basin aquifer system with plots of precipitation around the Minqin Basin and Hongyashan reservoir water trends (Zhu et al., 2007).

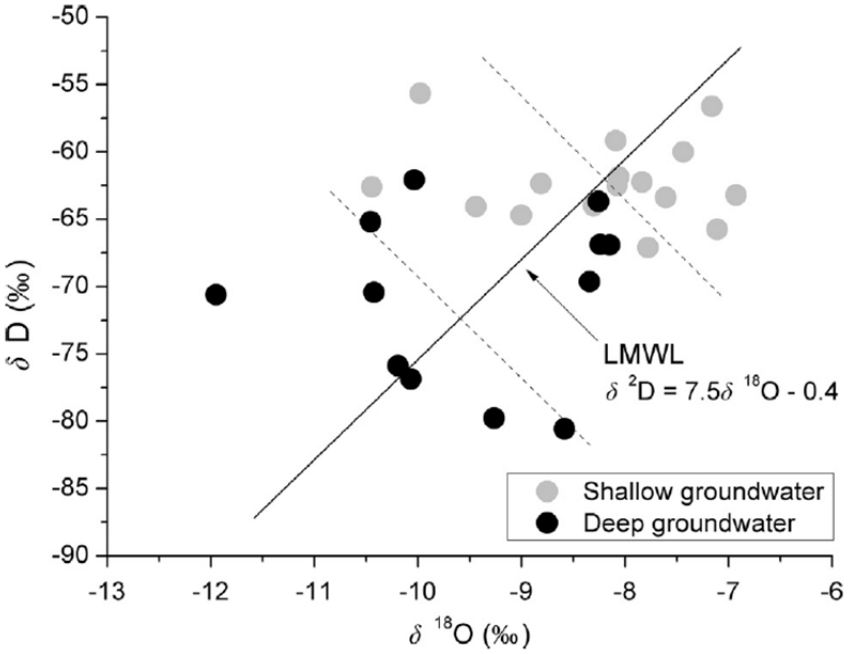

(a) The plot of $\delta^{18}O$ versus δD of water samples

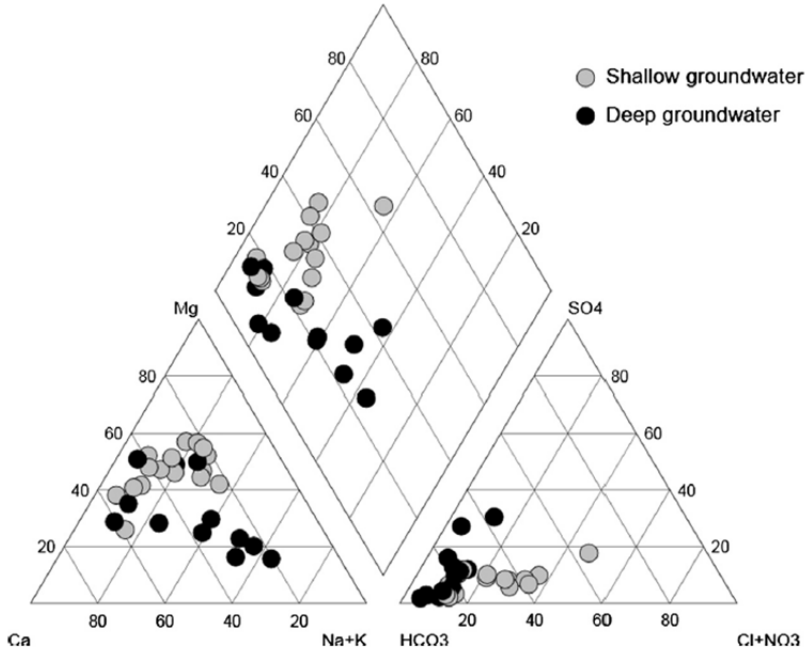

(b) The Piper plot of water samples.

Figure 5: Isotopic compositions and chemical types of water samples in a piedmont plain in North China Plain (Yuan et al. 2013).

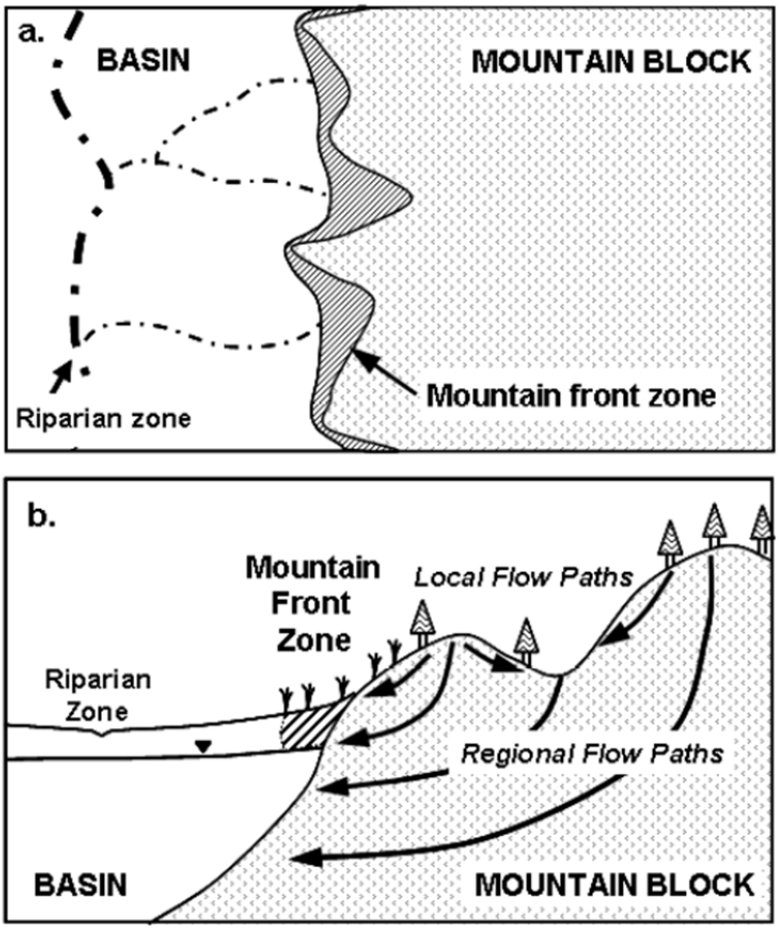

Figure 6: Schematic diagram showing four hydrologically distinctive units of the landscape in map view (a) and in cross-section (b) (Wilson and Guan, 2004).

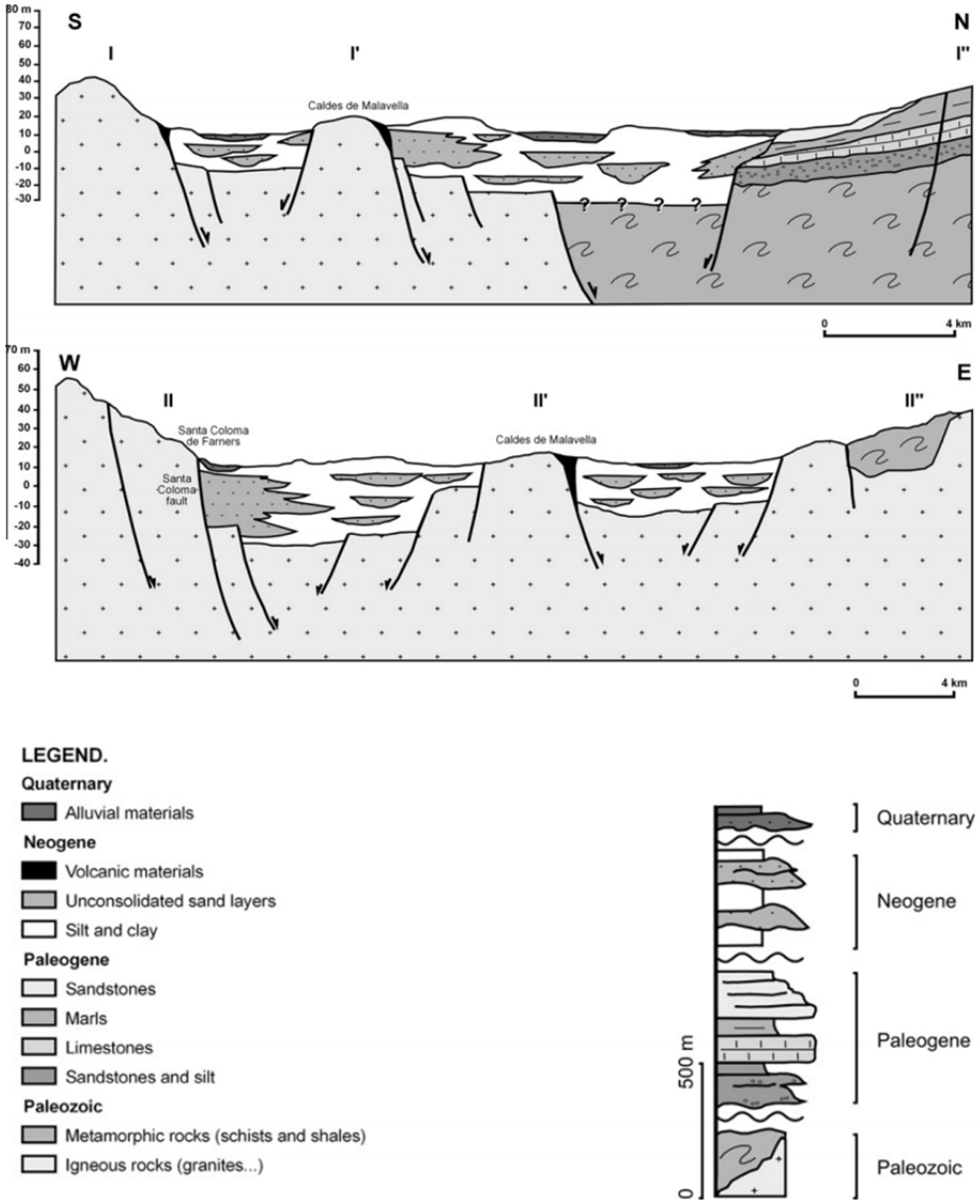

Figure 7: Schematic cross-sections of the Selva basin (Folch et al., 2011).

III. Groundwater recharge in piedmont plain

Despite numerous studies have investigated recharge mechanisms in (semi-) arid regions, the recharge process and water balance of fractured and alluvium aquifers in piedmont plain remain largely undescribed (Vanderzalm et al., 2011).

Piedmont plain corresponds to the recharge zone of Quaternary sediments, in which groundwater recharge has been estimated for the groundwater resource protection (Chen et al., 2004; Jiang et al., 2008; Wang et al., 2008). However, no agreement has been reached. Some recent studies have revealed the recharge regime in piedmont plain. For instance, Yuan et al. (2011) characterized a recharge regime of a fault-influenced aquifer in Beiyinshui River watershed in North China Plain (Figure 8), and it is concluded that the normal fault acts as a conduit for fracture water that mixes in the overlaying piedmont aquifer. Rohden et al. (2010) employed environmental tracers (^{3}H-^{3}He, noble gases, and stable isotopes) to study groundwater recharge and residence time in a strongly exploited alluvial plain aquifer system, which implied an effective recharge mostly due to infiltration of precipitation and irrigation water. Peng et al. (2014) employed stable isotopes and electrical conductivity to evaluate the recharge sources to groundwater in the proximal fan of Choshuichi alluvial plain. It is reported that precipitation in the alluvial plain is the major recharge source. Mountain groundwater's contribution is more notable in deep groundwater and Choshui Stream water's contribution decreases with increasing distance from the stream (Figure 9). In addition, Li et al. (2008) illustrated recharge source and hydrogeochemical evolution of shallow groundwater in a complex alluvial fan system in southwest of North China Plain, and a different recharge age and hydrochemical evolution is revealed in deep aquifer of Taihang Mt. alluvial fan based on the isotopic depletion and ion exchange (Figure 10).

However, these studies do not address the effect of groundwater withdrawal on the forced recharge towards the deep aquifer. In addition, recharge process in fault-influenced aquifer of alluvial/proluvial fan area in semi-arid region has not been revealed, especially the recharge regime of deep aquifer in piedmont plain has become an important issue for a better understanding of an accurate estimate of recharge.

Therefore, although remarkable progress has been made in groundwater recharge of piedmont plain over the past decade, the recharge mechanisms and the hydrochemical evolution of deep groundwater in semi-arid alluvial/proluvial fan area are still not well understood, especially considering the combined effects of groundwater withdrawal and normal fault formed along the mountainous region.

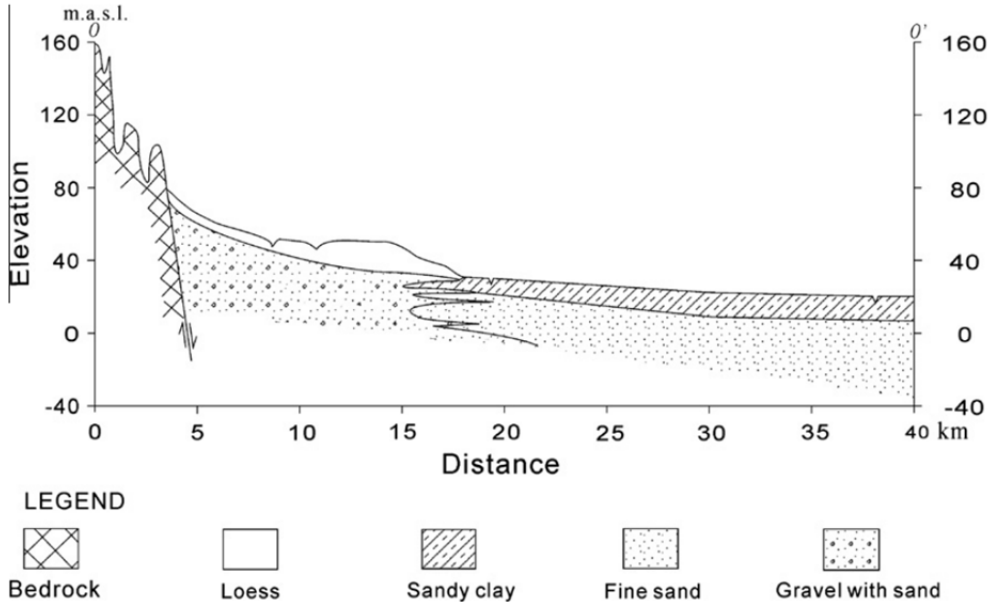

Figure 8: The sketch map of geological section in Beiyinshui River Watershed (Yuan et al. 2011).

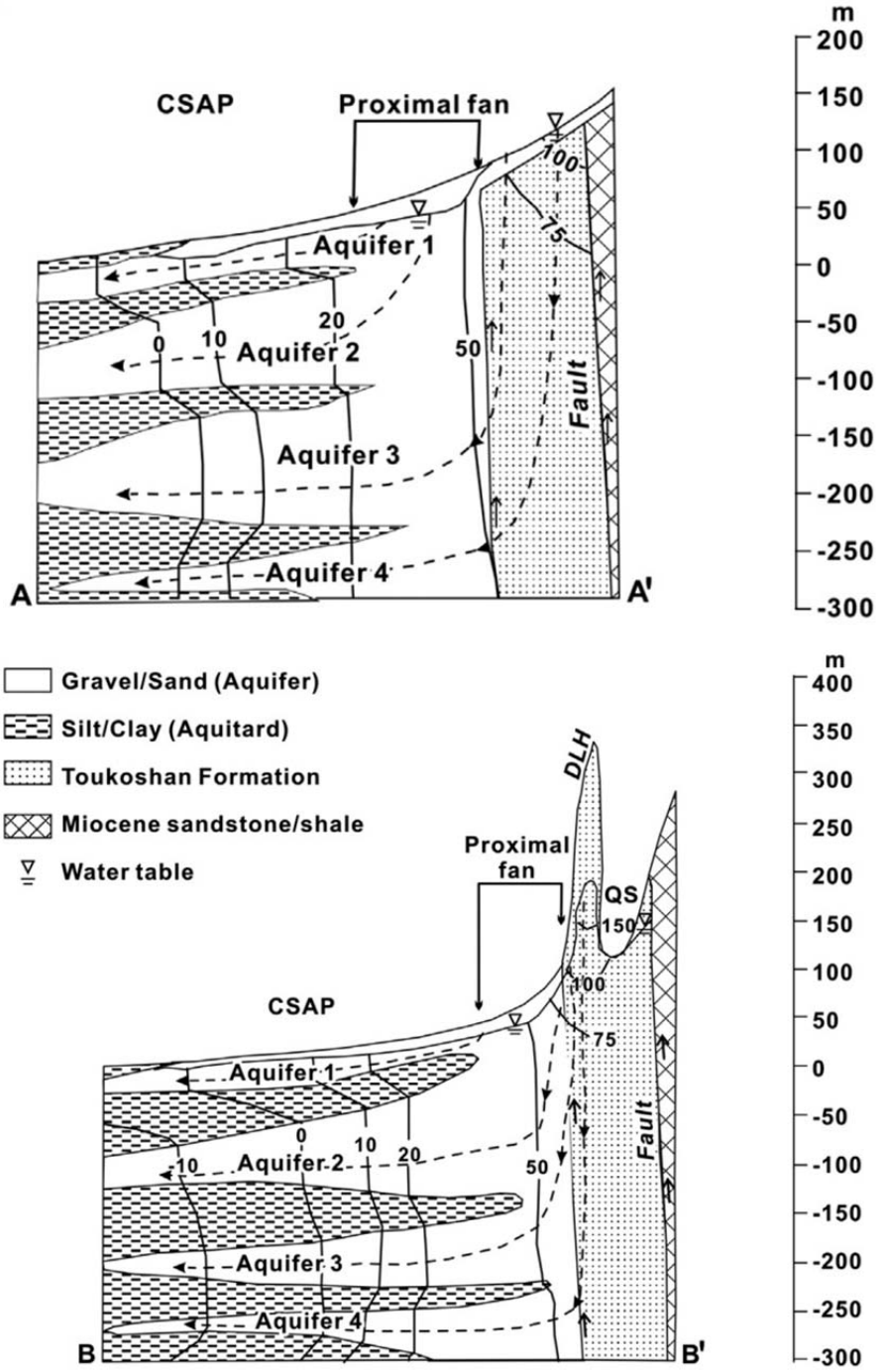

Figure 9: Two profiles illustrating the hydrogeological characteristics of the Choshuichi alluvial plain (Peng et al. 2014).

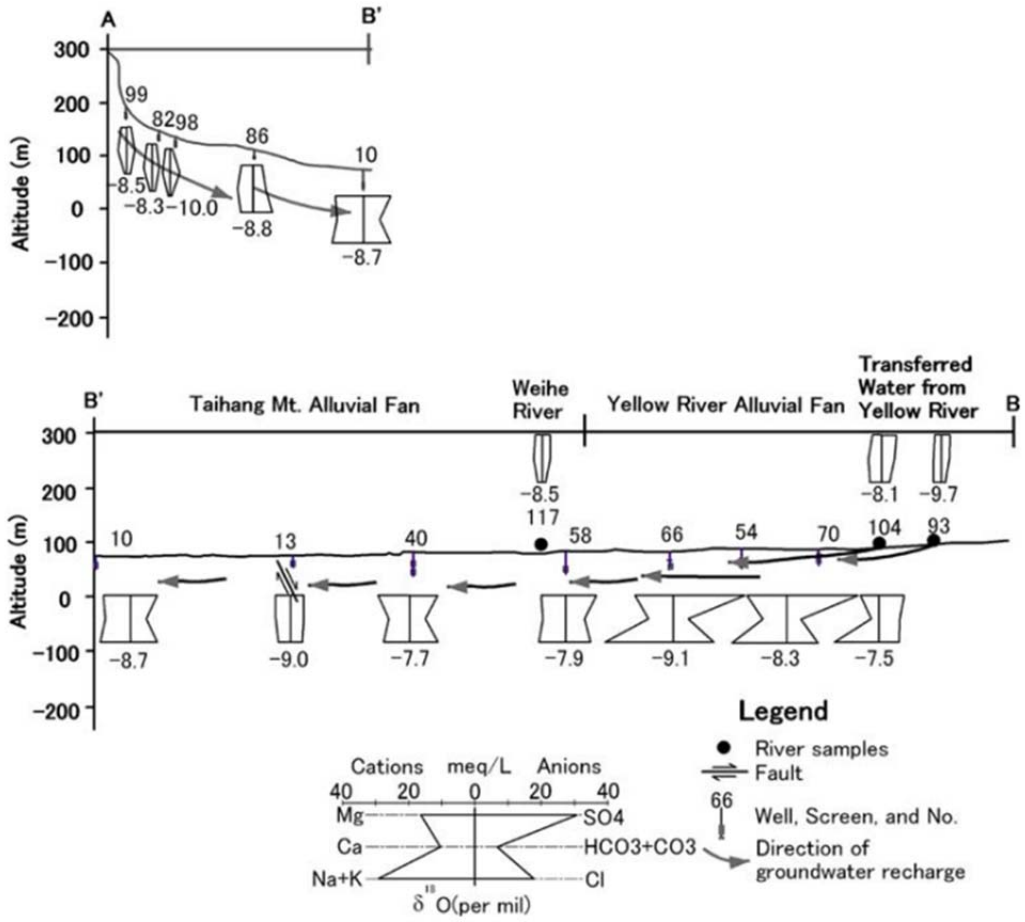

Figure 10: Conceptual model of a complex alluvial fan system showing hydrogeochemistry, $\delta^{18}O$, groundwater types, and groundwater flow direction (Li et al. 2008).

IV. Groundwater recharge in North Henan Plain

All these aspects coexist in North Henan plain, which belongs to the southern part of North China Plain. The population and agriculture activities have increased greatly over the last decades, which results in a growing water demand (Foster et al., 2004), however surface water resources are generally scarce and highly unreliable, which makes groundwater the primary source of water supply in this region (Yuan, R. et al., 2013). Meanwhile recent climatic variations and development of agricultural activities has resulted in the groundwater withdrawal continued, and deep groundwater that meets most of the local people's demands has been over-exploited. As a result, intensive groundwater exploitation may disturb the naturally steady flow system, even at a regional scale (Folch, A., et al., 2011).

North Henan plain is located at the complex alluvial-proluvial fans consisting of the Taihang MT. alluvial/proluvial fan in the northeast and the Yellow River alluvial fan in the southeast (Fig. 11). Alluvial/proluvial fans in piedmont plain form important aquifer systems supporting the potable water supply, local agriculture and industry development. Meanwhile groundwater in alluvial/proluvial fans represents the important water resource in semi-arid region.

Groundwater dynamics in North Henan Plain has been documented using hydrochemistry and isotopic techniques for the sustainable management of water resources. Pan et al. (2009) conducted a hydrochemical survey in North Henan Plain and demonstrated the interaction between shallow groundwater and surface water in the different landform unit in the Dashahe River basin, where exhibited a hydrochemical evolution of shallow groundwater in the proluvial fan area. Huang et al. (2010) investigated the hydrological geochemistry function in spatial distribution and evolution rules of groundwater in mining district of North Henan Plain. A quantitative hydrogeochemical simulation technology combined with hydraulic analysis and correlation matrices was utilized in this study. Their results indicated that exchange of positive ions of Ca^{2+}-Na^{+} and Mg^{2+}-Na^{+}, efflorescence and lioxiviation evaporation and concentration, non-congruent dissolution of dolomite are the major hydrological and chemical process to control the formation and the evolution of the

underground water, which provides a theoretical basis to infer the recharging sources of groundwater in the mining district. In addition, Zhang et al. (2010) investigated inland groundwater salinization in Jiaozuo area of North Henan Plain, with stable isotope (O^{18} and H^{2}) and hydrochemical compositions applied. The results demonstrated that chloride pollution in deep groundwater was connected with industrial waste water through tectonic structures, while chloride pollution of shallow groundwater was related with sewage mixed with industrial wastewater.

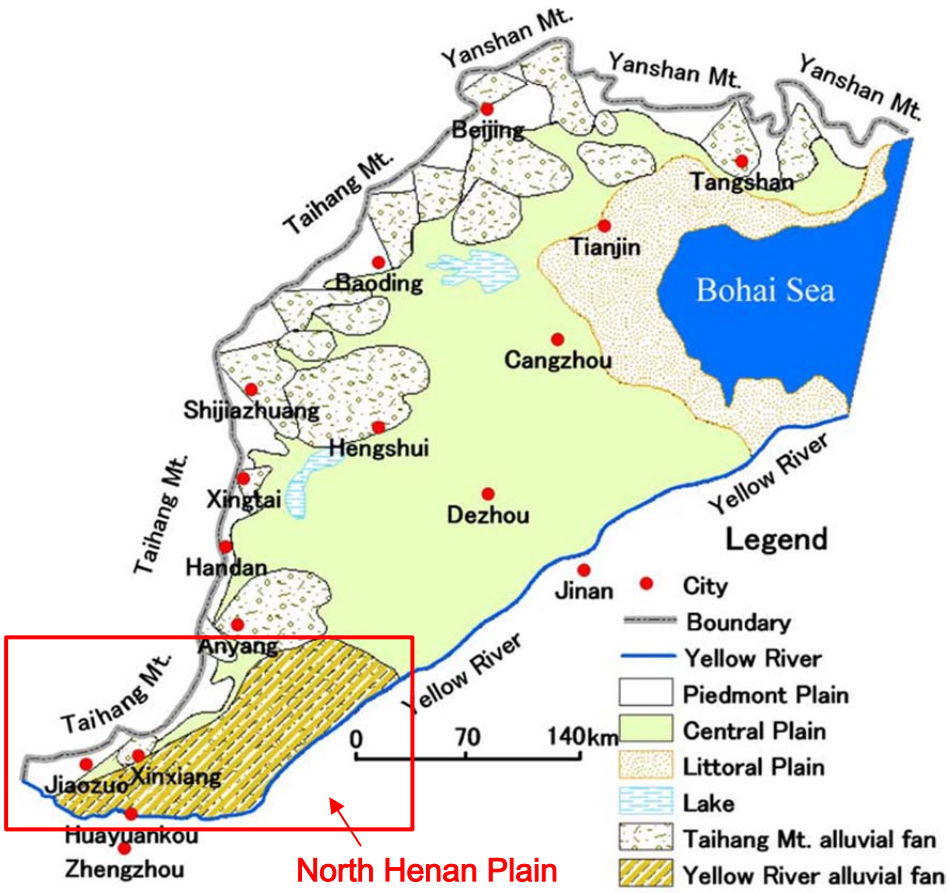

Figure 11: Alluvial fans in North China Plain (Li et al. 2008).

V. Summary

Previous research in North Henan Plain has shown that the geological formations and aquifer lithology are responsible for the specific groundwater flow pattern in the mountainous region and sedimentary infilling of the piedmont plain. In recent years, local government and scientists have performed significant surveys in North Henan Plain, with the groundwater flow systems of different landform units and aquifers described. In addition, much research has been carried out for focusing on the groundwater quality assessment and recognizing the way of practice sound water management (Pan et al., 1996; Guan et al., 2005).

Nevertheless, these documents paid more attention to the chemical evolution, interconnection between surface water and shallow aquifers, and contamination migration in individual aquifers on a regional scale. It is short of recharge information in a fault-influenced piedmont plain, and study of the isotopic geochemistry of deep groundwater resource is rather sparse, especially in alluvial-proluvial fan area. Furthermore, the efforts to use appropriate environmental tracers combined with hydrogeochemical data available to solve groundwater recharge issues in alluvial-proluvial fan area of piedmont plain are even fewer or non-existent.

Therefore in this scenario, it is important to establish a detailed groundwater recharge regime of piedmont plain in North Henan Plain for comparison with that based on other reginal and global scales. Meanwhile the effect of tectonic structure and deep groundwater withdrawal, as well the possible intrusion of shallow groundwater is of major interest in defining a reliable groundwater management of vulnerable piedmont ecosystem.

VI. Objectives

The objective of this thesis is to investigate the hydrochemical characteristics of different water systems in piedmont plain, and characterize the groundwater recharge processes in deep aquifer of alluvial/ proluvial fan with groundwater withdrawal, meanwhile the role of normal fault is expected to be identified.

Considering a reliable conceptual model of recharge regime with local scale can be constructed by groundwater isotopes combined with chemistry (Herczeg and Edmunds, 2000; Glynn and Plummer, 2005). Within this context, a schema of flow pattern integrated with hydrochemical evolution and EMMA (End member mixing analysis) is established to acquire insight into recharge regime of alluvial/ proluvial deep aquifer in piedmont plain using major ions and stable isotopes. It is expected that this study will reveal the groundwater hydrodynamics in alluvial/ proluvial fan under human pressures, and therefore applicable to similar water connectivity studies of piedmont plain.

Chapter 2: Study area and methodology

I. Site description

1. Location and topography

Jiaozuo area lies in the piedmont plain of North Henan plain in central China, extending between latitudes of 35.00°- 35.31°N and longitude of 112.95°- 113.26°E. This region covers an area of about 967 km^2 and is mainly included in Boai country, as illustrated in Figure 12.

Jiaozuo area borders Qinhe River basin to the west and south, Xishihe River basin to the east and to the north the Taihang mountain region, with the elevation ranging from 500 m to 1000 m.

Danhe River in the west of Jiaozuo area, originating in Gaoping country of Shanxi province, is the largest branch of Qinhe River and with a length of 162 km, which forms an alluvial fan and dries up in the mountain front region (Pan et al., 1996). Its mean annual flow rate is about 11.1m^3/s covering an area of the watershed around 3150 km^2. Qingtianhe reservoir is established in upstream of Danhe River and much of total runoff was stored, meanwhile the upper reach of Danhe River flows through limestone zones in Taihang mountain region, and recharges to local fracture water with a flow rate of 1.284- 1.734m^3/s, which causes an abrupt decline in runoff in downstream.

Xishihe River is the major tributary of Weihe River, upper reach of the Haihe River system, originates from the Lingchuan country of Shanxi province, with the length of channel in Jiaozuo area is approximately 74 km, which is a seasonal river and with no natural river water within the riverbed unless mountain torrent occurs in rainy season. This river forms a proluvial fan in the mountain-front (Pan et al., 2009).

Qinhe River, with a total length of 485 km and a mean annual discharge of 7.2×108 m3 from 1956 to 2010, is a major tributary of Yellow River (Bai et al., 2014). Five major reservoirs and massive canals for irrigation were constructed in the upper reaches and branches, which makes lower reach of Qinhe River becoming seasonal and usually dries up in dry season.

Two major geomorphic zones are included, mountainous area in the north and piedmont plain area in the south (Figure 13). With the average gradient of about 2‰, piedmont plain area can be subdivided into alluvial- proluvial fan area (elevation 100-200m) and alluvial plain area (elevation <100m).

2. Climate characteristics

Jiaozuo area belongs to the semi- arid zones and is characterized by a temperate continental monsoon climate (Figure 14), which is hot in summer (June- August) and cold in winter (December- March). The mean annual temperature is approximately 14.1- 14.4 °C. The mean annual precipitation ranges from 550 to 750 mm and mean annual evaporation is around 1170 mm (Figure 15). About 70% of annual rainfall concentrates in rainy season which is from June to September (Pan et al., 2009).

3. Land use and land-cover

In mountain region, the dominant land cover is forestland and grassland, with the predominant vegetation is deciduous broad-leaf forest, while farmland is the major land use type in piedmont plain, which accounts for about 31.7% of the total area of Jiaozuo site (Figure 16). Winter wheat and summer maize are the major crops widely cultivated and supported through pumping shallow groundwater (Liu et al., 2002), and agriculture irrigation consumes about 72% of the total exploitation quantity of groundwater (Jiao et al., 2005). In addition, fertilizer and manure has been widely utilized in local agriculture since 1965, which the amount significantly increases (Pan et al., 1996; Zhang et al., 2010).

4. Geological and hydrogeological settings

The study area represents a geotectonic piedmont plain, mountainous and hilly area in the north situates in the southern part of new cathaysian Taihang Mountain uplifting region, and the northern edge of the piedmont plain is bounded by a serious of hidden faults formed along the mountainous region, including Fenghuangling fault and Zhucun fault. Fenghuangling fault is an S- dipping high- angle (70°- 80°) normal fault which is buried beneath the Quaternary and Tertiary aquifer in mountainous region, with a total length of 70 km. Zhucun fault is also an buried S- dipping normal fault penetrating the basement and extending along the Taihang orogenic belt under aquifer,

with a total length of 160 km (Huang et al., 2010).

Groundwater in Jiaozuo area can be basically classified into two major groups: Carbonate karst water which is preserved in Cambrian- Ordovician limestone karst aquifer distributed in Taihang mountain region, Neogene- Quaternary pore water which is stored in sandy gravel deposits in piedmont plain (Figure 19). Two profiles are augured in western Danhe alluvial fan and eastern Xishihe proluvial fan in foothills region respectively to identify the recharge process in a alluvial- proluvial fan system (Figure 17). Although there is no available cross- section and no information about aquitard distribution, several boreholes in Jiaozuo area combined with the cross-section information of North Henan Plain (Figure 18) can show the reginal geological background. The Quaternary sediments aquifer forms the main aquifer of piedmont plain, the aquifer lithology is primarily gravel and clay- gravel in the alluvial- proluvial fan area, and sandy- clay in the alluvial plain area, meanwhile the size of aquifer media is diminished from the fan area to alluvial plain (Miao, 2011). The groundwater system is usually divided into shallow phreatic aquifer (buried depth of floor 40- 160 m) and deep confined aquifer (buried depth of floor 100- 400 m) (Figure 20), and a regional clay- mild layer generally exists between the two aquifers (Miao, 2010).

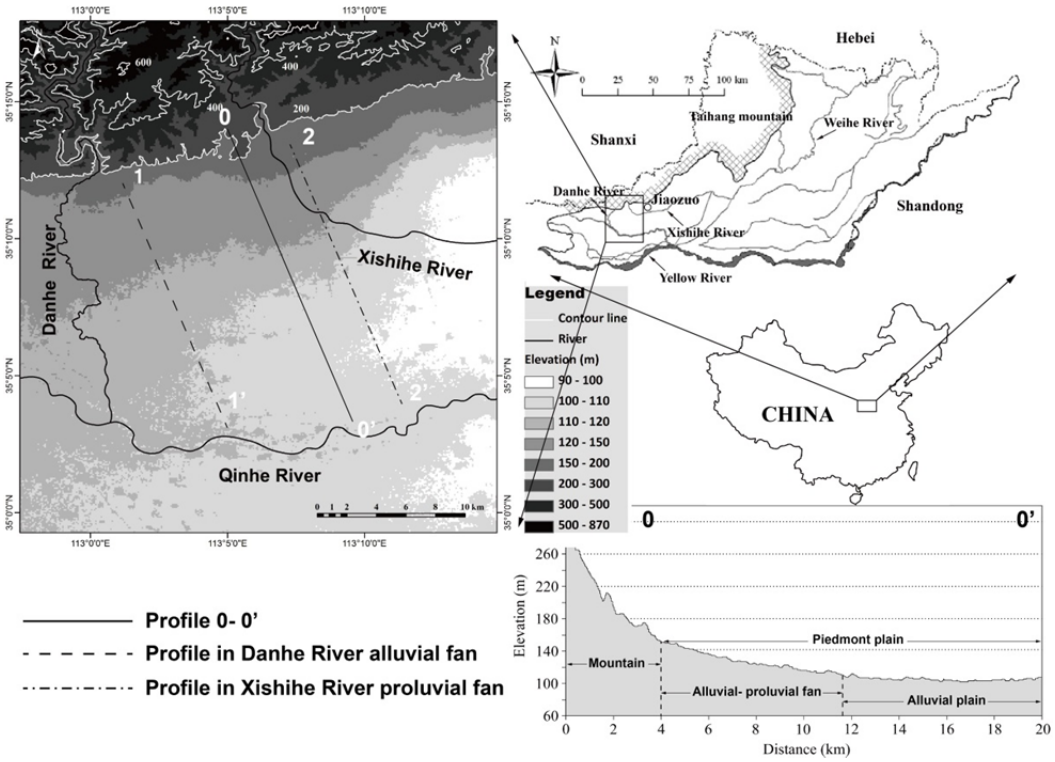

Figure 12: The location and DEM model (ASTER) of the study area. The longitudinal profile of DEM model along the 0- 0' cross- section.

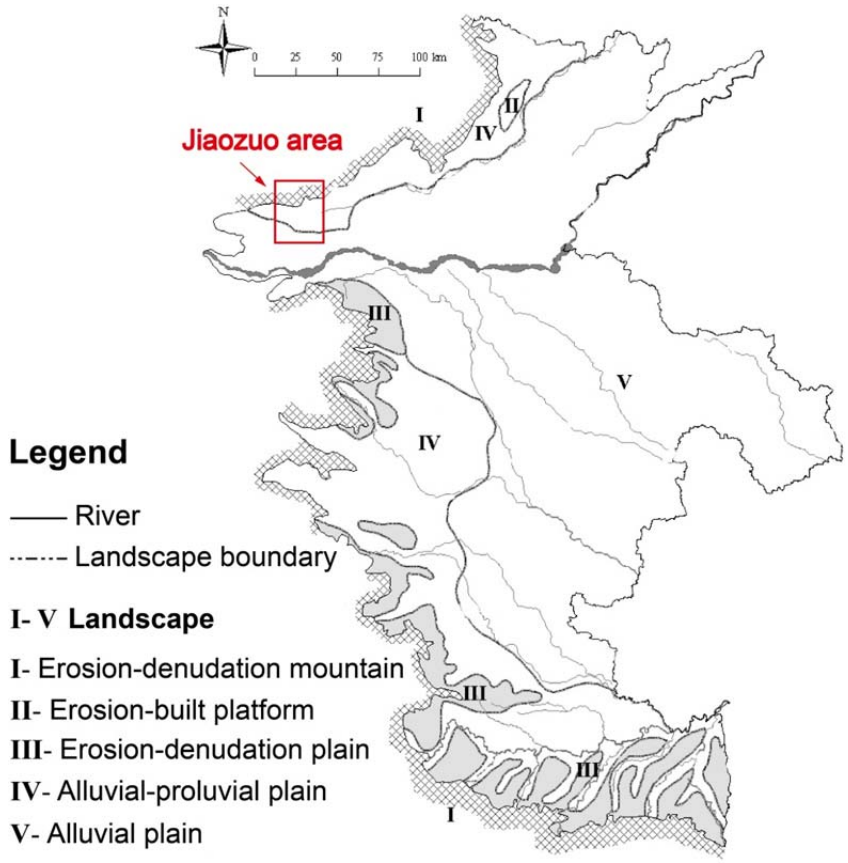

Figure 13: The landscape classification of North Henan Plain (Gao. 2008).

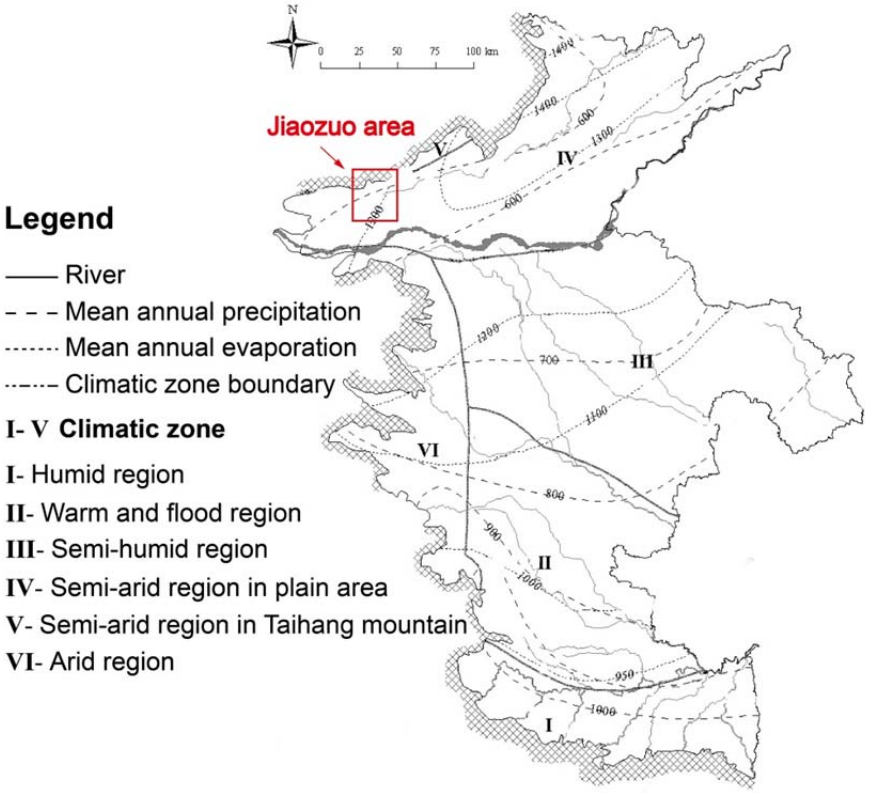

Figure 14: The climatic zones of North Henan Plain (Gao. 2008).

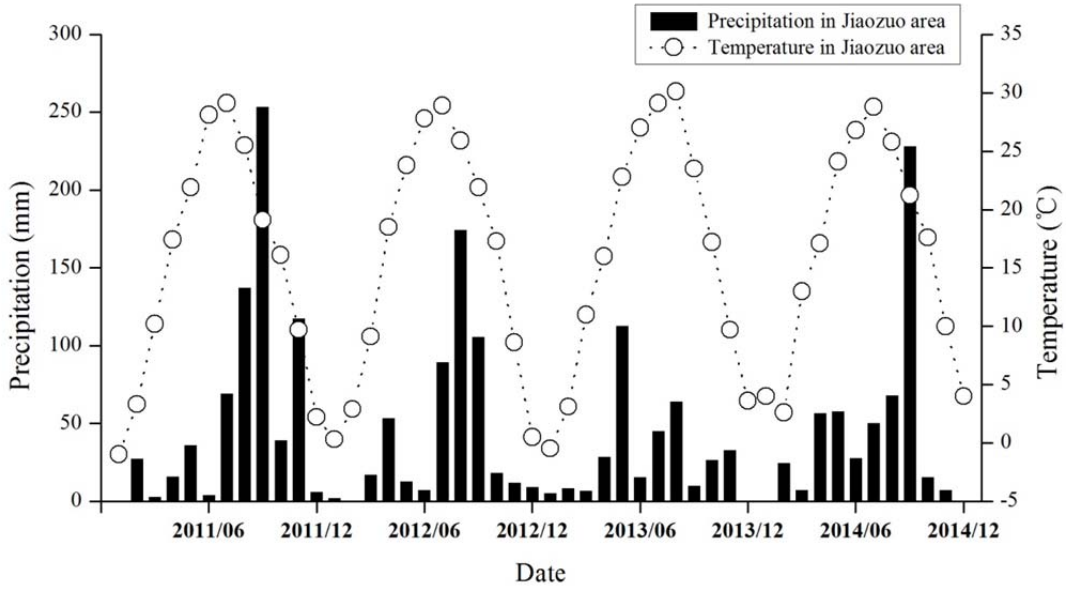

(a) Rainfall and temperature.

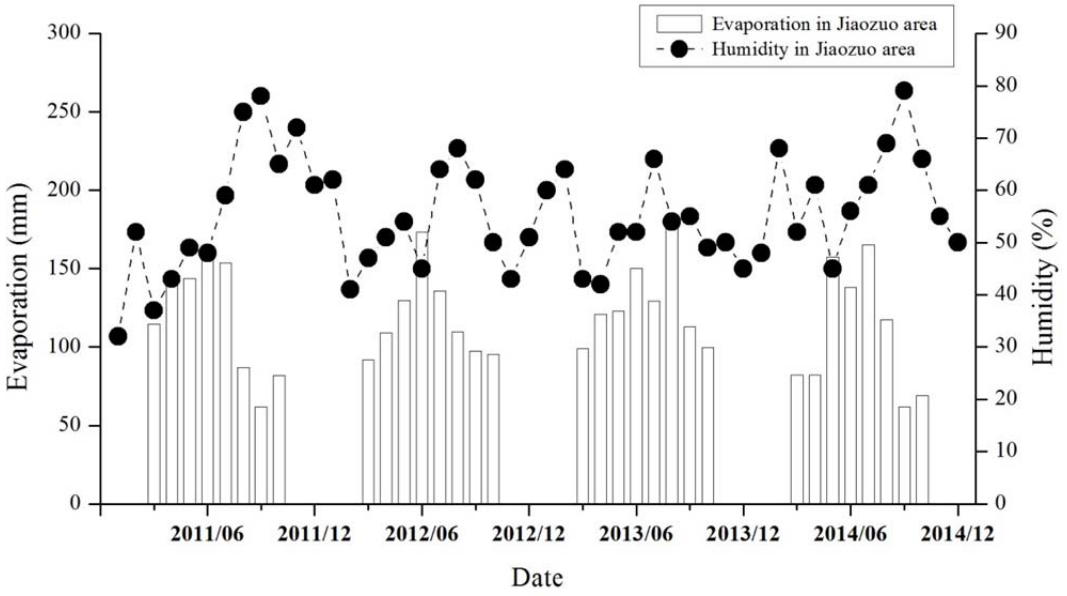

(b) Evaporation and humidity

Figure 15: Monthly values of climate data from January 2011 to December 2014.

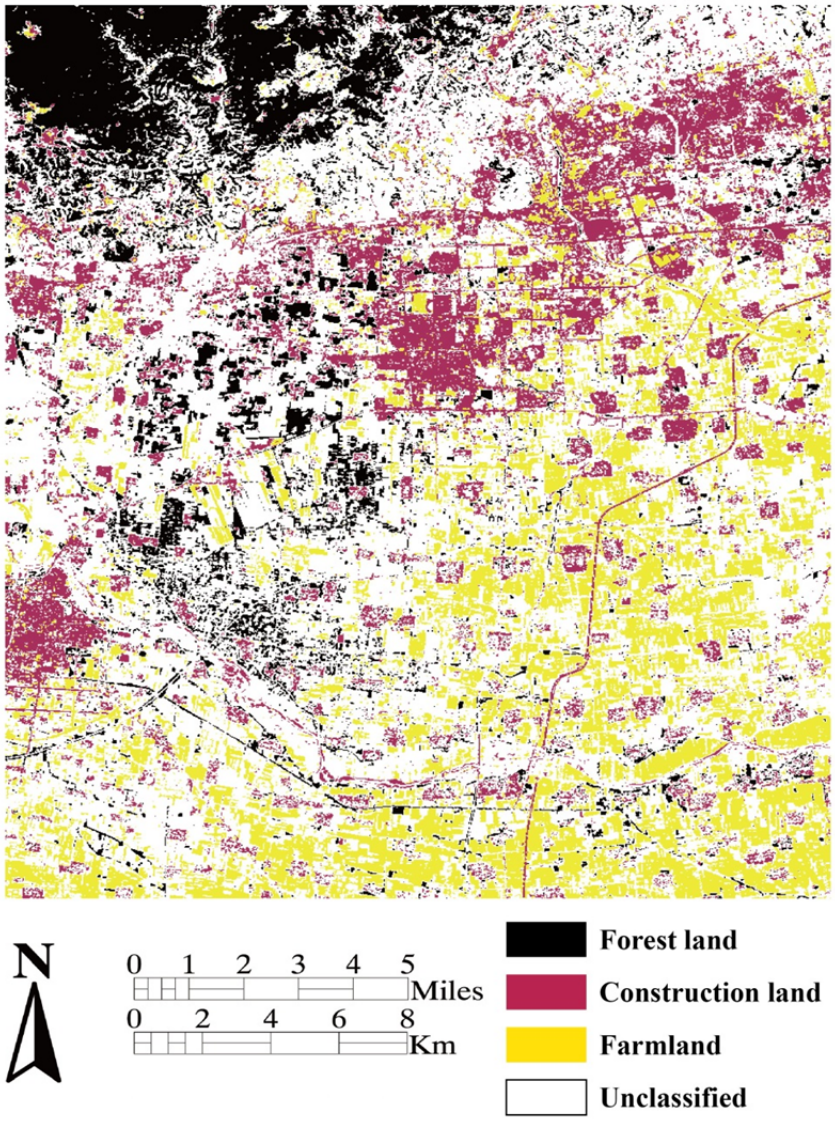

Figure 16: Land uses in the study area, 2014 (data from: NASA landsat remote sensing map, 2014).

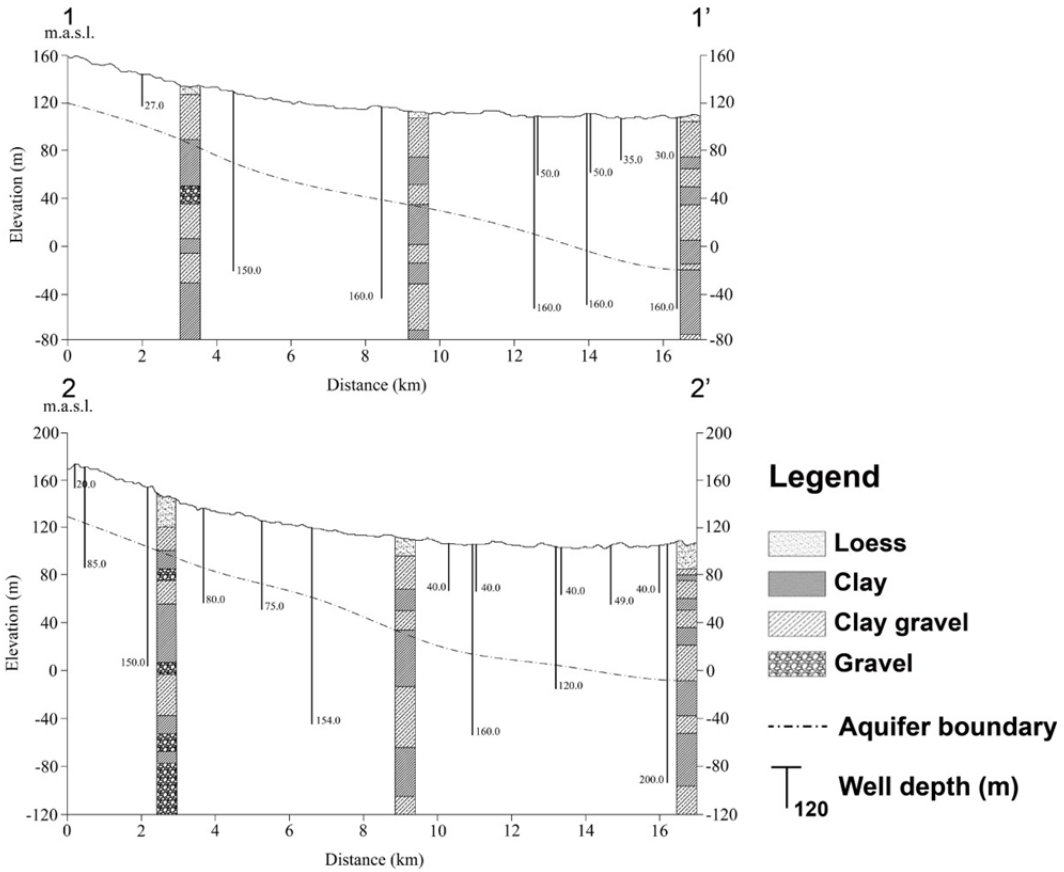

Figure 17: The sketch map of geological section along 1-1' and 2- 2' in Figure 12(according to local borehole information).

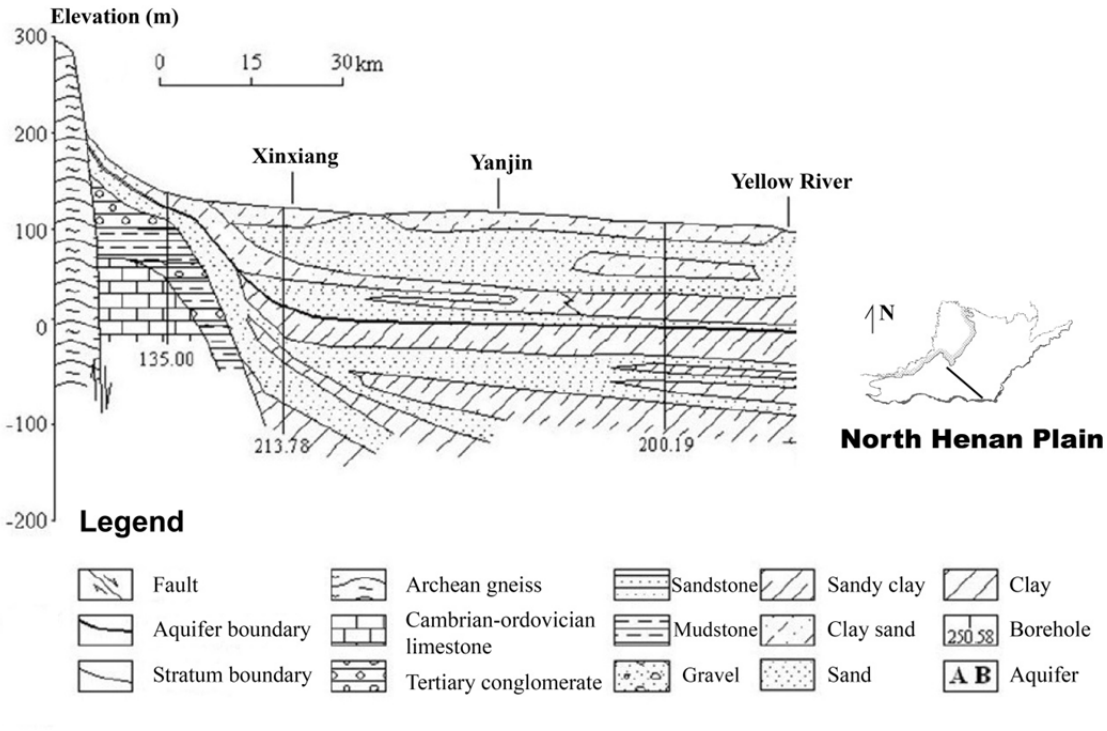

Figure 18: The SE- oriented cross-section in North Henan Plain.

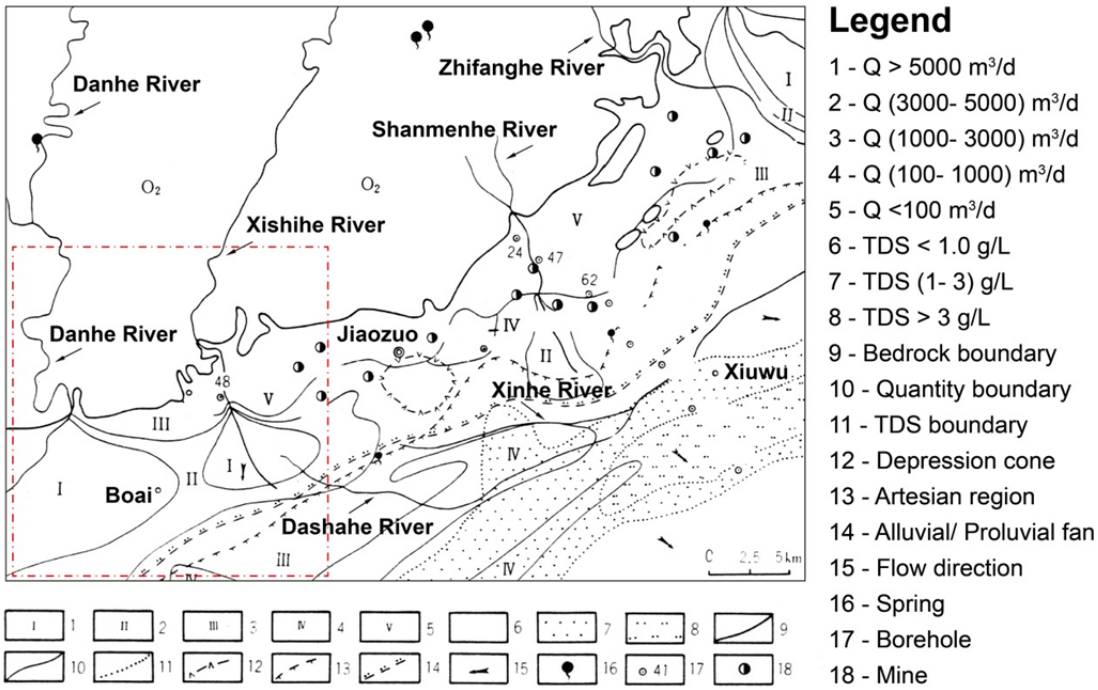

Figure 19: Hydrogeological map of Jiaozuo area.

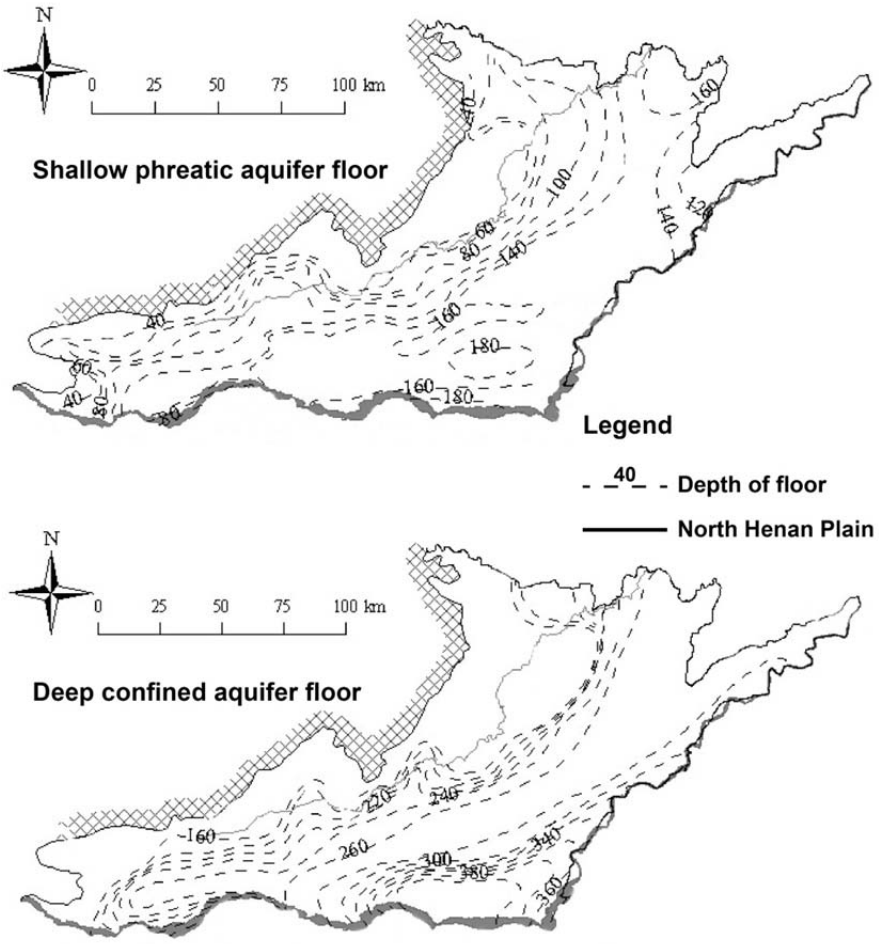

Figure 20: Depth of shallow and deep aquifer floor in North Henan Plain.

II. Methodology

1. Water sample information

Field surveys in Jiaozuo area were performed in successive years: 2013 (October), 2014 (August). Water samples collected in October represent dry season and those taken in August represent rainy season. Samples were collected from 77 locations in mountain region, as well as the alluvial- proluvial fan (northern margin of the piedmont plain) and alluvial plain (southern margin of the piedmont plain), including 15 mountain groundwater samples, 7 spring water samples, 6 river water samples and 86 groundwater samples in piedmont plain. River water samples were obtained from Qinhe River at two sites, as well as from Danhe River. Mountain groundwater samples were taken from the private and public wells in mountain villages, spring water samples were obtained along the fault zones (Figure 21). Considering the hydrogeological conditions in piedmont plain and potential impact of extraction on groundwater dynamics, samples of phreatic groundwater were typically collected from wells <70 m deep (private and irrigation wells), and deep groundwater samples were primarily obtained from public wells for potable water supply (60- 200 m depth).

2. Field and laboratory measurement

On site analyses included electrical conductance (EC), pH, oxidation- reduction potential (ORP) and bicarbonate ion measured by titration. All the water samples were collected in polyethylene bottles, filled to overflowing and capped, then filtered (0.45μm membrane filters) for isotope and major ions analyses. Chemical and isotopic compositions of water samples were analyzed in the laboratory of Graduate School of Life and Environmental Sciences, University of Tsukuba. Chemical compositions were analyzed at Research Facility Center of Science and Technology with Optima 7300DV ICP- AES for cations and Ion Chromatography (Shimazu Co. Ltd., HIC-SP/VP Super) for anions. Samples for stable isotope analysis (18O, 2H) were measured by Finnigan MAT 252, analyses for 18O and 2H are expressed in δ-notation relative to Vienna standard mean ocean water (V- SMOW) standards. The $\delta^{18}O$ and δD measurement were reproducible to ±0.1‰ and ±1‰, respectively.

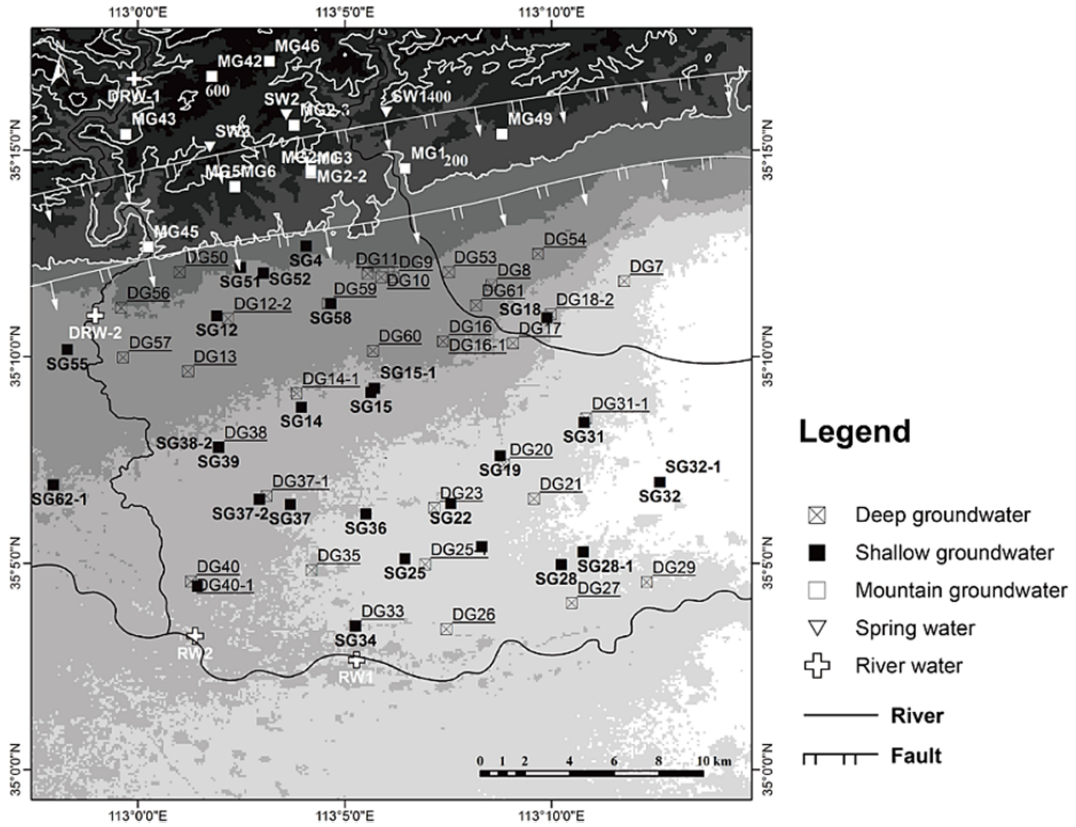

Figure 21: A map view of the Jiaozuo area and the normal faults with the locations of sampling sites.

III. Methods of data analysis

A variety of methods can been utilized for estimating recharge, and appropriate environmental tracers can reveal a general recharge mechanism especially with the limited hydrological data (Scanlon et al., 2002; Zhu et al., 2003). In addition, groundwater recharge regime on both local and reginal scale can be established by hydrochemical composition combined with groundwater isotopes (Mahlknecht et al., 2004; Glynn and Plummer, 2005).

Hydrochemical and isotopic methods have been successfully applied as an effective tool to clarify local and regional groundwater system in alluvial fan, for instance to determine different water system in the arid and semiarid region (Schu ¨rch and Vuataz 2000); to clarify groundwater recharge sources (Tsujimura et al. 2007); and to study the interaction of different aquifers (Dassi et al. 2005).

1. Graphical methods of representing analyses

The hydrochemical evolution of regional groundwater flow can be generalized by the typical water types that are found in different zones of groundwater systems (Ingebritsen et al., 2006). Considering the major ions (Cl^-, NO_3^-, SO_4^{2-}, K^+, Na^+, Ca^{2+}, Mg^{2+}, HCO_3^-) dissolved in groundwater determine the differences of water type, graphical procedures do this discrimination much more effectively than numbers presented in tables, in which the methods of trilinear diagram and hexa diagram are useful principally for emphasizing differences and similarities of water quality. In addition, the chemical results are only accepted when the charge balance error is within ±5%.

Trilinear diagram, which is also called Piper diagram (Piper, 1944), is a graphical representation of the water chemistry and has been widely used to clarify the hydrochemical evolution of different water bodies (Subrahmanyam and Yadaiah, 2001). As shown in Figure 22, it can be seen that trilinear diagram consists of one rhombus area and two triangles areas. The triangle area in left bottom represents the mill equivalent percentage of cations (K^+, Na^+, Ca^{2+} ,Mg^{2+}), and the one in right bottom indicates the mill equivalent percentage of anions (Cl^-, SO_4^{2-} , HCO_3^-).

Water samples distributed in different zones of the rhombus area indicates various

water types. Zone 1: alkaline earths (Ca + Mg) exceed alkalis (Na + K); zone 2: alkalis exceed alkaline earths; zone 3: weak acids (CO_3 + HCO_3) exceed strong acids (SO_4 + Cl); zone 4: strong acids exceed weak acids; zone 5: carbonate hardness >50% (alkaline earths and weak acid dominate); zone 6: non-carbonate hardness >50% (water usually originates in hot spring water or fossil water); zone 7: non-carbonate alkali >50% (with sea water characteristics); zone 8: carbonate alkali >50% (groundwater is inordinately soft in proportion to the content of TDS); zone 9: no cation–anion pair >50% (Piper, 1944).

Hexa diagram, which also refers to Stiff diagram (Hem, 1985), it depicts an irregular polygonal shape or pattern with the major ionic compositions connected, as illustrated in Figure 23. It uses three parallel horizontal axes extending on each side of vertical zero axes. Contents of cations and anions can be plotted on each side of vertical axes, which the cation on each horizontal axis situates in the left side of vertical axis, and anion in the right. The width of the pattern represents the ion concentration which is in mill equivalents per liter. Therefore, the Hexa diagram can be a relatively distinctive method of describing the divergence and similarity of water chemical composition.

2. Stable isotopic analysis

The utilization of stable isotopes to solve hydrogeochemical issues in ecosystem has been significantly increasing because stable isotopic data can provide both source-sink (tracer) and process information (Peterson, B. J. and Fry, B., 1987), for instance ^{18}O and ^{2}H variation can be used as a hydrological tool for investigating local sources of groundwater (Dansgaard, 1964).

Precision measurements of deuterium and ^{18}O in natural waters are always made by a mass spectrometer. However no means are available for an accurate determination of the absolute ^{18}O content and it is much easier to measure relative or absolute differences between two samples (Dansgaard, 1964). Considering the variations in isotopic composition are mainly concerned, the ^{18}O data will be given as the relative deviation (denoted by δ) of the heavy isotope content of a sample from that of a standard. Therefore, δ may be considered as

$$\delta\,(‰) = \frac{R_{sample} - R_{standard}}{R_{standard}} \times 1000$$

Where, R_{sample} and R_{sample} are the measured isotopic ratio for sample and for standard, respectively. The reference standard is SMOW (Standard Mean Ocean Water, Craig, 1961).

Isotopic fractionation of water is caused by several processes in nature, and the fact that the volatility of H_2O^{16} is higher than those of the heavy isotopic components causes the fractionation in all condensation processes and also in the evaporation of well mixed liquid water (Dansgaard, 1964). Considering the seasonal isotopic divergence is primarily controlled by large scale monsoon activities with distinct isotopic compositions (Yamanaka et al., 2004), and a meteoric water line can be defined with the isotopic compositions of precipitation (Craig, 1961), which provides the basis for the interpretation of water recharge sources and processes.

$$\delta D = a\,\delta^{18}O + b\ (‰)$$

Where *a* and *b* are constants that varies in specific region.

Isotopic signature of groundwater is not influenced by water-rock/soil ion exchange and with negligible evaporation impact in aquifer of certain depth (McCarthy et al., 1992; Gat, 1996). Therefore, the isotopic divergence in groundwater may due to the infiltration of surface water or the precipitation (Kendall and Mcdonnell, 1998).

3. End-member mixing analysis

End-member mixing analysis (EMMA) is an effective tracer approach in hydrogeological research, which utilizes chemical/isotopic components to differentiate the potential sources contributing to a mixed item (Clark and Fritz, 1997; Bosley et al., 2002).

EMMA is based on tracer mass balance, which has been conventionally applied in hydrograph separation (Burns et al., 2001). In addition, this approach can also be utilized to clarify the contribution ratio of each recharge source of groundwater (Nakaya et al., 2007).

This method assumes the following conditions (Barthold et al., 2011): (1)

groundwater is a mixture of various sources with a constant composition; (2) the mixing process is linear and completely dependent on hydrodynamic mixing; (3) the tracers selected for calculating the contribution ratio are conservative; (4) the sources are with extreme concentrations.

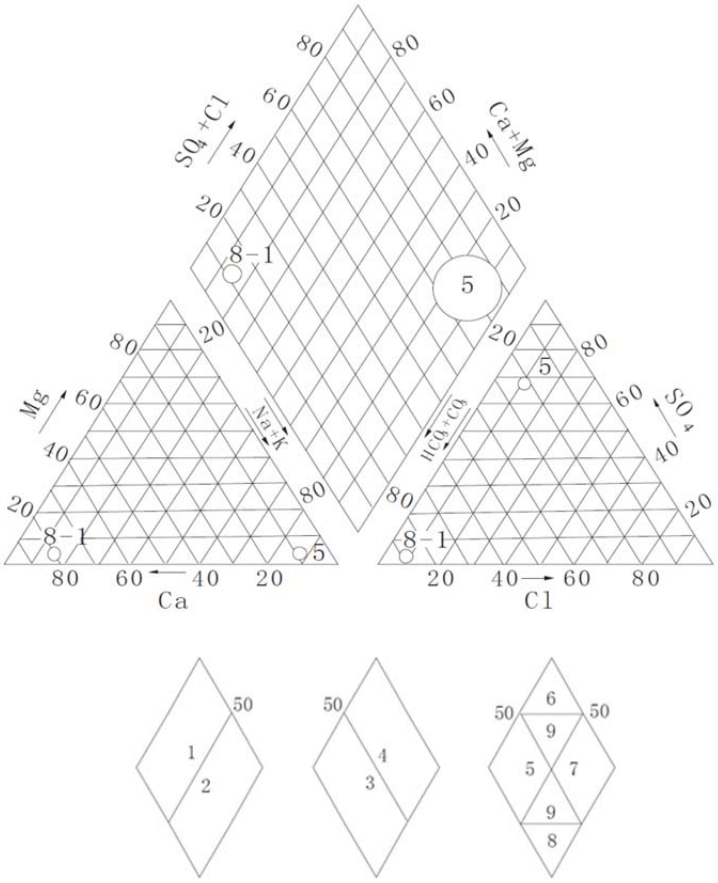

Figure 22: The Piper diagram. Zone 1: alkaline earths (Ca + Mg) exceed alkalis (Na + K); zone 2: alkalis exceed alkaline earths; zone 3: weak acids (CO_3 + HCO_3) exceed strong acids (SO_4 + Cl); zone 4: strong acids exceed weak acids; zone 5: carbonate hardness >50% (alkaline earths and weak acid dominate); zone 6: non-carbonate hardness >50% (water usually originates in hot spring water or fossil water); zone 7: non-carbonate alkali >50% (with sea water characteristics); zone 8: carbonate alkali >50% (groundwater is inordinately soft in proportion to the content of TDS); zone 9: no cation–anion pair >50%.

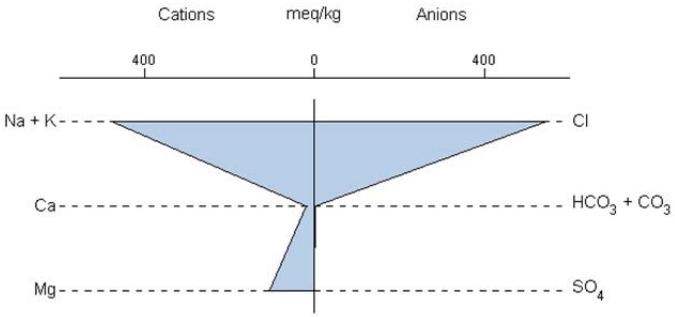

Figure 23: The Hexa diagram (Hem, 1985).

Chapter 3: Hydraulic and hydrochemical results of different water systems in Jiaozuo area

I. Groundwater table and variation in Jiaozuo area

Groundwater table contour line is drawn separately for the upper unconfined aquifer and confined aquifer underneath, which includes alluvial-proluvial formations and Quaternary sedimentary units (Figure 24). Phreatic water flow is controlled by elevation gradients, and it is consistent with water flow system of piedmont plain in Jiaozuo area. Phreatic water table decreases with the elevation declines, which results in the phreatic water flows toward down gradient direction of elevation with SE-oriented. Meanwhile, deep groundwater level variation is in accordance with phreatic water.

It is worth noting that a depression cone of the phreatic water in site of SG25 was formed in alluvial plain, where water level depth reaches 9.3m, and another depression cone was formed in deep aquifer of Xishihe River proluvial fan, where water table depth of wells DG9, DG10 remained at 50m during dry and rainy season.

The variation of water table depth in alluvial- proluvial fan and alluvial plain was markedly different during the studied period (Figure 25). Water table depth significantly raised in deep aquifer occurs in alluvial plain during the rainy season, with the average depth increases 3.23m, while the deep water table depth in alluvial-proluvial fan remained fairly steady (exception of DG8 and DG9), the average depth only increases 0.44m. Nevertheless, the variation of water table depth in phreatic aquifer in alluvial- proluvial fan is relative close to alluvial plain during the rainy season, with the average depth raised by 2.05m and 2.06m respectively.

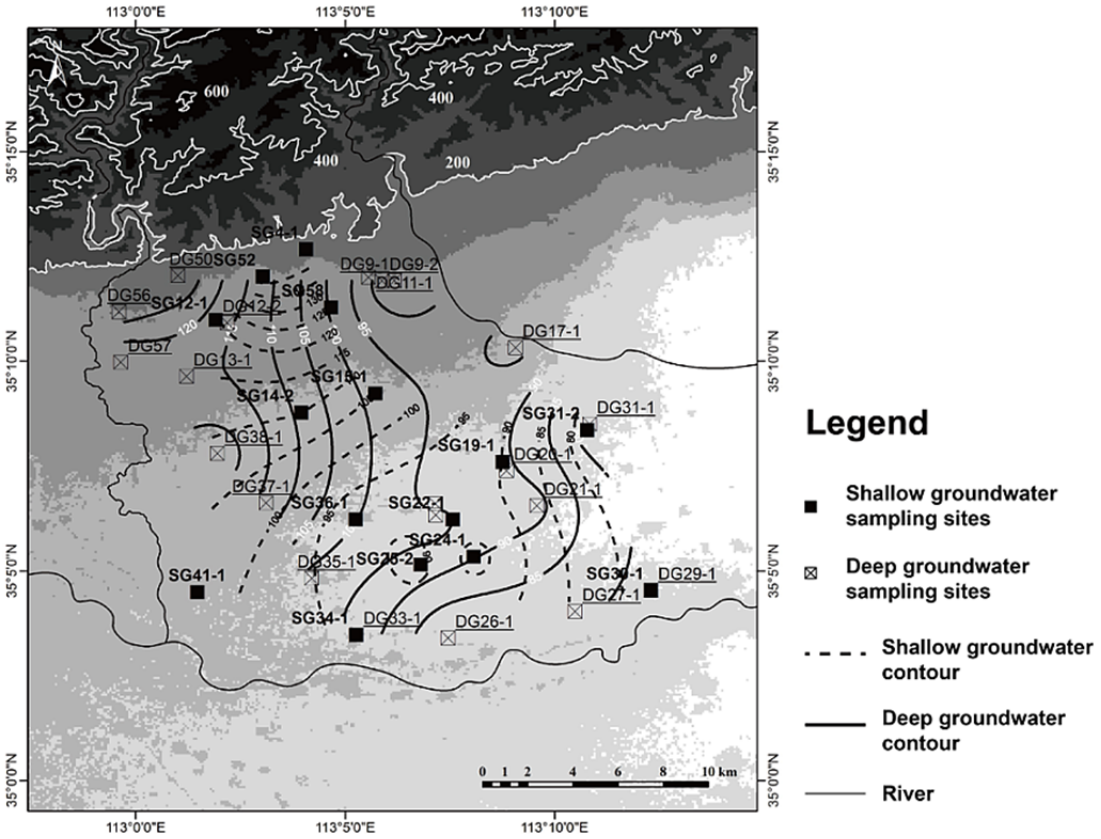

Figure 24: Contour map of shallow and deep groundwater table in August 2014.

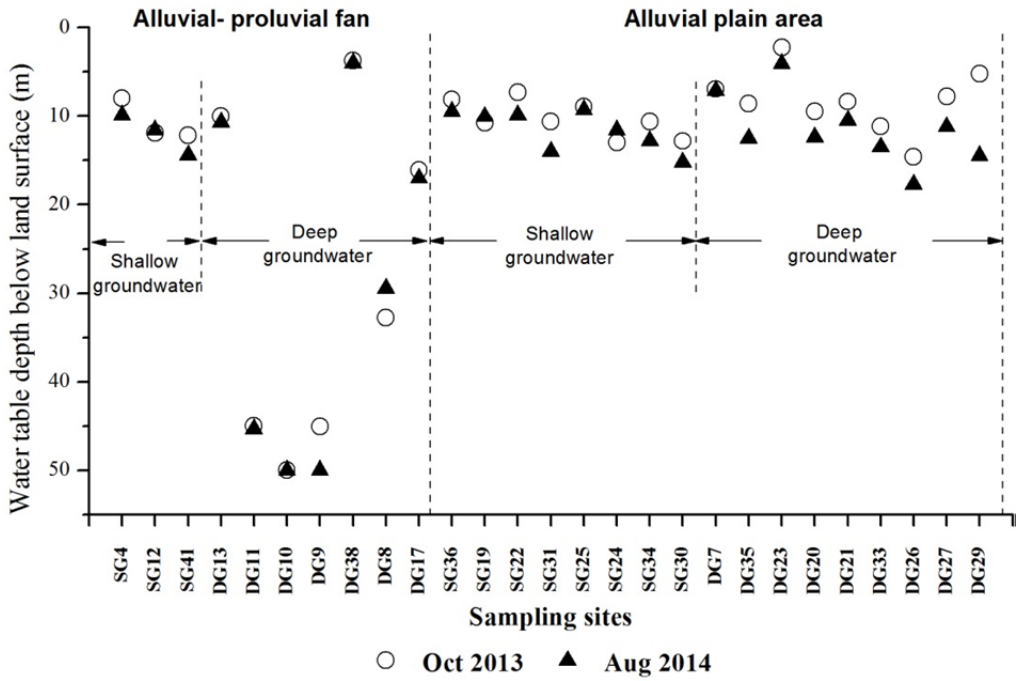

Figure 25: Variance of water table depth below land surface measured in field surveys.

II. Hydrochemical characteristics of different water systems

Hydrochemical results (field data, site information and physicochemical parameters) of the surface water and groundwater are presented in Table 1, which is arranged according to three different water systems: mountain water, shallow and deep groundwater system.

1. Characteristics of pH ORP and EC

The mean pH value of most mountain groundwater samples was 7.7 with no obviously variation during the dry and rainy season, except for sites of MG2, MG3, MG5, MG2-2 were with a relative lower mean value of 6.9.The pH value of spring water varied from 7.18 to 8.12 in fault zones, meanwhile the mean pH value of river water is almost the same with some spring water, which is an indicator that recharge from spring water happened. The pH of shallow and deep groundwater in piedmont plain were neutral to alkaline, and lower than the value in hilly area, with the value of 7.3 and 7.5 respectively.

The ORP values of some shallow groundwater in alluvial plain were negative, while shallow groundwater in fan area and deep groundwater in piedmont plain were almost positive, with the average values were 138 mV and 121 mV respectively.

The mean EC value of deep groundwater (700 μs/cm) in alluvial plain was always much lower than the value of shallow groundwater (610- 3600 μs/cm) in piedmont plain and mountain groundwater (560- 1860 μs/cm), except the deep water samples in sites of DG21 and DG29 were characterized by a high degree of variability. However the EC of deep groundwater increases from the southern alluvial plain aquifer to northern alluvial-proluvial fan aquifer, which has a mean value of 955 μs/cm (Figure 26 and Figure 27).

2. Spatial distribution of water chemistry in Jiaozuo area

Shallow groundwater samples were characterized by a high degree of variability with respect to major ion concentrations, and fall predominantly in the category of $Ca{\cdot}Mg\text{-}HCO_3{\cdot}SO_4$ in alluvial-proluvial fan, which indicates the quality of groundwater varied greatly and impact of human activities (Figure 28).

Calcium (ranging from 3.17 meq/L to 8.58 meq/L) and magnesium (ranging from

2.53 meq/L to 5.16 meq/L) were the dominant cations of deep groundwater in northern alluvial- proluvial fan, meanwhile bicarbonate (varying from 4.34 meq/L to 7.67 meq/L) and sulfate (1.04- 4.39 meq/L) predominated as for the anions. The major water type of deep groundwater changed from Ca·Mg-HCO_3·SO_4 in alluvial-proluvial fan to Ca·Mg-HCO_3 in southern alluvial plain along the flow direction of groundwater, and a number of deep groundwater samples in foothills region have mixed ionic composition (Figure 28 and Figure 29). Additionally, deep well DG21 in alluvial plain are chloride enriched only in dry season and another deep well DG29 is dominated by sodium during the studied period.

In the spring water of site SW3, the concentrations of calcium and sulfate were much higher than the other water samples in hilly areas (Figure 30), which suggest the existence of gypsum stratum considering the geological setting. Meanwhile, it is inferred that some mountain groundwater could be recharged by spring water due to the similar water type.

3. Stable isotopic composition in waters

The seasonal isotopic divergence is primarily controlled by large scale monsoon activities with distinct isotopic compositions (Yamanaka et al., 2004). The basis for the interpretation in this study was provided by a local meteoric water line (LMWL) for Jiaozuo area, which was established by the isotopic compositions of local rain water in 1986 and 1987 (Pei et al., 1993), and could be defined as $\delta D = 8.03\ \delta^{18}O + 12.68$ (correlation coefficient: $R^2 = 0.96$).

The δ values of Qinhe River water was -7.13‰ for $\delta^{18}O$ and varied from -57.1 to -56.2‰ for δD in October (dry season) (Figure 31), which tended to be heavier than river water in $\delta^{18}O$ (-7.90 to -7.81‰) and δD (-58.6 to -57.9‰) in August (rainy season) (Figure 32) due to evaporative enrichment. Meanwhile, the $\delta^{18}O$ values ranged from -8.90 to -8.85‰ and δD changed from -65.8 to -64.3‰ in Danhe River water in rainy season, which exhibited a more depleted stable isotopic composition than Qinhe River water.

Mean values of $\delta^{18}O$ and δD in mountain groundwater were -9.00‰ and -65.5‰ in rainy season which is similar to the mean values in dry season, with the $\delta^{18}O$ and

δD were -9.03‰ and 64.0‰ respectively. Meanwhile spring water and most mountain groundwater exhibited similar isotopic compositions. It is suggested that some wells in mountain region should be intimated with spring water in tectonic areas.

The shallow groundwater in piedmont plain exhibited a relative wide range of values for $\delta^{18}O$ and δD, falling between -10.68‰ and -7.31‰ for $\delta^{18}O$ and between -81.0‰ and -47.6‰ for δD (Figure 31 and Figure 32). Meanwhile, although surveys were conducted in different seasons, isotopic composition of deep groundwater in alluvial plain exhibited a relative narrow range, with the mean values of $\delta^{18}O$ and δD were -9.66‰ and- 72.1‰ in dry season, -9.75‰ and 71.5‰ in rainy season, which is very close to the mean values of deep confined groundwater in North Henan Plain. Additionally, deep groundwater in alluvial- proluvial fan area differed from the deep groundwater in alluvial plain in its isotopic pattern, which was more enriched in foothills region and its isotopic composition was similar to the shallow groundwater in the overlying aquifer.

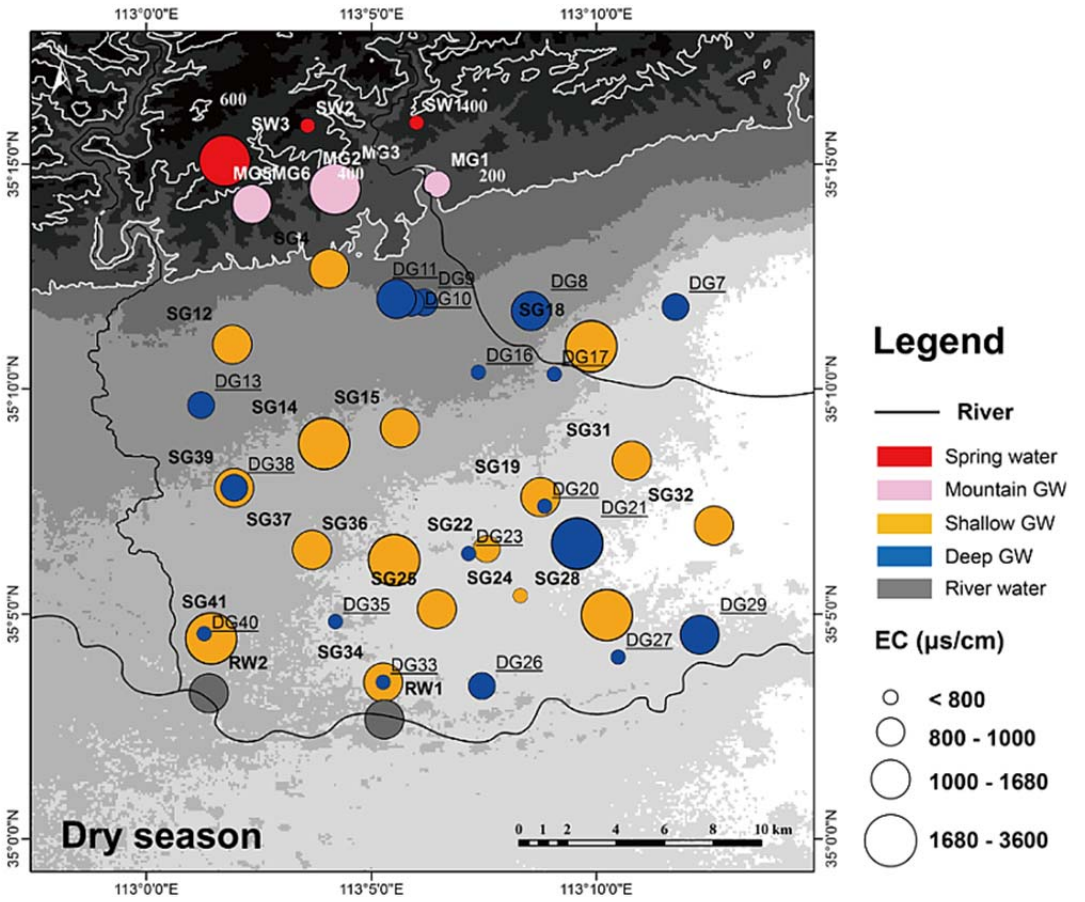

Figure 26: Spatial distribution of EC (Electrical Conductivity) value during the dry season.

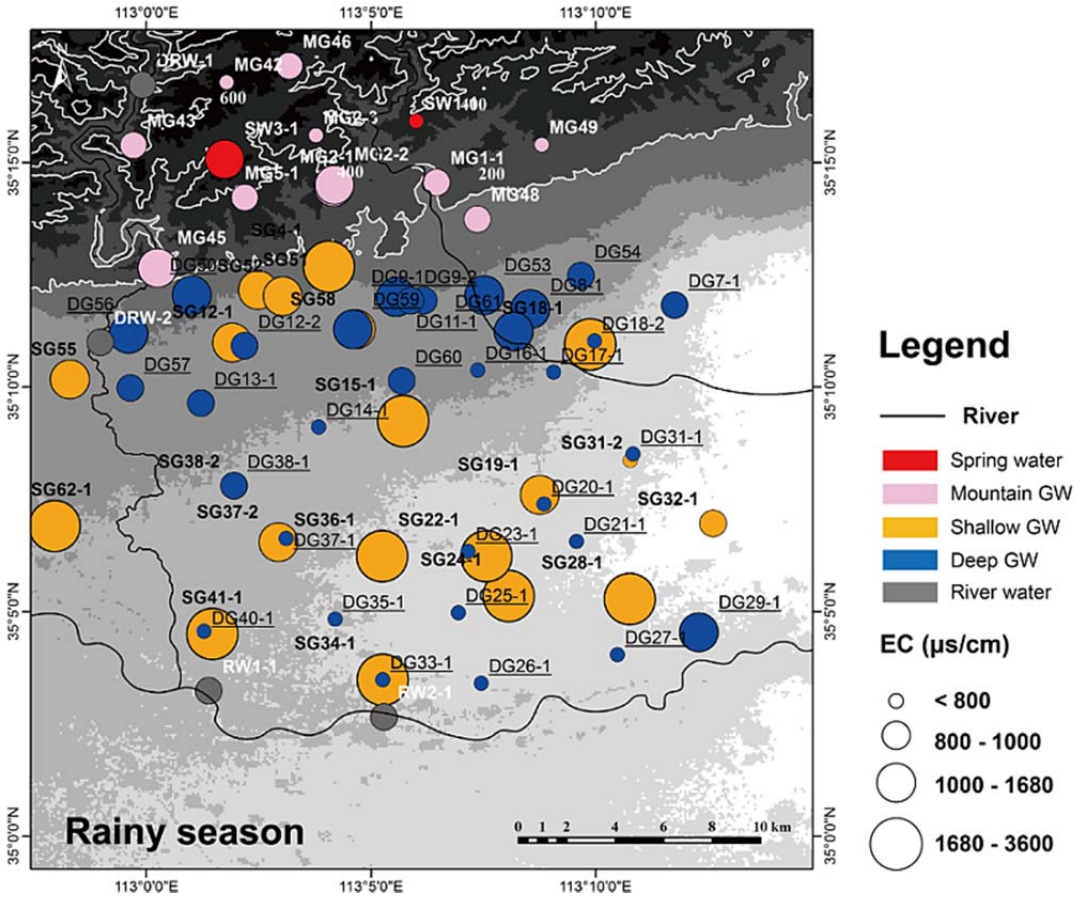

Figure 27: Spatial distribution of EC (Electrical Conductivity) value during the rainy season.

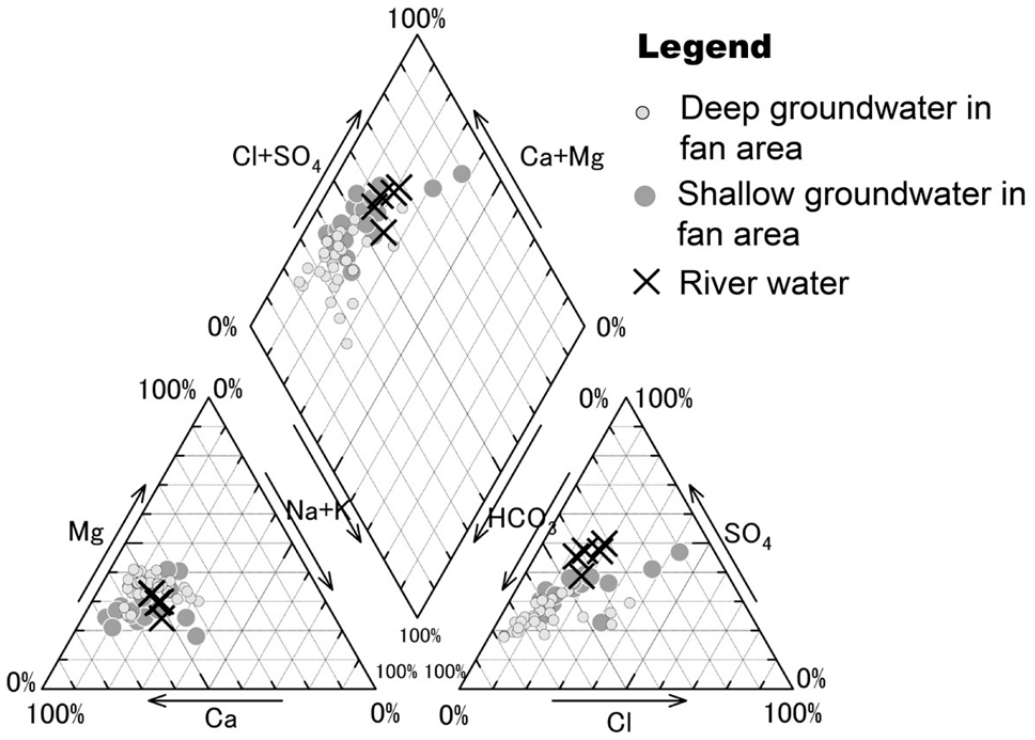

Figure 28: Piper diagram of water samples in alluvial-proluvial fan area.

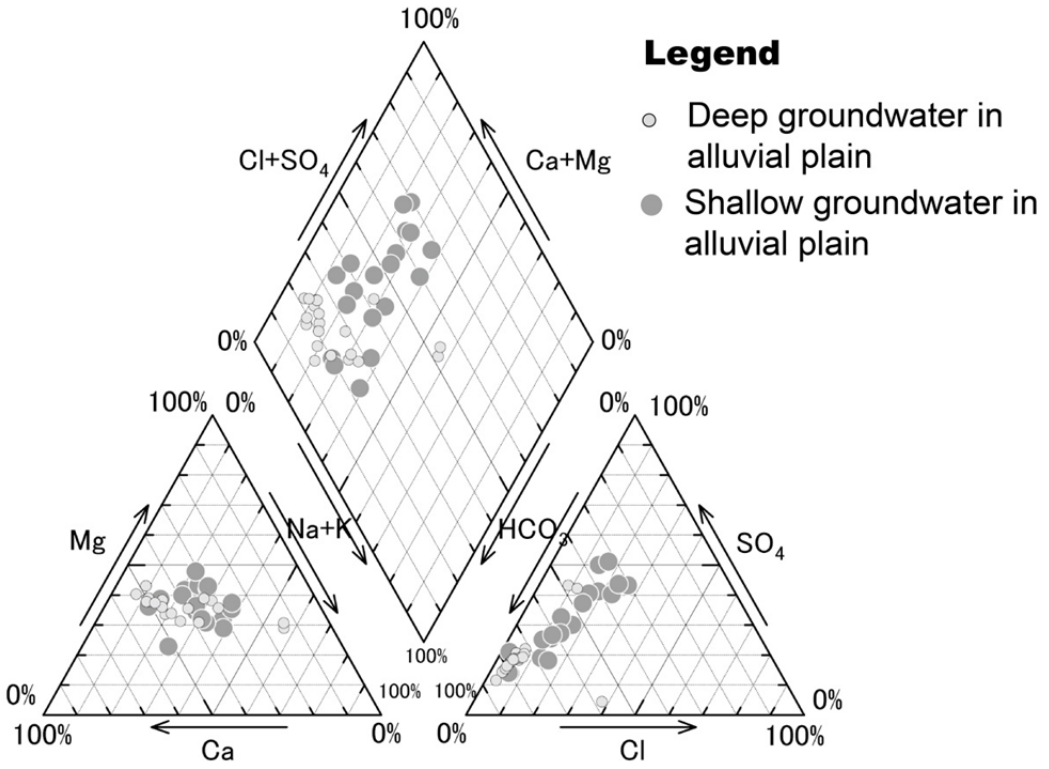

Figure 29: Piper diagram of water samples in alluvial plain area.

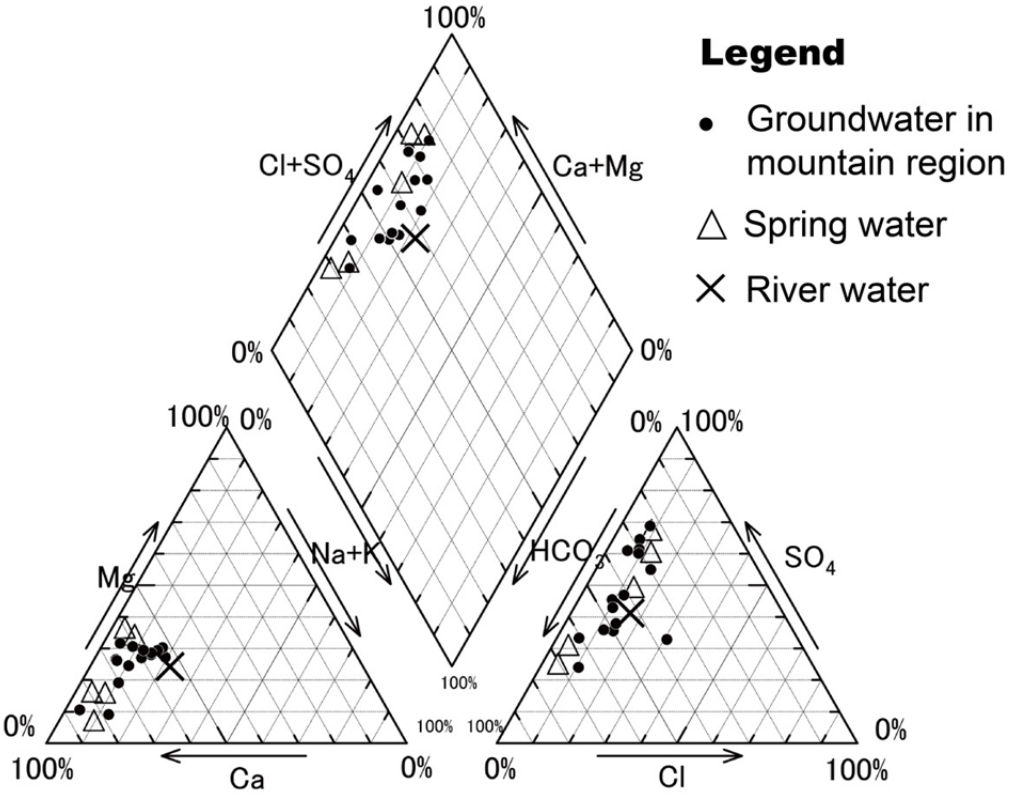

Figure 30: Piper diagram of water samples in mountain region.

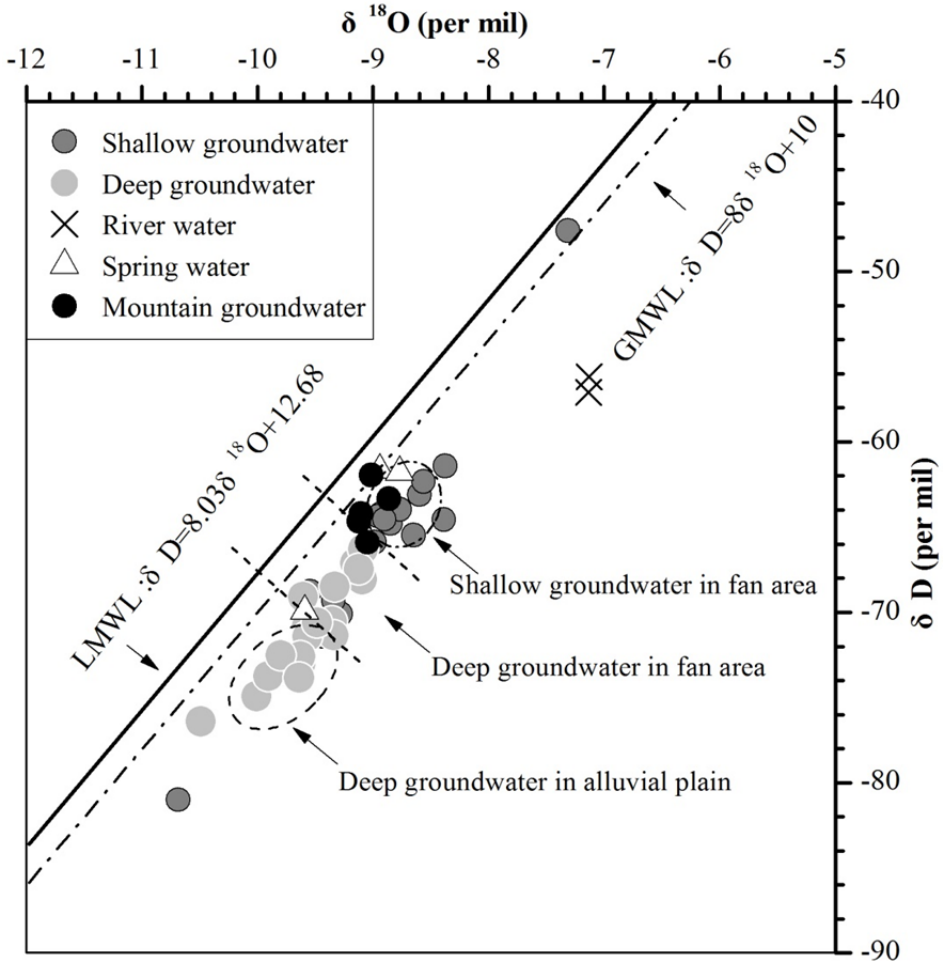

Figure 31: Isotopic composition of water samples in dry season.

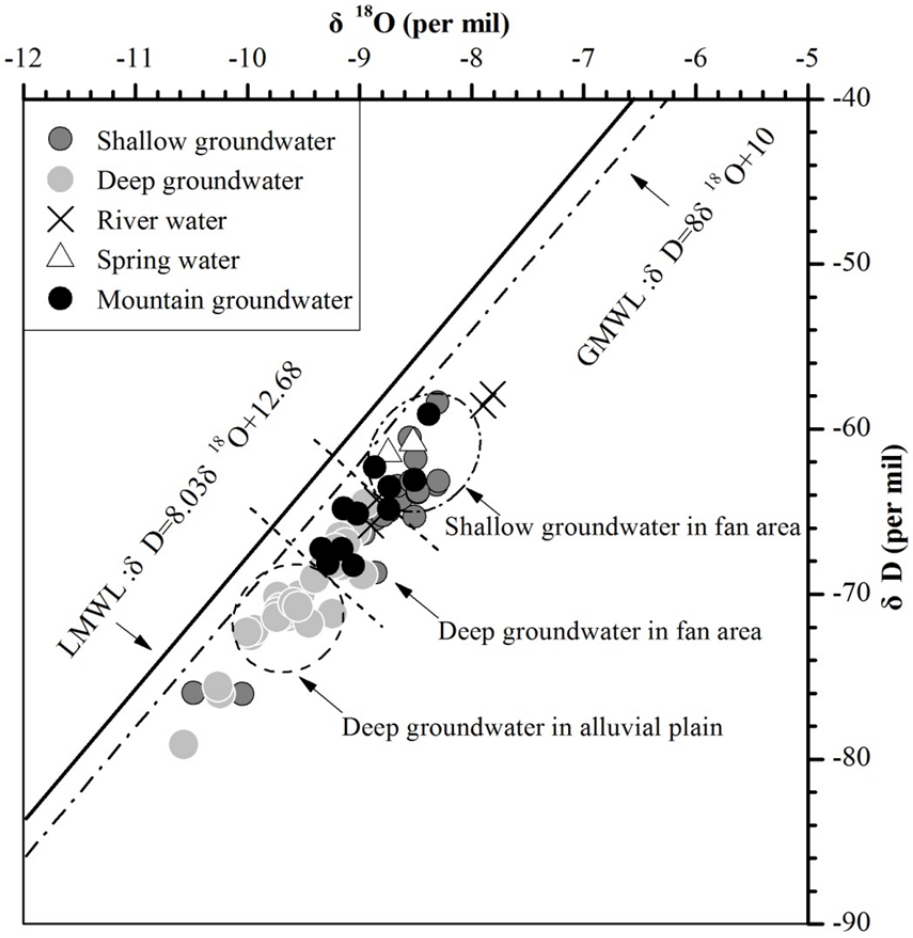

Figure 32: Isotopic composition of water samples in rainy season.

Chapter 4: Groundwater flow processes in fault-influenced aquifers of piedmont plain in Jiaozuo area

I. Introduction

As mentioned in mountain-block recharge, recharge of aquifers that situate in tectonic area is significantly influenced by the regional groundwater flow paths. Because tectonic structure, particularly fault, exerts an important role in groundwater flow process and makes the aquifer recharge complex. For instance, structure permeability and related architecture may form potential controls on water flow.

Relations between tectonic structure and groundwater recharge have been recently documented. In some cases, faults can form a preferential path between different aquifers and make opportunities for transmitting water. However some basin-bounding faults may act as a flow barrier to block mountain subsurface water recharging the basin aquifer. In Jiaozuo area, a reginal normal fault is located along the mountain edge, buried by quaternary deposits in piedmont plain. Therefore, it is necessary to illuminate whether the fault acts as a conduit or a barrier, when the recharge of aquifers of piedmont plain is focused on.

II. The role of normal fault in the recharge process of piedmont plain

Zhucun fault is buried beneath the Quaternary aquifer in northern edge of piedmont plain and penetrates the basement. Quaternary aquifer in piedmont plain in North Henan Plan mainly incorporates local precipitation, lateral flow of fracture water in bedrock and karst water (Gao. 2008). However, Drop height of hanging wall and footwall of the Zhucun fault varies from 700 to 1000 m, which results in the Ordovician karst aquifer of the footwall joined to the Carboniferous- Permian aquitard and Cenozoic stratum of the hanging wall, and such tectonic structure suggests the Zhucun fault act as a barrier hindering karst water flow to the basin and meanwhile may form a conduit for the water moving along the normal fault. Additionally, Quaternary aquifer only reaches a total thickness of less than 100m in foothill region, while the Ordovician karst aquifer is buried beneath the Carboniferous- Permian stratum with the thickness ranges from 350 to 400m, indicating a very limited vertical

hydraulic conductivity between the karst aquifer and the overlying Quaternary sedimentary layers. Meanwhile, considering the occurrence of bedrock outcrop and few wells drilled in mountain boundary, it is possible to conclude that aquifer in mountain boundary is not widely distributed, indicating no effective geological connectivity between mountain aquifer and Quaternary aquifer in piedmont plain.

Hydrochemical facies allow distinct groundwater sources to be differentiated in mountain and plain aquifers. The mountain water samples are variable in their major ion compositions, though spring water (exception of SW1) are generally Ca+Mg rich with sulfate the dominant anion type (Figure 33), meanwhile the similar facies are also encountered in mountain wells (e.g., MG2, MG5), provided they are in the vicinity of fault zones, suggesting an efficient flow path through tectonic structures. However, groundwater in alluvial- proluvial fan has a different water type, which defines a Ca·Mg-HCO_3·SO_4 facies (Figure 34 and Figure 35). It is suggested that groundwater in fan area could possibly be formed by the different hydrochemical processes.

To summarize, this hydrochemical information, together with tectonic structure characteristics, indicate that there is no lateral or vertical upward recharge from the mountain region provides water to the sedimentary aquifer in the basin, which is inferred that Zhucun normal fault forms the southern boundary of water movement in mountain region.

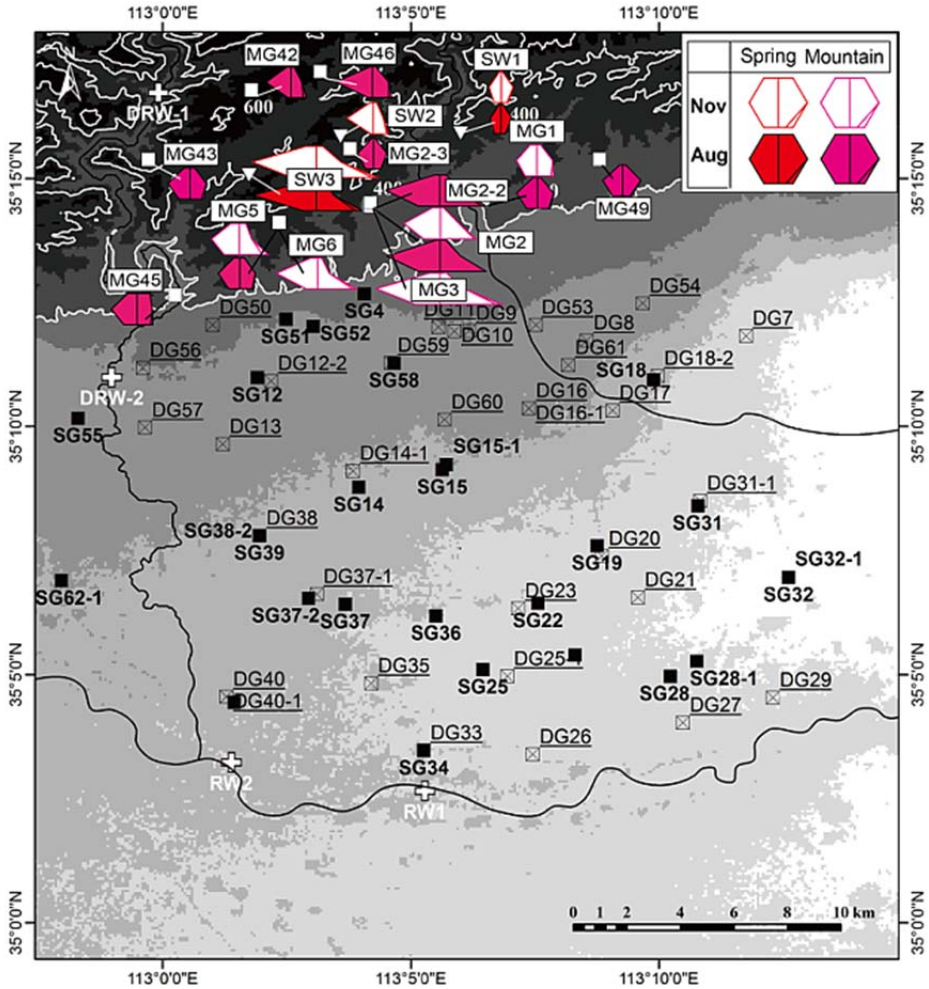

Figure 33: Hexa diagram of water samples in mountain region.

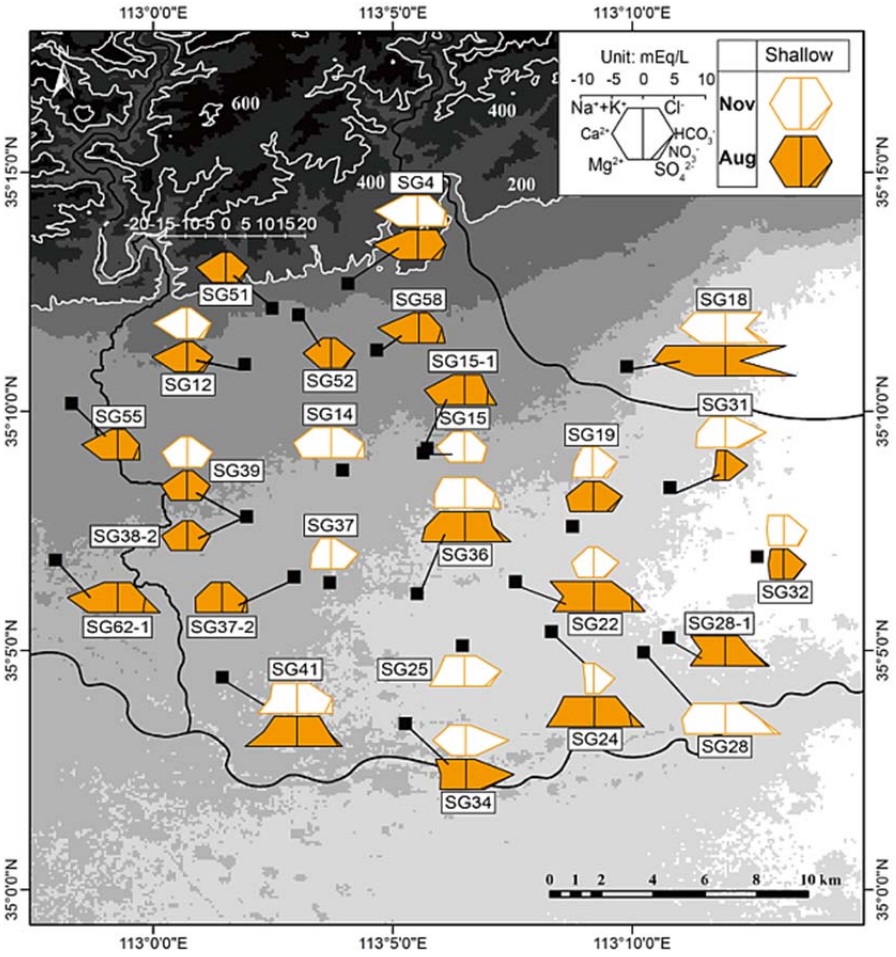

Figure 34: Hexa diagram of shallow water samples in piedmont plain.

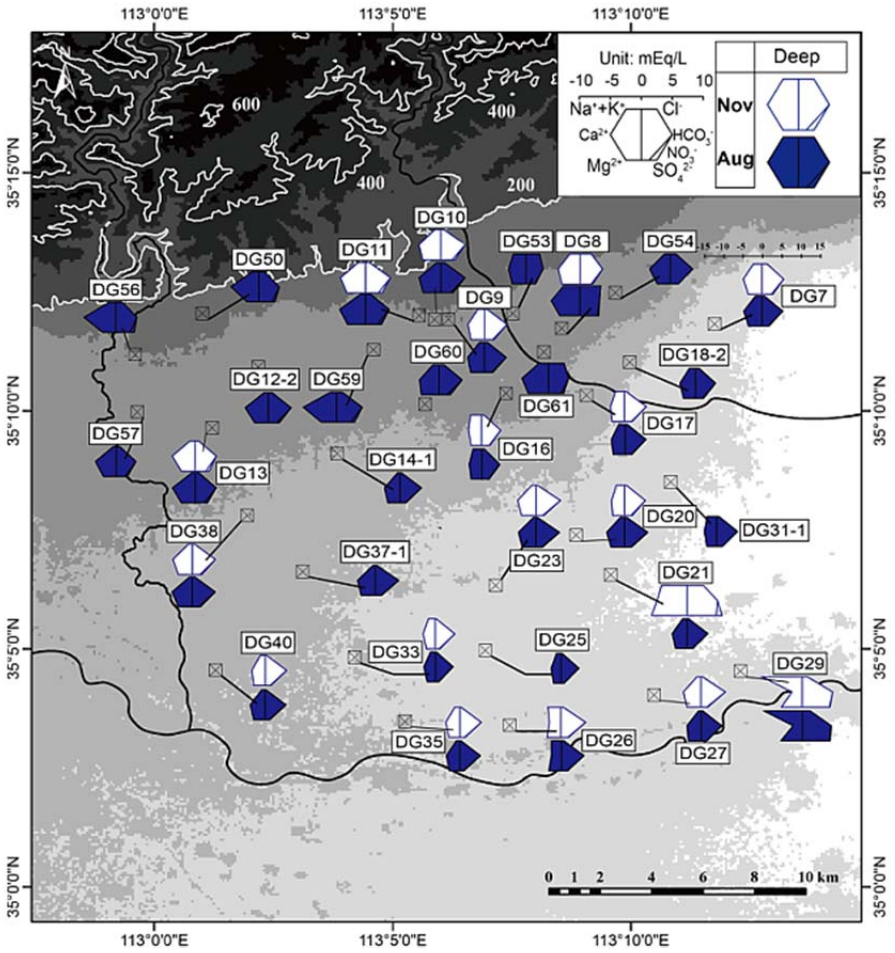

Figure 35: Hexa diagram of deep water samples in piedmont plain.

III. Hydrochemical evolution in deep groundwater system in piedmont plain

The evolution of hydrochemical composition of groundwater during regional flows can be generalized by considering the water types typically found in different groundwater flow systems (Ingebritsen et al., 2006). The variability of EC value of deep groundwater reveals the possible mixture behavior in deep aquifer of alluvial-proluvial fan area in Jiaozuo area. (Aji et al., 2006; Yuan et al., 2011) reported that EC value of groundwater in river basin increased along the regional groundwater flow direction. However, the trend is not observed along the deep groundwater flow path in Jiaozuo area. High EC values appear in the deep aquifer of northern alluvial- proluvial fan area and low EC values occur in the southern alluvial plain (Figure 36), except the amount of dissolved ions in deep water of DG21 and DG29 is spatially variable which may suggest the preferential path way between aquifers at different depths. Additionally, the mean EC value of deep groundwater in alluvial- proluvial fan area is similar to the overlying phreatic aquifer, suggesting the influence of the possible phreatic aquifer recharge in foothills region.

Stiff diagram corresponding to the surveys identify the deep groundwater in each geological environment in piedmont plain with a different hydrochemical facies along its reginal flow path. Comparing with deep groundwater in alluvial- proluvial fan and alluvial plain area (Figure 37), the deep water in fan area is of an HCO_3-SO_4 type, in which HCO_3 accounts for 34.2-77.7% and SO_4 17.9-33.6% of the total anions with the mean nitrate concentration around 41.3 mg/L, while deep water in alluvial plain appears to be dominated by HCO_3 and has the much lower nitrate values (<10 mg/L), which is close to the background value of nitrate in North Henan plain. Considering agriculture activities in the piedmont plain, it is inferred the excessive NO_3^- could be introduced by the utilization of manure which results in the existence nitrate contamination. In addition, positive ORP values and moderate pH values of deep groundwater in piedmont plain suggest almost no reduction of nitrate (Environmental, Y. S. I., 2008), so it is suggested that deep groundwater in piedmont plain is expected to be characterized by the confined groundwater in North Henan Plain, meanwhile a possible mixture with shallow groundwater of high nitrate concentrations (average

106.2 mg/L) controls the hydrochemical features of deep groundwater in alluvial-proluvial fan area, and results in the order of hydrochemical evolution.

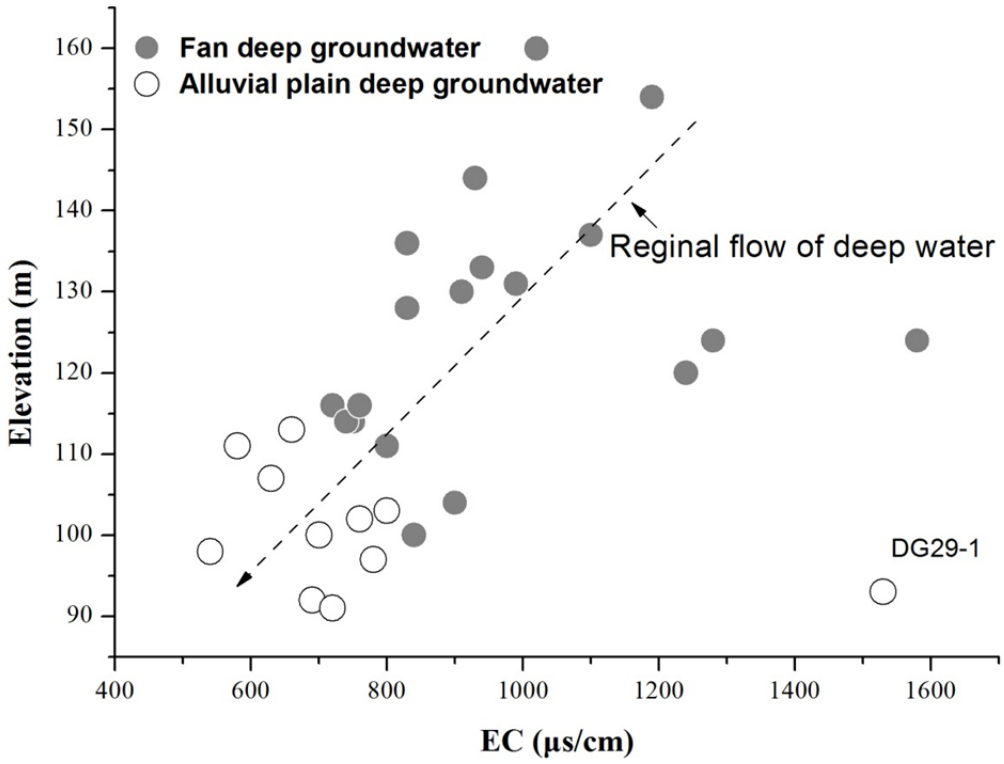

Figure 36: EC values of deep water samples in fan area and alluvial plain. The dash line shows a regional flow of deep groundwater.

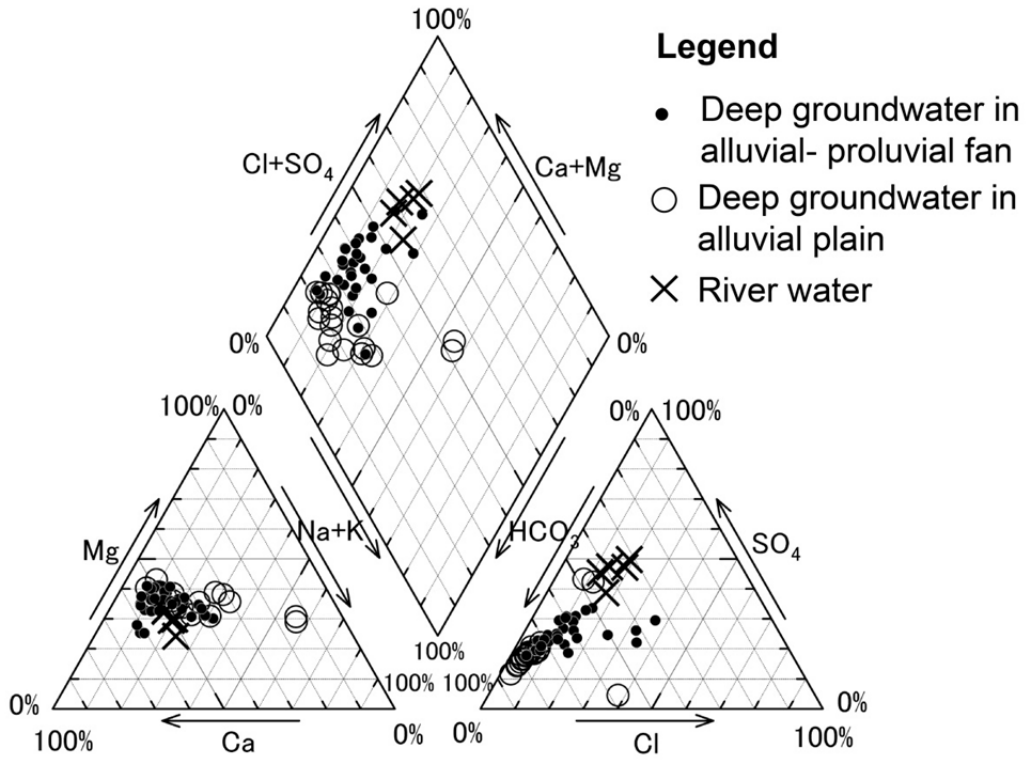

Figure 37: Piper diagram for the major ions of deep groundwater in different landscapes.

IV. Groundwater recharge processes of the piedmont plain aquifers

Piedmont plain is usually considered as the recharge zone receiving infiltrating precipitation (Li et al., 2008; Lu et al., 2008). However, due to the intensive groundwater exploitation in phreatic aquifer, water table declines greatly within the piedmont plain. In this study, the average depth to the shallow water table increased from 9.8m in dry season to 11.9m in rainy season (Figure 25), even in the alluvial-proluvial fan with aquifer lithology is primarily gravel and sand which is available for receiving the rainfall infiltration, water table depth has reached to more than 12.0m below land surface in rainy season, suggesting the direct infiltration of rainfall could not form the rapid recharge in the short term owing to the large depth to the water table and it may be difficult for the phreatic aquifer to receive direct precipitation recharge in piedmont plain under the impact of water table decline (Yuan et al., 2011). Considering the local average annual precipitation and evaporation during the studied period (447mm and 944mm respectively), it is suggested that local rainfall infiltration is not dominated for the phreatic water recharge and most of the rainwater underground is discharged by evapotranspiration before it reaches the water table in piedmont plain. In addition, wheat- maize double cropping system is largely supported through pumping shallow groundwater in Jiaozuo area, and the irrigation water is supposed to be the primary recharge of phreatic aquifer.

The average depth to the deep water table in alluvial- proluvial fan remains steady at nearly 10m during dry and rainy season, except of DG9, DG 10 and DG11 which lie in the deep water depression cone with a significant drawdown of water level, meanwhile water table fluctuations in DG8, DG9 are notable due to the variation of extraction intensity in different seasons. However, deep groundwater in alluvial plain exhibits a significant reduction of water level, with the average depth to the water table raised from 8.3m to 11.5m in rainy season. Considering the deep water in total piedmont plain is over- pumped, it is supposed that shallow groundwater percolates to deep aquifer in alluvial- proluvial fan, resulting in the smooth connection between phreatic and deep water in fan area.

As shown in Figure 31 and Figure 32, the isotopic data on all water samples

distribute along the local meteoric water line (LMWL), indicating their meteoric origin. The isotopic composition of most deep groundwater (exception to sampling site DG21 in dry season) in alluvial plain exhibits a narrow range, falling between -9.91‰ and -9.48‰ for $\delta^{18}O$ and between -73.8‰ and -69.1‰ for δD in dry season, between -10.26‰ and -9.55‰ for $\delta^{18}O$ and between -72.3‰ and -69.0‰ for δD in rainy season. It is confirmed these deep groundwater is expected to be characterized by the same general recharge source due to the similar isotopic composition (Figure 38 and Figure 39), as well the deep water in fan area due to the continuous confined aquifer. In addition, the extremely depleted isotopic composition suggests a residence time of 7000- 15000 years for the deep groundwater in alluvial plain, which is confirmed by the interpretation of groundwater radiocarbon data in North Henan Plain (Gao. 2008), implying the deep groundwater within Jiaozuo area was formed in a relative cold and wetter climatic phase during the late Pleistocene and Holocene (Gao. 2008). On the other hand, shallow groundwater in piedmont plain is enriched to values between -10.68‰ and -7.31‰ $\delta^{18}O$ and varies widely during both dry and rainy seasons (Figure 38 and Figure 39), and this isotopic divergence can be attributed to the incorporation of different recharge source, including the local precipitation after experiencing evaporation, local irrigation water and other water inhered with depleted δ values. However the shallow groundwater in alluvial- proluvial fan exhibits a relative narrow range, with the mean values of $\delta^{18}O$ were -8.73‰ in dry season and -8.64‰ in rainy season, which is close to the mean value of unconfined groundwater in North Henan Plain, with a residence time of 30- 44 years (Gao. 2008).

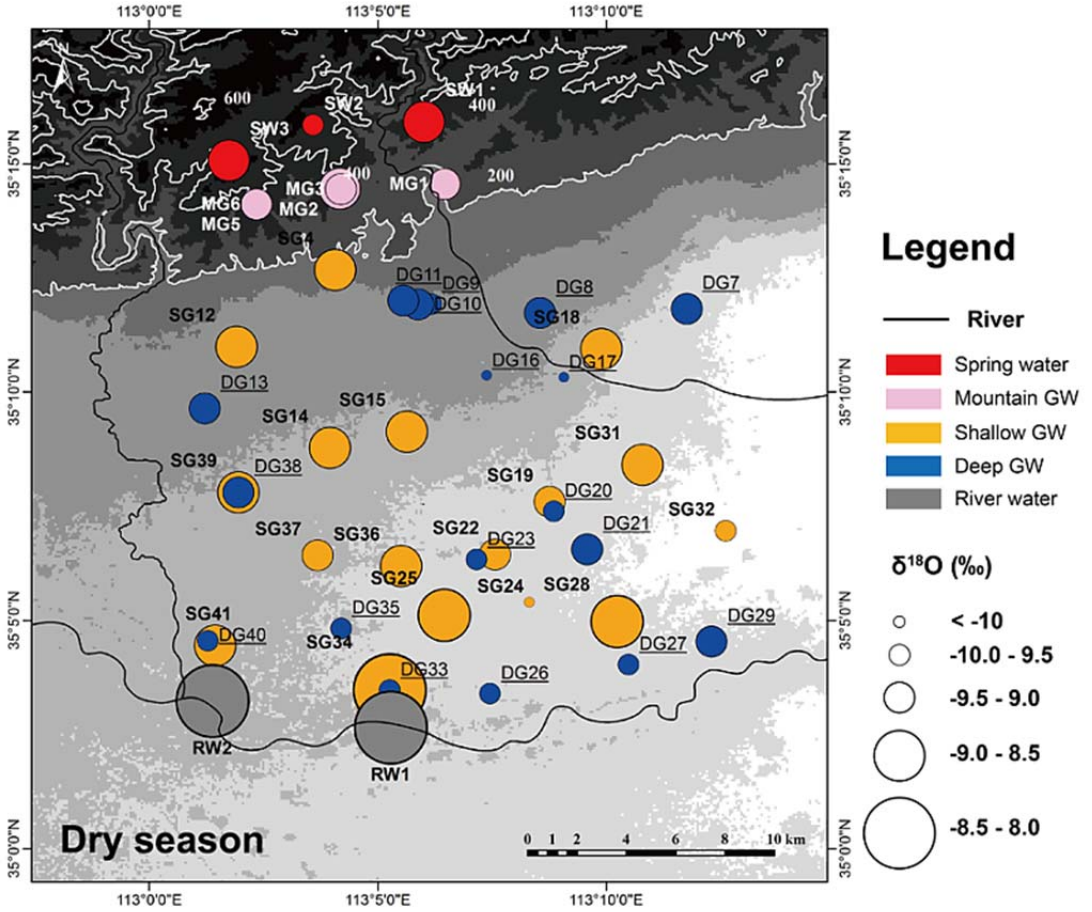

Figure 38: Spatial distribution of $\delta^{18}O$ value in different landscapes during dry season.

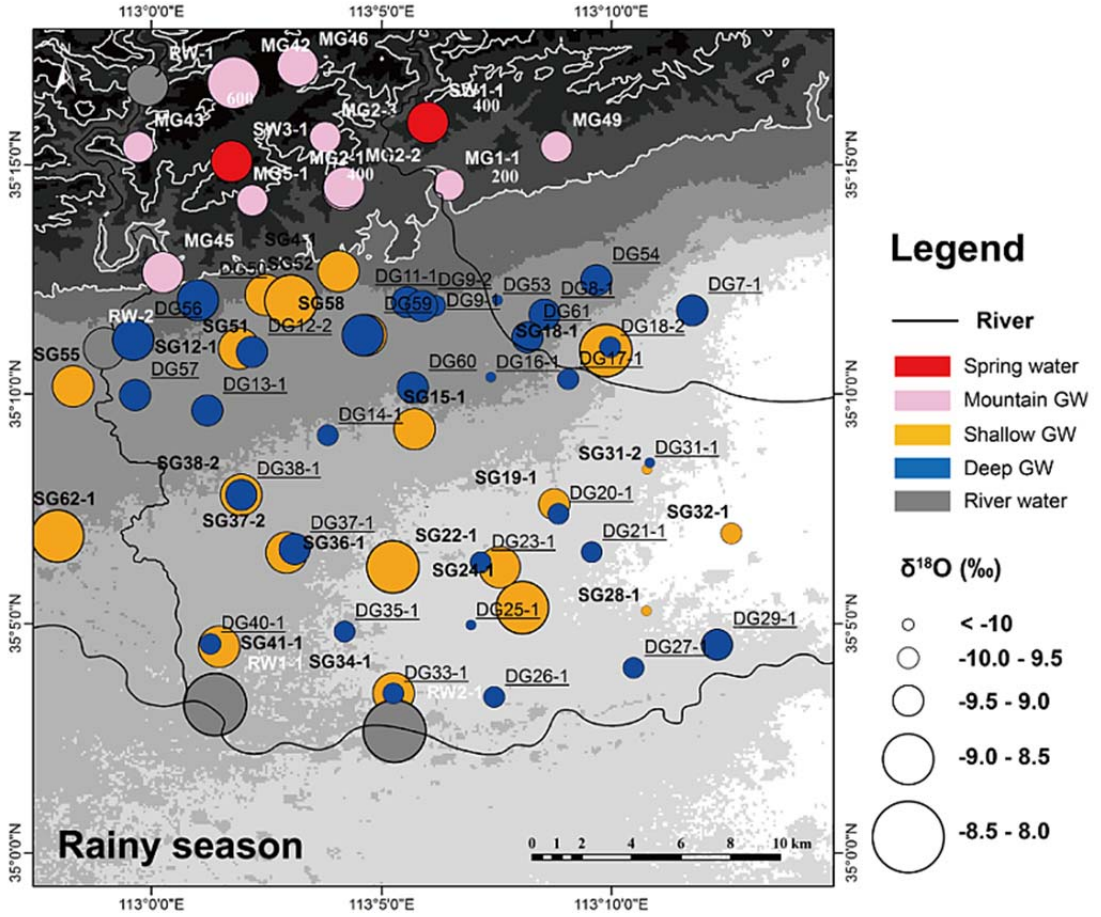

Figure 39: Spatial distribution of $\delta^{18}O$ value in different landscapes during rainy season.

Chapter 5: Groundwater mixing processes and a conceptual model of groundwater flow path in piedmont plain

I. Hydrogeochemical facies along the groundwater flow direction from alluvial-proluvial fan to alluvial plain

The hydrogeochemical facies reflected the response of chemical processes occurring within the lithologic framework and also the pattern of groundwater flow (Back. 1960). The Stiff plotting technique (Stiff. 1951) was applied to describe the chemical evolution of water along the groundwater flow path.

Combined with the aquifer lithology (aquifer floor depth and composition) and hydrological data (hydraulic head and water table), the Stiff diagram of samples are shown in Figure 40 and Figure 41 along the groundwater flow direction 1-1' and 2-2' from the alluvial-proluvial fan area to the Qinhe River alluvial plain during dry and rainy season. The variations of $\delta^{18}O$ are also indicated in the figures.

Along the section 1–1' (Danhe River alluvial fan) (Figure 40), sulfate concentration in deep groundwater decreased significantly from the proximal-fan to the alluvial plain with remarkable isotopic variation. Deep groundwater evolved from Ca-SO_4-HCO_3 type in alluvial fan area, to Ca-HCO_3 type in the alluvial plain area. Considering the contour line of hydraulic head in the cross-section reveals the potential to transmit phreatic water to the deeper aquifer and shallow water type of Ca-SO_4-HCO_3, shallow water intrusion occurred and led to the variation of water types. This process can also be evidenced by the deep water isotopic depletion and content of nitrate diluted from proximal-fan to alluvial plain. However, deep water sample DG12-2 represents much depleted $\delta^{18}O$ value in proximal-fan area where is more likely to be influenced by shallow water infiltration, which implies the possible distribution of aquitard overlying this deep water.

Along the section 2–2' (Xishihe River proluvial fan) (Figure 41), there is a notable depression cone in proximal-fan and mid-fan region which is indicated by the sharp decline of deep groundwater table. However, the deep water withdrawal does not significantly influence the $\delta^{18}O$ value distribution in proximal-fan area of proluvial

fan, and $\delta^{18}O$ value of most deep water samples are even more depleted than alluvial plain. In addition, water sampling location DG9 reveals the extremely depleted $\delta^{18}O$ value, which is similar as the isotopic composition of deep confined water in alluvial plain. Considering proluvial fan aquifer is usually formed by the gravel and gravel sand, which tends to be convenient for the infiltration occur. It is supposed that the leakage of shallow water to deep aquifer is widely influenced by the impermeable clay layer overlying the deep aquifer of proluvial fan. The chemical evolution of deep water in proluvial fan is consistent with the alluvial fan, suggesting the similar shallow water intrusion behavior.

The deep aquifer in alluvial plain, which is illustrated in southern part of the two cross-sections, appears markedly lower in sulfate than other groundwater in the alluvial-proluvial fan, and its water chemistry is Ca-HCO_3 type rather than mixing type as in the fan area. The $\delta^{18}O$ composition and water chemistry suggest that the deep water in alluvial plain has not been influenced by the shallow water intrusion in fan area and still remains the hydrochemical signature of deep confined groundwater in North Henan Plain.

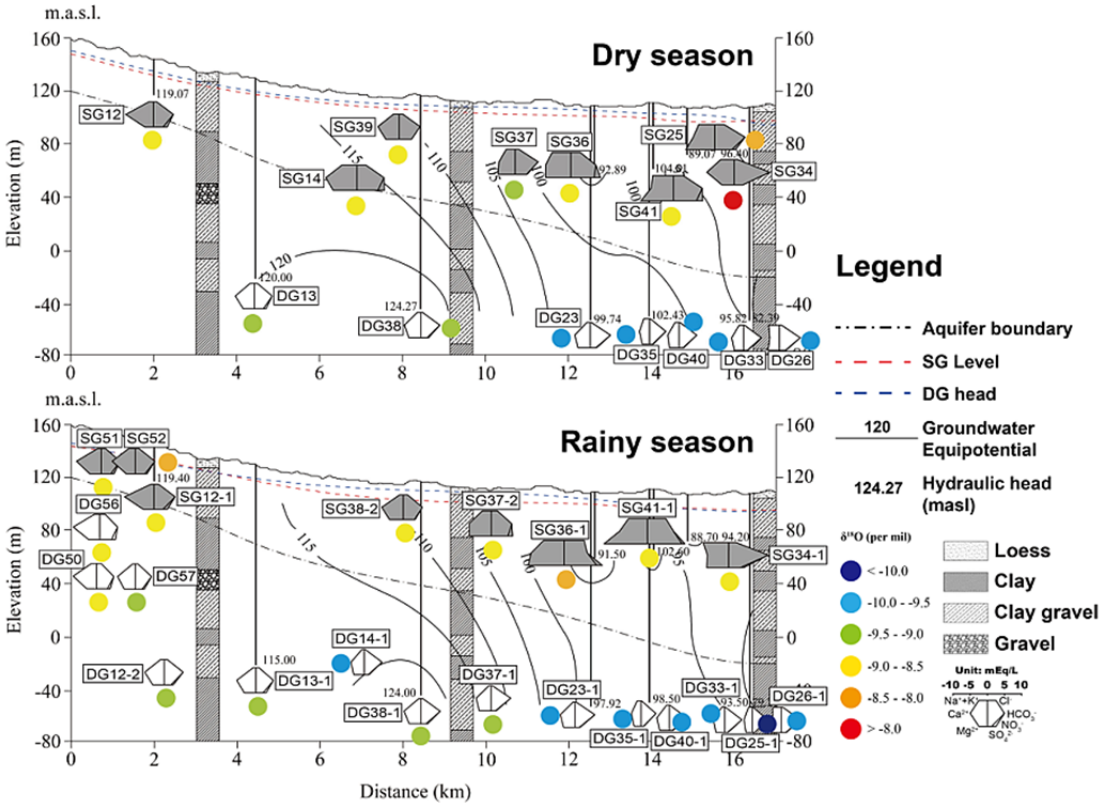

Figure 40: Distribution of Stiff diagram and $\delta^{18}O$ value of water samples along the cross-section 1-1' (Danhe River alluvial fan).

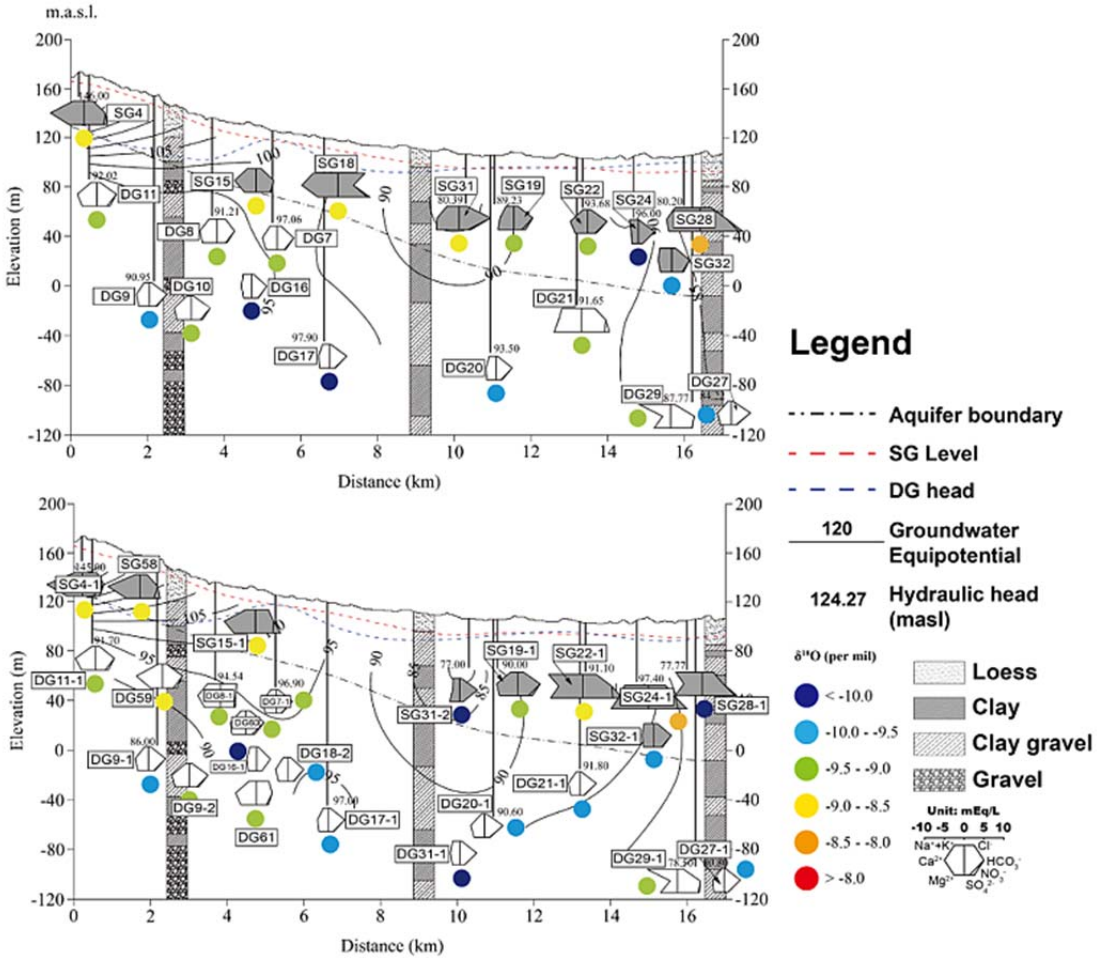

Figure 41: Distribution of Stiff diagram and $\delta^{18}O$ value of water samples along the cross-section 2-2' (Xishihe River proluvial fan).

II. Contribution of alluvial-proluvial fan shallow groundwater to the deep aquifer

As mentioned, deep groundwater in both fan area and alluvial plain should be recharged during the same period and therefore with the similar isotopic composition. However, deep groundwater in alluvial- proluvial fan area reveals the different isotopic composition with the mean value of $\delta^{18}O$ is -9.28‰ in dry season and -9.27‰ in rainy season, which is significantly heavier than that of deep water in alluvial plain. Considering no recharge from mountain region provides water to the sedimentary aquifer, it is supposed that shallow groundwater in fan area contributes a relatively enriched $\delta^{18}O$ value to the deep water in alluvial- proluvial fan, supporting the assertion that deep groundwater incorporates shallow groundwater infiltration in fan area revealed by water table variations and hydrochemical evolution.

Considering the hydraulic head data indicates the flow direction and potential to transmit water to the receiving water body (T Praamsma et al., 2009), deep water in fan area incorporates overlying shallow groundwater can also be evidenced by the contour line of hydraulic head indicated in Figure 40 and Figure 41, in which the hydraulic head value is calculated by the water table and well screen depth during dry and rainy season. Additionally, the possible mixing process in alluvial and proluvial fan area can also be clearly identified by the vertical distribution of nitrate. As mentioned, nitrate acts as a valuable tracer that defines the possible mixing process in deep aquifer within the fan area due to the diluted concentration. Figure 42 show that shallow and deep water systems has the high nitrate concentration in fan area related to agriculture pollution within the basin, while Figure 43 indicates that the mean content of NO_3^- in deep groundwater in alluvial- proluvial fan is diluted to less than half of that in the overlying phreatic aquifer following the downward flow potential indicated by the variation of hydraulic head, and remains the background value in the alluvial plain. Consequently, it can be confirmed that the mixing process occurs in deep aquifer in alluvial and proluvial fan area.

In Figure 44, the isotopic composition of groundwater in alluvial and proluvial fan during dry and rainy season arrange in a line, which shows a two end member mixing

trend. One end- member should be vertical inflow from shallow aquifer in fan area, which contributes a relatively enriched δ value to the subjacent deep water. The other end- member is characterized by depleted δ values of stable isotopes in piedmont plain, which meets the requirement of a much depleted δ value source. Additionally, the δ value of deep groundwater in fan area distributes along the mixing line between the mean values of overlying shallow groundwater and deep groundwater in piedmont plain, which can be taken as a mixing end- member.

Previous studies have shown that oxygen stable isotope composition of water have the potential for use in tracing groundwater sources (Nakaya et al., 2007), which makes $\delta^{18}O$ value the optimal tracer for the mixing model. Meanwhile the average isotopic compositions of the two end- members are employed to calculate the mixture ratio. The relative contribution to deep water in fan area (*f-DW*) between shallow water in fan area (*f-SG*) and deep water in piedmont plain (*p-DW*) can be derived from a conventional two end member mixing equation in terms of δ values (Clark and Fritz, 1997):

$$R_{f\text{-}SG}=(\delta^{18}O_{f\text{-}DW}-\delta^{18}O_{p\text{-}DW})/(\delta^{18}O_{f\text{-}SG}-\delta^{18}O_{p\text{-}DW}) \quad (1a)$$

and

$$R_{p\text{-}DW}=1-R_{f\text{-}SG} \quad (1b)$$

where $R_{f\text{-}SG}$ and $R_{p\text{-}DW}$ are the fractions of shallow water in fan area and deep water in piedmont plain, respectively.

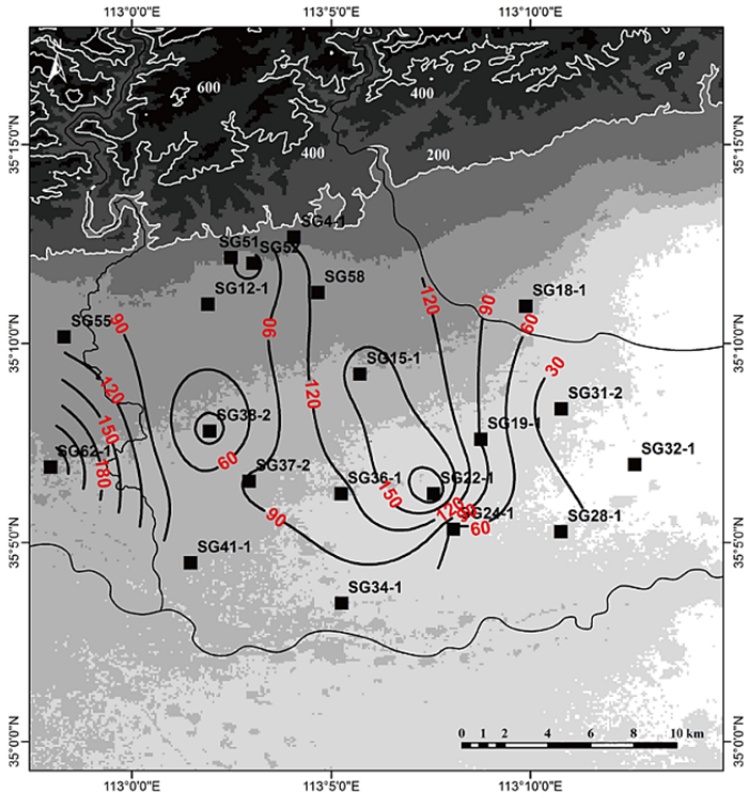

(a) Contour of nitrate concentration (in NO_3^-mg/L) in shallow groundwater

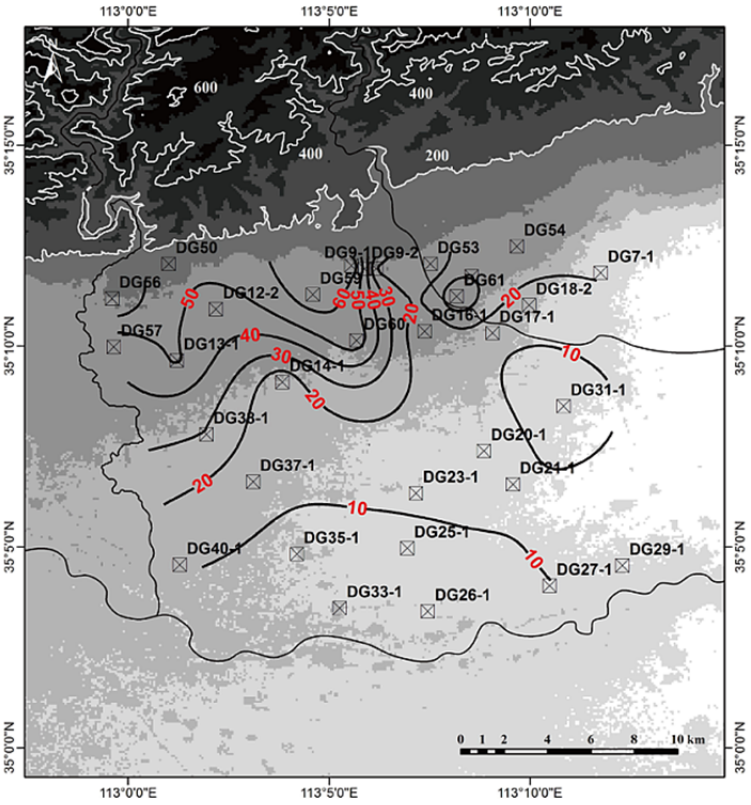

(b) Contour of nitrate concentration (in NO_3^-mg/L) in deep groundwater

Figure 42: Nitrate contamination in shallow and deep aquifers of different landscapes.

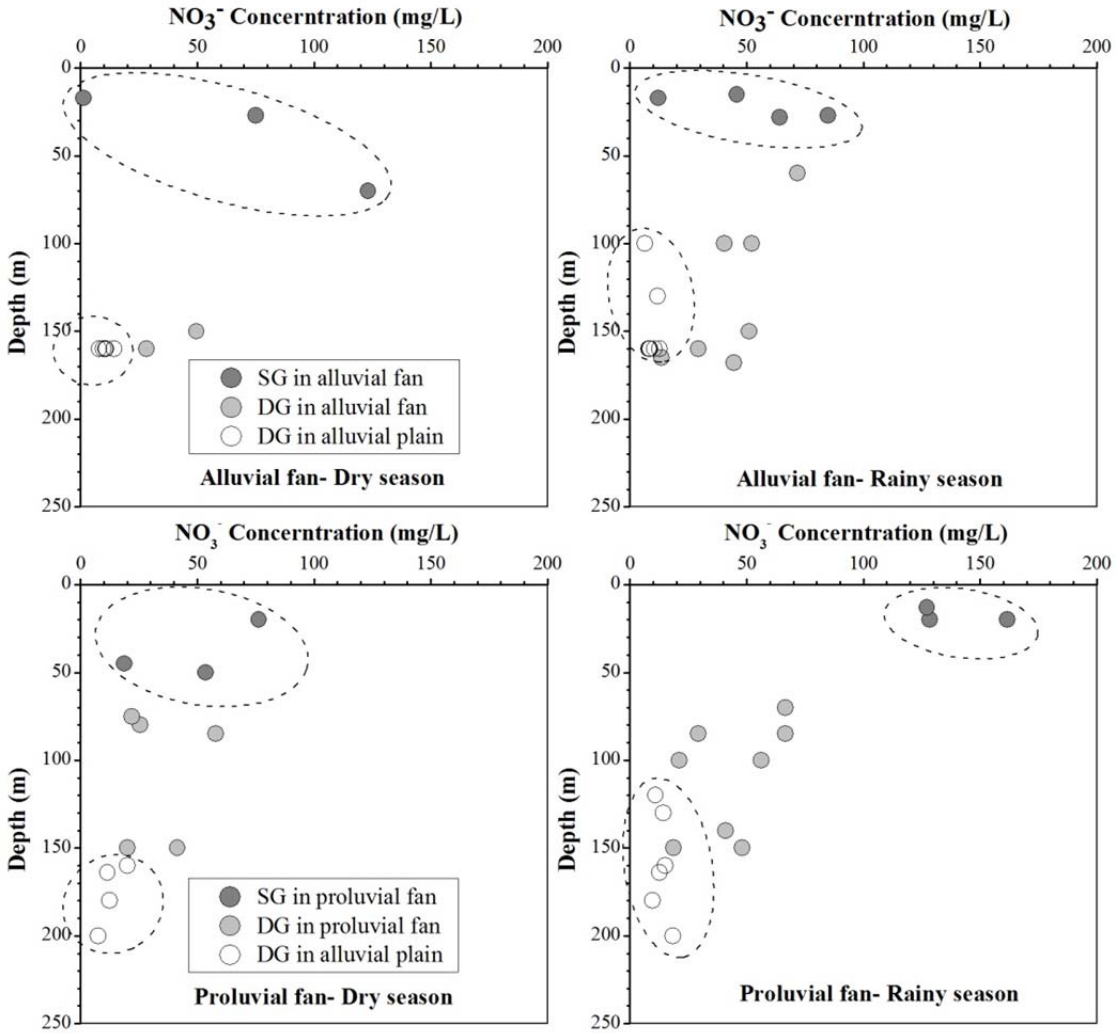

Figure 43: Vertical distribution of nitrate in alluvial- proluvial fan (SG = shallow groundwater, DG = deep groundwater).

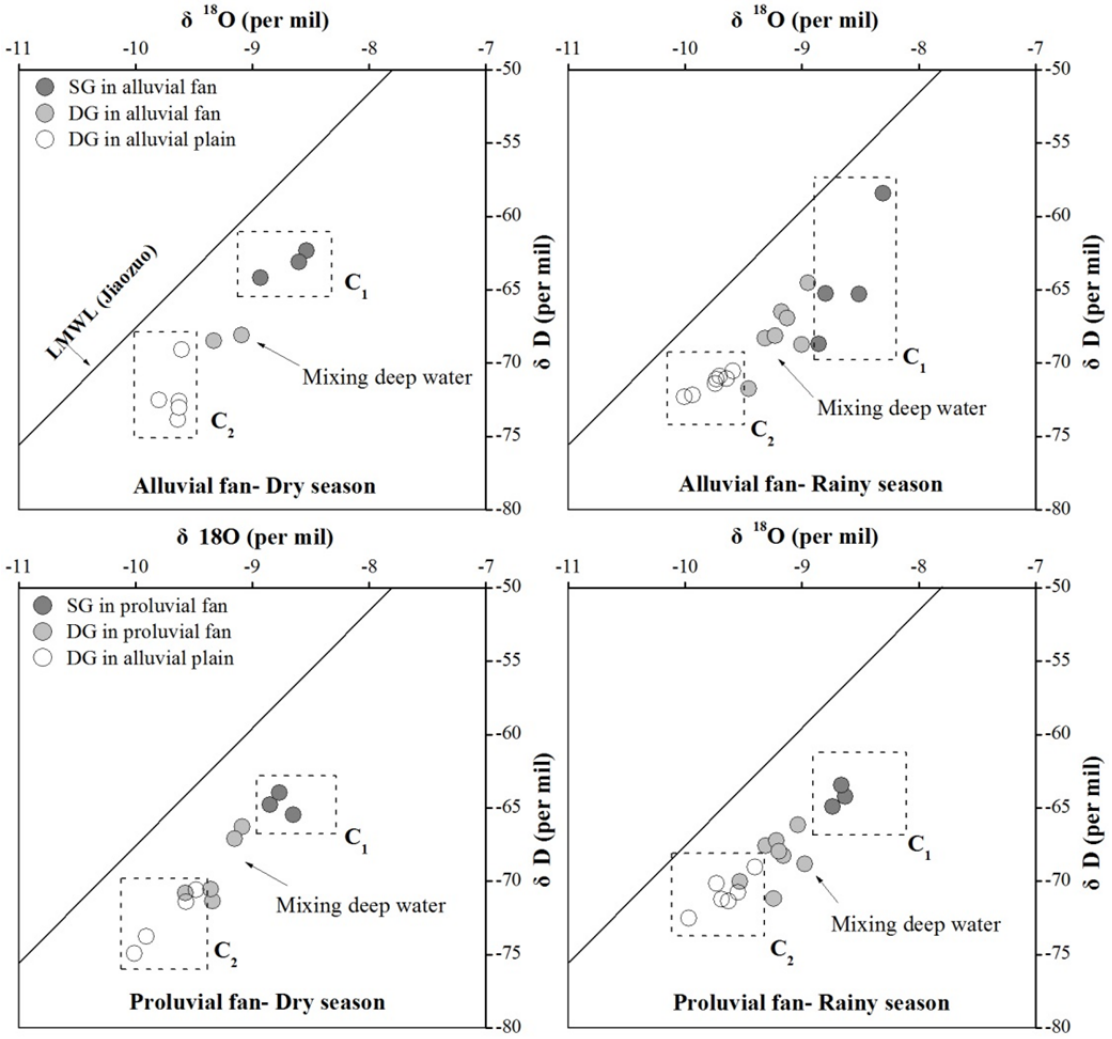

Figure 44: Isotopic composition of groundwater samples in different geomorphic units (SG = shallow groundwater, DG = deep groundwater).

III. Schema of groundwater mixing processes in alluvial-proluvial fan area

Integrated with a mixing model of groundwater with $\delta^{18}O$ value and the variations of hydraulic head during dry and rainy season, the water samples in Jiaozuo piedmont plain are respectively shown in Figure 45 and Figure 46 along the profile 1-1' in western Danhe River alluvial fan, and 2-2' in eastern Xishihe River proluvial fan, meanwhile constitute a schematic diagram of groundwater mixing processes. It is hoped that this schema will enhance the understanding of shallow groundwater intrusion in alluvial-proluvial fan area.

Along the profile 1-1' (Danhe River alluvial fan) (Figure 45), it is noted that infiltration of shallow groundwater is greatest in the foothills (DG50) and its contribution decreases with increasing distance from the fault. The hydraulic gradient is expected to produce groundwater flow from Danhe River alluvial fan to the alluvial plain and the shallow groundwater recharge system is as far as 10 km to the south. Thus, the distance can be considered an important factor controlling the mixing process. However the limited contribution of shallow water to proximal-fan (DG57) can be attributed to the possible impermeable layers that somewhere overly the deep aquifer in proximal fan. Additionally, the water table decline in alluvial plain in rainy season exhibits a hydraulic head variation and may result in the shallow water contribution in distal-fan (DG38-1) increased, however no discernable change occurred in the isotopic results of deep wells in alluvial plain during the period of water table drawdown, indicating no isotopic evidence of deep water in alluvial plain incorporates the mixing water.

Along the profile 2-2' (Xishihe River proluvial fan) (Figure 46), the result of mixing analysis shows a similar mixing trend as in Danhe River alluvial fan, which the mixture ratio declines with the increasing distance away from the fault. However the shallow water contribution is much reduced especially in mid- fan region (DG9-1) located in a depression cone. Considering the remarkable high hydraulic gradient in depression cone and the aquifer lithology of proluvial fan, the shallow water contribution in proluvial fan should not differ greatly among locations compared with alluvial fan, therefore reducing the shallow water contribution will indicate the

vertical connections between different aquifers are not consistent with the variation of hydraulic head in mid- fan region in Xishihe River proluvial fan. It is supposed that the downward groundwater flow to deeper aquifer is hindered by the possible aquitard widely distributed above the deep aquifer of proluvial fan. Meanwhile, mixing process in Xishihe River proluvial fan reaches about 6 km away from the fault, which exhibits a relative limited scale, indicating that the shallow groundwater to deep groundwater connections are more limited in proluvial fan area compared with alluvial fan. In addition, impact of hydraulic head decline of deep groundwater in alluvial plain on groundwater mixing process is negligible in the short term, indicating that the aquifer lithology is a more limiting factor in Xishihe River proluvial fan when compared to Danhe River alluvial fan, which may form a more complex groundwater flow pattern in proluvial fan area.

The possible groundwater flow pattern in alluvial/proluvial fan area can also be identified by the nitrate tracer. The profile of nitrate concentration along the Danhe River alluvial fan (Figure 47) clearly reveals the shallow water intrusion, in which shallow water system has the highest nitrate concentration related to the agriculture contamination within the alluvial fan area, and a relative high nitrate concentration is found in the deep aquifer of about 120 m depth below land surface, indicating a strong mixing effect of shallow groundwater and original/old groundwater in deep aquifer. Additionally, the shallow water intrusion behavior revealed by the profile of nitrate is in accordance with the recharge process estimated by EMMA (Figure 45). When the shallow water contribution decreases along the flow path, the nitrate content is also diluted following the downward flow. It can be assumed that the nitrate plume will reach to the deeper aquifer in southern alluvial plain with the continuous agriculture pollution.

Meanwhile, the profile of nitrate concentration along the Xishihe River proluvial fan (Figure 48) exhibits a relative limited intrusion scale, which is similar to the results of EMMA (Figure 46), indicating the possible impermeable layers in the mid-fan deep aquifer disturbs the groundwater flow path, and prevents the deep water in distal-fan area from being mixed by the lateral flow. Additionally, EMMA shows

deep water in proluvial fan has been mixed with shallow water except DG9-1 which is considered as a semi-confined deep groundwater. However profile of nitrate in proluvial fan reveals a much reduced nitrate content in proximal-/mid fan deep aquifer, indicating the downward flow of shallow water with high nitrate concentration is hinder by the aquitard, and shallow water flow with relative low nitrate content recharges the deep aquifer underneath. It is concluded that the groundwater flow pattern is greatly disturbed by the aquitard in proluvial fan area.

By mapping hydrochemical facies in different water systems and the isotopic divergence in deep aquifer of piedmont plain, the groundwater flow path in the alluvial-proluvial fan can be described using a schema of the flow pattern in Jiaozuo area (Figure 49).

In this schema diagram, the northern part of the study area is bounded by a buried impermeable fault that behaves as an aquiclude, which has been illuminated. This buried normal fault separates the piedmont plain aquifers from mountain aquifers/mountain blocks. The isotopic composition of piedmont plain deep water is relatively enriched in alluvial-proluvial fan area due to the leakage of shallow water with high $\delta^{18}O$ value, and the accumulation of nitrate contaminant in deeper aquifers is also implied in the shallow water intrusion. In addition, alluvial-proluvial fan is characterized by downward groundwater flow, which is revealed by the contour line of hydraulic head. Therefore, contribution of shallow groundwater is more notable in deep aquifer of proximal-fan area, and its contribution decreasing with distance from the normal fault. However, shallow water intrusion seems to be limited in deep aquifer somewhere located in proximal-fan region, which implies the influence of relatively impermeable confining layers, and such kind of limitation may also reduce the impact of deep groundwater table withdrawal on the regional groundwater flow path. Meanwhile it is important to recognize the possibility of contaminant transport with the intrusion of shallow groundwater into deeper aquifers of alluvial-proluvial fan area, where groundwater flow pattern is specific due to the complex aquitard distribution.

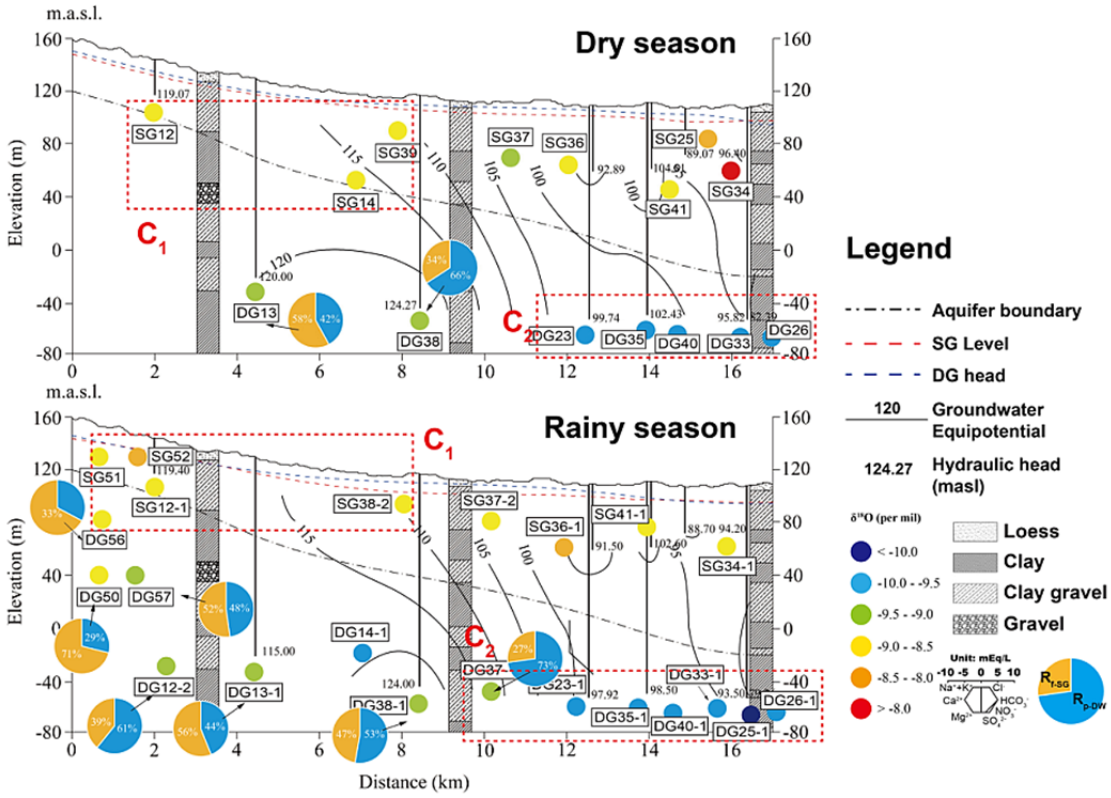

Figure 45: Results of end member mixing analysis in Danhe River alluvial fan ($R_{f\text{-}SG}$ and $R_{p\text{-}DW}$ is the mixture ratio of shallow groundwater and deep groundwater).

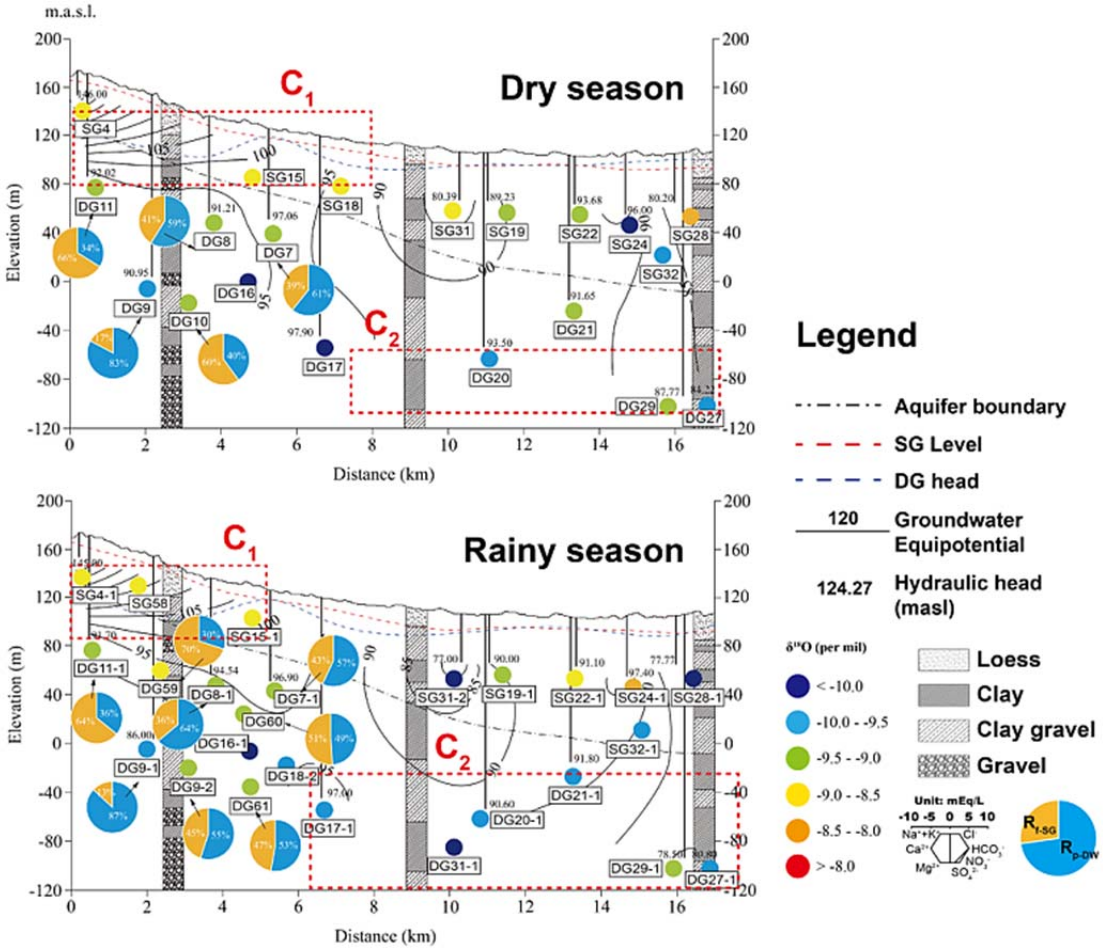

Figure 46: Results of end member mixing analysis in Xishihe River proluvial fan ($R_{f\text{-}SG}$ and $R_{p\text{-}DW}$ is the mixture ratio of shallow groundwater and deep groundwater).

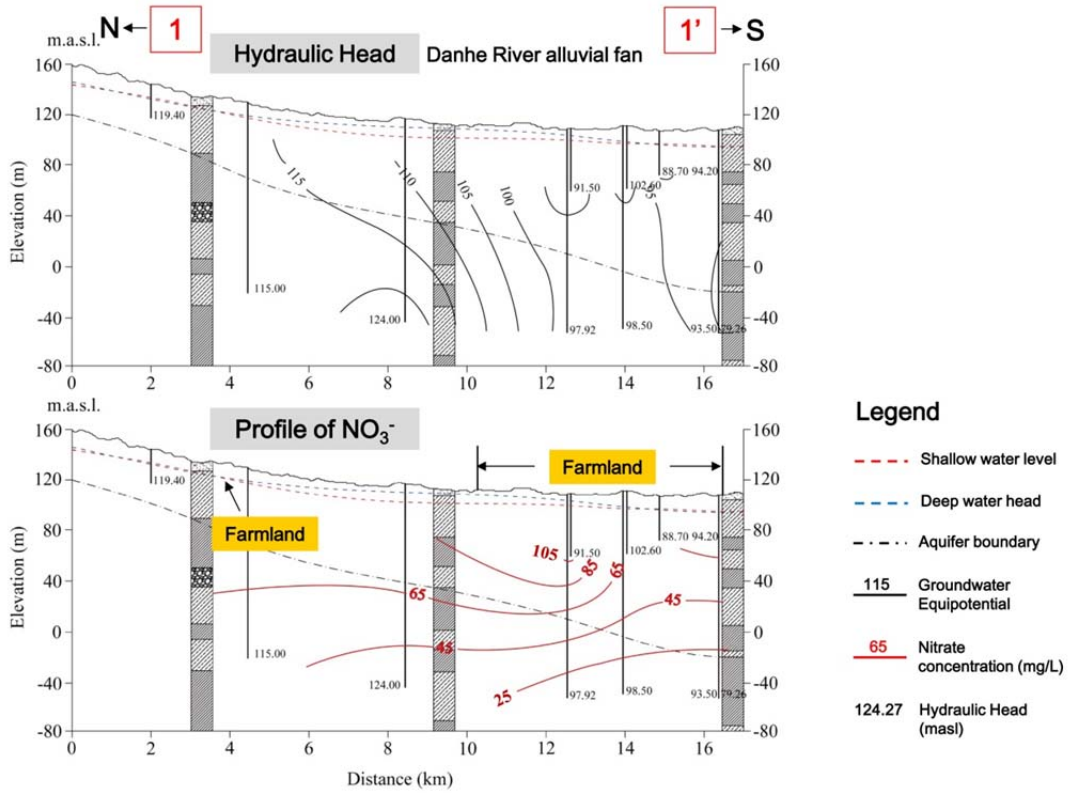

Figure 47: Profiles of nitrate concentration along the vertical cross section of 1-1' in Danhe River alluvial fan (Rainy season).

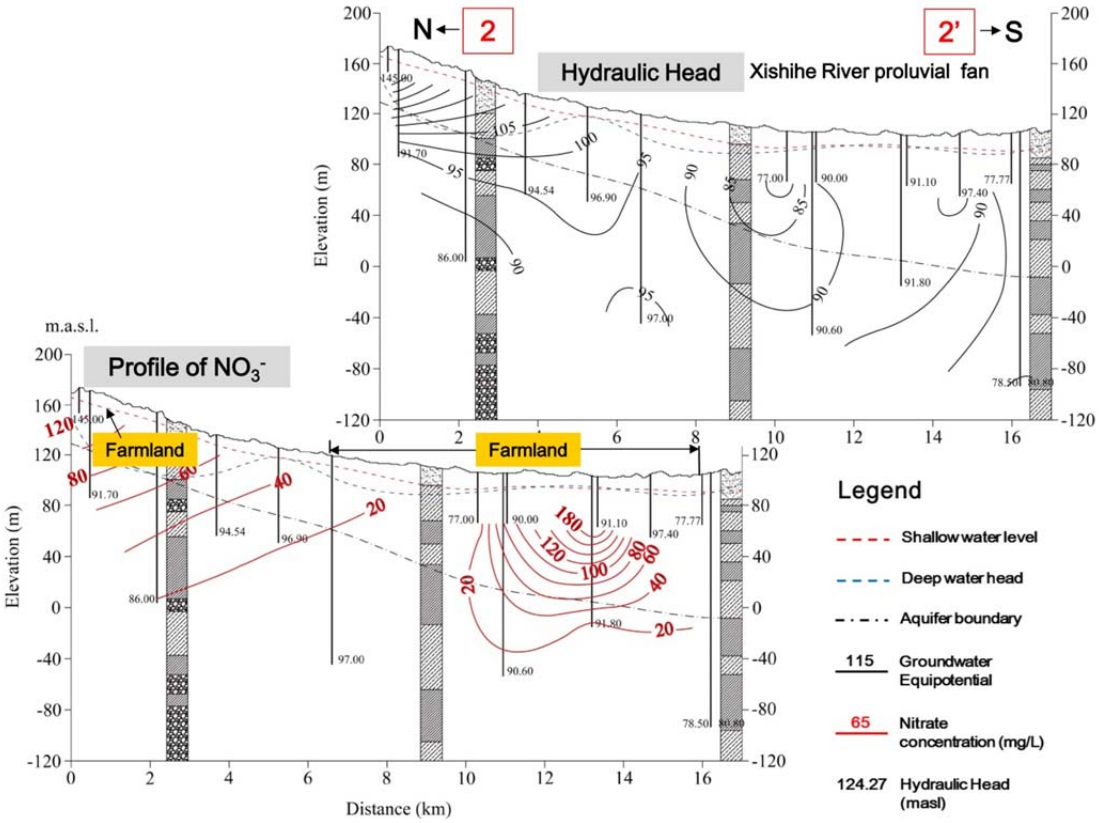

Figure 48: Profiles of nitrate concentration along the vertical cross section of 2-2' in Xishihe River proluvial fan (Rainy season).

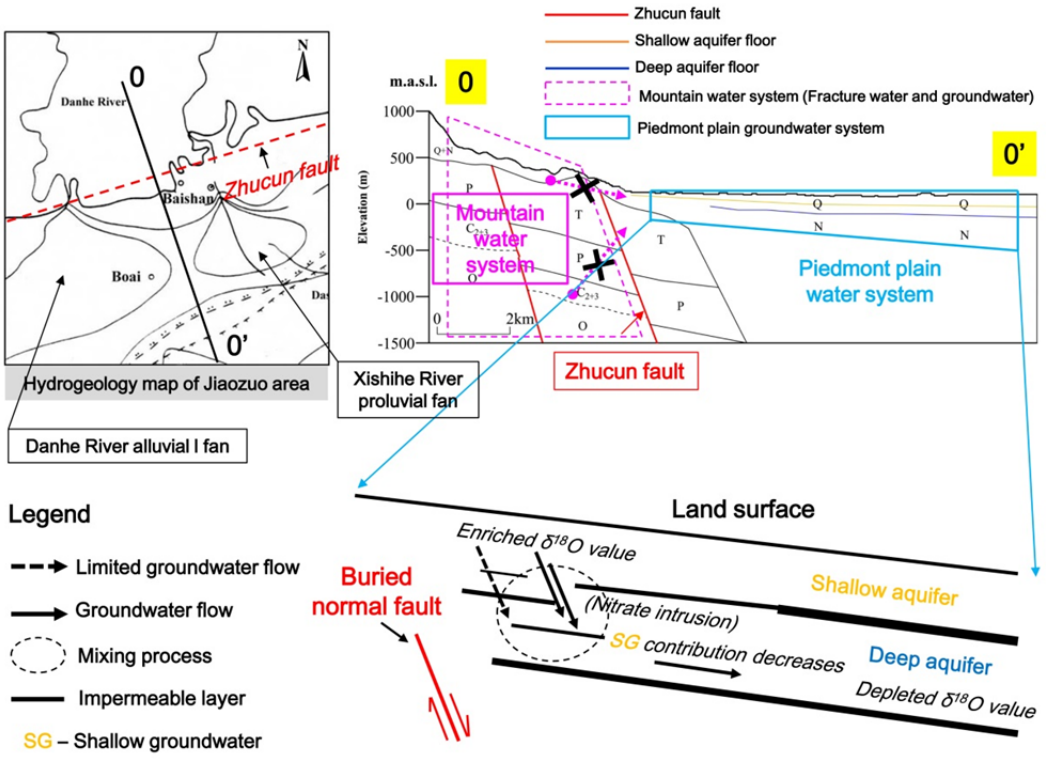

Figure 49: Schematic diagram of the current condition of groundwater flow.

IV. Recharge mechanism and a three-dimensional space conceptual model of groundwater flow processes in piedmont plain

Based on the current hydrochemical and isotopic data and supported by the earlier studies, a three-dimensional space conceptual model of groundwater recharge is proposed in the Jiaozuo piedmont plain, exception to the south region (Figure 50).

As mentioned, Zhucun fault behaves as a barrier, which separates the piedmont plain aquifers from mountain aquifers, indicating there is no lateral or vertical upward recharge from the mountain region provides water to the sedimentary aquifer in the piedmont plain. Therefore deep groundwater recharge of alluvial-proluvial fan is not influenced by the mountain-front recharge.

Runoff generated from Taihang Mountain used to be the source of surface water and shallow groundwater for the alluvial-proluvial fan area, in which Danhe River and Xishihe River ultimately reaches the Qinhe River and the Weihe River, respectively. In addition, Danhe River is also the important recharge source of karst water in mountain region. By the 1990s, surface and groundwater were abundant in the alluvial-proluvial fan area, and the shallow aquifer was recharged by direct infiltration from Danhe River and Xishihe River. Meanwhile, shallow groundwater table depth was approximately less than 2.0m below land surface. However in the last two decades, with the decrease in the surface water from the Danhe River and Xishihe River as a result of reservoirs constructed in its up reaches and less rainfall, downstream of Danhe River and Xishihe River dried up even during rainy season, respectively. It is implied that direct infiltration from river water does not remain the source of shallow groundwater. Due to the changes in surface water recharge and groundwater exploitation, the shallow and deep groundwater level in the piedmont plain has markedly dropped in the last decades. Recently, the regional decline of the groundwater level in the whole plain has continued to occur.

Piedmont plain area is usually considered as the recharge zone receiving infiltrating precipitation. However, it may be hard to receive direct recharge in Jiaozuo area under the impact of intensive human activities. This situation has been clarified by the spatial variance of depths to the water table during dry and rainy season. The water

table continuously declined from November 2013 to August 2014 in the piedmont plain, even in the front of the alluvial-proluvial fan after rainy season, the drawdown of water level still occurs. Considering local rainfall cannot meet the need of the crop and agricultural irrigation results in the drawdown of shallow water level, more shallow wells will be abandoned or drilled again to a deeper depth. Therefore, it is supposed that the local precipitation is not the dominant recharge source for phreatic aquifer and most of the infiltration is discharged by evapotranspiration before it reaches the water table in the Jiaozuo area. In addition, irrigation return flow is not influenced by the evaporation below land surface due to the relative consistent isotopic value and meanwhile is insufficient to support the current shallow groundwater levels.

The origin of shallow water in piedmont plain phreatic aquifer may be the modern rainfall in North Henan Plain. The isotopic compositions of the most shallow water samples from the Jiaozuo area tend to conform to the same pattern as the groundwater isotopic signature of North Henan Plain, which have been similarly enriched by evaporation. However, several shallow water samples are considered to be isotopically heavier than the other shallow water due to the rainfall infiltration with the impact of strong evaporation. In addition, a few shallow water samples extremely depleted in isotopic value suggests that deep groundwater extracted in some separate farmlands is used for irrigation and infiltrates to the phreatic aquifer.

Additionally, it is noted that the deep groundwater in alluvial plain extremely depleted in both $\delta^{18}O$ and $\delta^{2}H$, suggesting that the deep groundwater in the confined aquifer must be of a paleo-water origin. This conclusion has been confirmed by the groundwater radiocarbon data. In contrast, the isotope composition of the deep groundwater in the alluvial-proluvial fan area shows a different pattern than the isotope composition in alluvial plain. Considering the mixing of groundwater flow could lead to a controlling influence on water chemistry, the deep groundwater in alluvial-proluvial fan area (Ca-Mg-HCO_3-SO_4) is indicated as a mixture of shallow groundwater (Ca-Mg-HCO_3-SO_4) with deep confined groundwater (Ca-Mg-HCO_3) in the piedmont plain. Additionally, the shallow groundwater intrusion is consistent with

the variation of nitrate and sulfate concentration from fan area to the alluvial plain, with the content diluted along the groundwater flow path.

According to the determined isotopic and hydrochemical characteristics, deep groundwater in the area of alluvial-proluvial fan is connected to the shallow aquifer system, and direct recharge of deep water comes from the vertical leakage from the overlying phreatic aquifer, which represents a gradually decreased shallow water contribution with the increasing distance away from the fault. In addition, as groundwater flows from the proximal-fan to distal-fan regions, the contribution of shallow water to deep groundwater in some sampling locations of the proximal-fan and mid-fan regions seems to be much limited. The limitation can be attributed to relatively impermeable layers somewhere overlying the deep aquifer. Furthermore, groundwater flow path in proluvial fan is more influenced by the aquitard distribution than alluvial fan, which forms a relatively much limited mixture scale and a specific groundwater flow pattern.

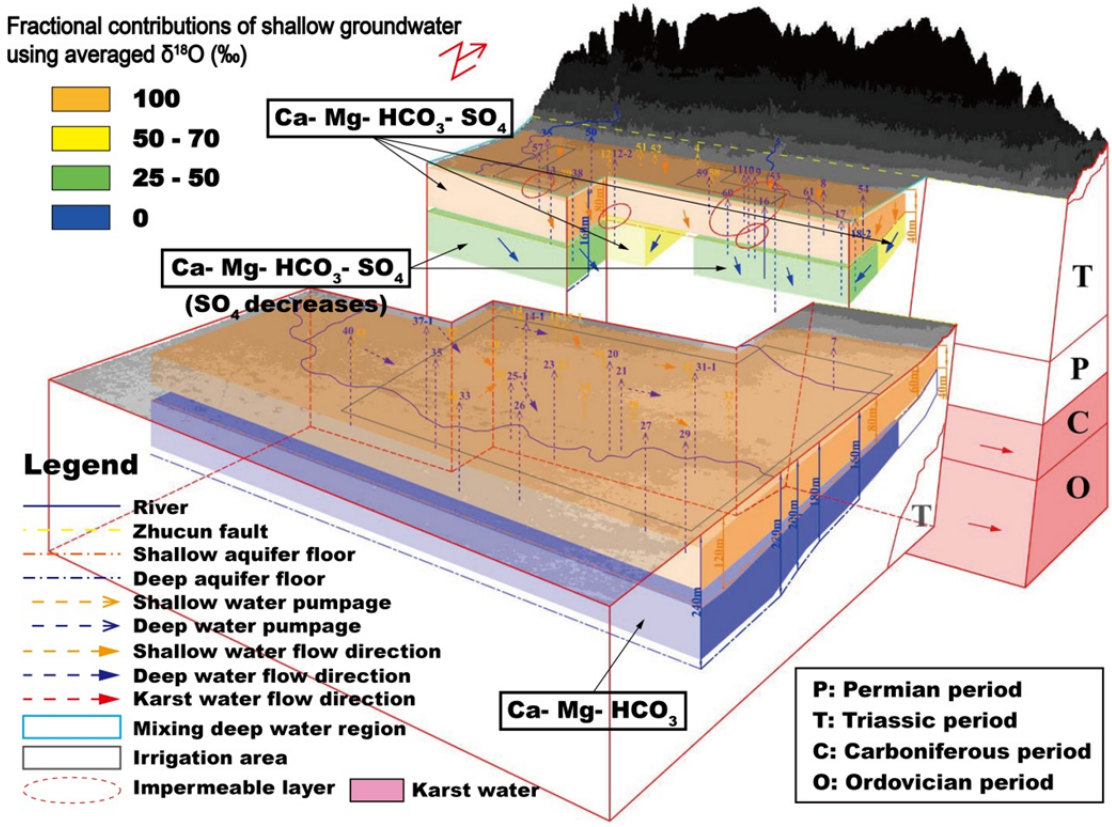

Figure 50: Three-dimensional space conceptual model of groundwater flow processes in Jiaozuo piedmont plain.

Chapter 6: Conclusions and perspectives

I. Conclusions

This study employed water isotopes, hydraulic and hydrochemistry analysis to evaluate the importance of potential recharge sources to deep groundwater in the alluvial-proluvial fan area of a semi-arid piedmont plain in North Henan Plain. To this end, first clarifying hydrological connections among precipitation, surface water, mountain groundwater and fracture water is essential.

The isotopic and water table variation results specified that precipitation is not the recharge source of groundwater in the piedmont plain due to the large depth to the water table and strong evaporation effect leaves little opportunity for precipitation infiltrates to the aquifer beneath. Meanwhile, direct infiltration from river water is no longer the source of phreatic water as a result of reservoirs constructed in its up reaches and less rainfall recharge, which makes the downstream of the river dried up even during rainy season. In addition, it has been concluded that the normal fault in the piedmont plain boundary acts as a barrier, suggesting no lateral or vertical upward recharge provides water to the basin aquifer. Therefore, it is implied that the deep groundwater recharge of alluvial-proluvial fan is not influenced by the surface water infiltration or mountain-front recharge.

Based on the spatial distribution of the hydrochemical constituents of the deep groundwater, the alluvial-proluvial fan area which situates in the front range of the piedmont plain could be considered as recharge zones. The major anion contents decrease continuously along the deep water flow paths, and evolve from a HCO_3-SO_4 type in the fan area toward a more diluted HCO_3 type in the alluvial plain. The gradual chemical evolution implies that shallow water infiltrates to the deep aquifer and with the content diluted along the deep water flow direction.

The isotopes linked with groundwater hydraulic head data have proven to be effective in helping understand recharge process within the aquifer. This comprehensive analysis leads to the identification of shallow water intrusion to the deep aquifer of alluvial-proluvial fan area of piedmont plain in North Henan Plain.

The receiving water body is formed in deep aquifer of piedmont plain, which was recharged in a colder and wetter climate during the late Pleistocene and Holocene. Considering shallow water in fan area the only potential recharge source of deep water and hydraulic gradient in different aquifers, it is suggested that shallow groundwater leakage in alluvial-proluvial fan area and deep groundwater in piedmont plain are the two main end sources of mixing deep water in alluvial- proluvial fan. In addition, the nitrate intrusion in deep aquifer of fan area (mean value of 40.7mg/L) indicates that shallow water leakage may facilitate the penetration of persistent contaminants into deep aquifer.

The end-members mixing model using stable isotope is shown to be useful for estimation of the contribution ratio of different recharge sources. The results demonstrate that the average contribution of the shallow groundwater is estimated to be 25% - 70% in deep aquifer of fan area according to binary end-member mixing analysis (EMMA) for $\delta^{18}O$ values, and the mixing ratio of shallow groundwater declines with increasing distance away from the fault.

Additionally, the results of recharge process also represent a good example of impermeable layer influence in alluvial- proluvial fan groundwater system, which impacts the groundwater flow patterns in piedmont plain. It is implied that impermeable layer would primarily influence the mixing process in proluvial fan area more than alluvial fan on this site, and meanwhile makes groundwater recharge in proluvial fan exhibit a relatively more limited mixture scale and a specific groundwater flow pattern. Furthermore, a detailed conceptual model integrated with groundwater flow path and EMMA exhibits the shallow water intrusion behavior in alluvial-proluvial fan area and consistent variations of hydrogeochemistry. It will be applicable to similar water connectivity studies of piedmont plain.

These main outcomes conclude that groundwater systems in alluvial-proluvial fan are greatly disturbed by the impermeable layers distribution, which modify the groundwater flow paths in different aquifers. Such modifications, which exert a control on the shallow water intrusion to deeper aquifer within the fan area and the amount of natural deep water resources, can be identified with the aid of hydrological

information, hydrochemical and isotopic data. Furthermore, structural elements, such as buried normal fault, represent a much different role in specific geological setting, therefore the mountain-block recharge contribution is fundamental to be clarified during the study of piedmont plain groundwater recharge.

Therefore, the groundwater flow patterns in fan area without detailed geological information are extremely difficult to be predicted, where one cannot simply refer to the traditional hydrogeological conclusions to understand the specific recharge process. The results of this study will provide a stepping stone for deep groundwater management in piedmont plain area which borders a normal fault and it also highlights the need for caution in the interpretation of groundwater mixing process with limited geological information, which may result in a specific flow pattern. Furthermore, the improvement of groundwater quality in piedmont plain area must be based on the phreatic aquifer in the alluvial-proluvial fan area, where the hydraulic linkage between shallow and deep aquifer may facilitate the penetration of persistent contaminants into deep confined aquifer of piedmont plain.

II. Perspectives

In this study, relationship between hydraulic head variation and mixture ratio of shallow water indicate that the impact of deep groundwater over-exploitation in alluvial plain is negligible during the study period.

However, data from the surveys in Jiaozuo piedmont plain only covers the recent two years after intensive deep groundwater abstraction, and the reduction of hydraulic head continued only for short periods of time, which can hardly provide a contribution to the depiction of linkage between different aquifers under human pressure, because the interconnection between deep and phreatic aquifer takes place with a long delay time. Thus, the deep water flow system in alluvial plain may at a first glance seems to be steady in the short term, they may in reality be highly disturbed after decades of years. An additional result of this is that the initial hydrological process of groundwater in a piedmont plain may be judged wrongly only on the basis of isotope and hydrochemical research when long term groundwater abstraction is neglected in the data interpretation.

Therefore, the influence of long term over-exploitation of deep water on the reginal groundwater flow pattern should be considered in Jiaozuo piedmont plain, especially in alluvial-proluvial fan area, and more hydraulic head data combined with water sample hydrochemical information should be collected every a few years. This future work will reveal the impact of deep water table withdrawal on the shallow water intrusion, and contribute to the sustainable management of deep groundwater bodies under the demand of human pressures.

Moreover, in this paper, hydrogeological surveys were conducted in alluvial-proluvial fan area based on the very limited geological information, and it is encountered many difficulties in the flow process interpretation and conceptual model construction. It is hoped that more boreholes which penetrates in the deep aquifer should be installed, especially in mountain edge and fan area. Therefore it can provide a more detailed aquifer lithology and is highly appropriate for the establishment of groundwater movement simulation model.

Acknowledgements

This research was supported by the State Scholarship Fund of the China Scholarship Council, China (File No. 201206400018), and study fund of Tsujimura lab of Graduate School of Life and Environmental Sciences, University of Tsukuba, Japan. Therefore, I would like to give the sincere thanks to the above two departments which offer me the precious opportunity to study abroad and complete the hydrology Ph.D work.

My deepest gratitude goes first and foremost to Professor Maki Tsujimura, my supervisor, for his constant encouragement and guidance. He has walked me through all the stages of the Ph.D work. Without his consistent and illuminating instruction, this thesis could not have reached its present form. I do appreciate his patience, encouragement, and professional instructions during the journal paper review and presentations for special exercise. Additionally, I am deeply moved by his serious attitude towards academic work.

I also owe a special debt of gratitude to the professors of Ph.D thesis evaluation committee, for their instructive suggestions and valuable comments on the thesis draft.

Besides, I would like to express my heartfelt gratitude to Professors of the Watershed Research group: Honorary Professor Dr. Norio TASE, Professor Dr. Michiaki SUGITA and Professor Dr. Atsushi KAWACHI, who offered me valuable suggestions in the academic studies.

I gratefully acknowledge the sincere help of Professor Huanzhen ZHANG, Professor Chuanping FENG and Professor Zhenya ZHANG, who offered me this valuable chance to achieve the state scholarship and recommended me to the hydrology Professor Maki Tsujimura. Without their pushing me ahead, the Ph.D academic work in Japan would be impossible to be carried out.

In addition, I would like to give my thanks to the professors in Environmental Diplomatic Leadership Program, especially Professor Dr. Naomi WAKASUGI and Professor Dr. Xiaogang SUN, from whose devoted teaching and enlightening lectures

I have benefited a lot and academically prepared for the thesis.

Furthermore, I feel grateful to all the members of Tsujimura lab, especially Mr. Ikeda and Mr. Sakakibara, who provided me with valuable suggestions for the Ph.D work and guidance for the water analysis instruments. I also acknowledge the kind support of Dr. Jie ZHANG for his collaboration and assistance with field work and data interpretation.

Last my thanks would go to my beloved family for their loving considerations and great confidence in me all through these years. I also greatly appreciate to my wife's support and endless love. My gratitude also extends to my friends in University of Tsukuba and fellow classmates in China University of Geoscience (Beijing) for their continuous support and generous encouragement.

References

Aji, K., Tang, C., Song, X., Kondoh, A., Sakura, Y., Yu, J. and Kaneko, S. 2008. Characteristics of chemistry and stable isotopes in groundwater of Chaobai and Yongding River basin, North China Plain. Hydrol. Process. 22, 63–72.

Back W. 1960. Origin of hydrochemical facies of ground water in the Atlantic Coastal Plain. Internat Geol Cong, 21st, Proc, pt 1, Copenhagen, pp 87–95

Bai, P., Liu, W. and Guo, M. 2014. Impacts of climate variability and human activities on decrease in streamflow in the Qinhe River, China. Theoretical and applied climatology, 117(1-2), 293-301

Barthold, F.K., Tyralla, C., Schneider, K., Vaché, K.B., Frede, H. and Breuer, L. 2011. How many tracers do we need for end member mixing analysis (EMMA)? A sensitivity analysis. Water Resour. Res. 47, W08519. http://dx.doi.org/10.1029/2011WR010604.

Bense, V. F. and Person, M. A. 2006. Faults as conduit‐barrier systems to fluid flow in siliciclastic sedimentary aquifers. Water Resources Research, 42(5).

Bosley, K.L., Witting, D.A., Chambers, R. and Wainright, S.C. 2002. Estimating turnover rates of carbon and nitrogen in recently metamorphosed winter flounder (Pseudopleuronectes americanus) with stable isotopes. Mar. Ecol. Prog. 236, 233–240.

Burns, D.A., McDonnell, J.J., Hooper, R.P., Peters, N.E., Freer, J.E., Kendall, C. and Beven, K. 2001. Quantifying contributions to storm runoff through end-member mixing analysis and hydrologic measurements at the Panola Mountain Research Watershed (Georgia, USA). Hydrol. Process. 15 (10), 1903–1924.

Chen, J., Tang, C., Sakura, Y., Kondoh, A., Yu, J., Shimada, J. and Tanaka, T. 2004. Spatial geochemical and isotopic characteristics associated with groundwater flow in the North China Plain. Hydrol. Process. 18, 3133–3146.

Chen, Z., Nie, Z., Zhang, G., Wan, L. and Shen, J. 2006. Environmental isotopic study on the recharge and residence time of groundwater in the Heihe River Basin, northwestern China. Hydrogeol. J. 14 (8), 1635–1651.

Chowdhury, A.H., Uliana, M. and Wade, S. 2008. Ground water recharge and flow characterization using multiple isotopes. Ground Water 46(3), 426–436.

Clark, I.D., Fritz, P. 1997. Tracing the hydrological cycle. In: Environmental Isotopes in Hydrogeology. CRC Press, Florida, pp. 35–60.

Craig, H. 1961. Standard for reporting concentrations of deuterium and oxygen-18 in natural waters. Science, 133,pp. 1833-34.

Dansgaard, W. 1964. Stable isotopes in precipitation. Tellus, 16(4), 436-468.

Dassi L, Zouari K, Seiler KP, Faye S and Kamel S. 2005. Flow exchange between the deep and shallow groundwaters in the Sbeı¨tla synclinal basin (Tunisia): an isotopic approach. Environ Geol 47:501–511

Devlin, J. F. and Sophocleous, M. 2005. The persistence of the water budget myth and its relationship to sustainability. Hydrogeology Journal, 13(4), 549-554.

De Vries, J.J. and Simmers, I. 2002. Groundwater recharge: an overview of processes and challenges. Hydrogeol. J. 10, 5–17.

Dogramaci, S., Skrzypek, G., Dodson, W. and Grierson, P. F. 2012. Stable isotope and hydrochemical evolution of groundwater in the semi-arid Hamersley Basin of subtropical northwest Australia. Journal of hydrology, 475, 281-293.

Environmental, Y. S. I. 2008. ORP Management in wastewater as an indicator of process efficiency. YSI, Yellow Springs, OH http://www. ysi. com/media/pdfs/A567-ORP-Management-in-Wastewater-as-an-Indicator-of-Proces s-Efficiency. pdf (accessed on 15.08. 13).

Folch, A., Menció, A., Puig, R., Soler, A. and Mas-Pla, J. 2011. Groundwater development effects on different scale hydrogeological systems using head, hydrochemical and isotopic data and implications for water resources management: the Selva basin (NE Spain). Journal of Hydrology, 403(1), 83-102.

Foster, S., Garduno, H., Evans, R., Olson, D., Tian, Y., Zhang, W. and Han, Z. 2004. Quaternary aquifer of the North China Plain—assessing and achieving groundwater resource sustainability. Hydrogeology Journal, 12(1), 81-93.

Gao, S. Q. 2008. Groundwater cycle pattern and renewability evaluation of groundwater in the Quaternary aquifer in Henan plain. Ph.D Thesis, Jilin University, 89-99 (in Chinese)

Gat, J.R. 1996. Oxygen and hydrogen isotopes in the hydrologic cycle. Annu. Rev. Earth Pl. Sc., Vol. 24, pp. 225-262.

Gee, G.W. and Hillel, D. 1988. Groundwater recharge in arid regions: review and critique of estimation methods. Hydrol. Process. 2, 255–266.

Glynn, P.D. and Plummer, L.N. 2005. Geochemistry and the understanding of groundwater systems. Hydrogeology Journal 13, 263–287.

Guan, E. T., Wu, Q. and Li, D. 2005. Protection and utilization of groundwater resource in Jiaozuo city. Coal Geology & Exploration, 1 (in Chinese).

Hem, J.D. 1985. Study and interpretation of the chemical charateristics of natural water. Water chemistry. U.S. Geological Survey, Water Supply Paper 2254.

Herczeg, A.L. and Edmunds, W.M. 2000. Inorganic ions as tracers. In: Cook, P.G., Herzeg, A.L. (Eds.), Environmental Tracers in Subsurface Hydrology. Kluwer, Boston, 31–78.

Huang, P. H., Chen, J. S., Ning, C. and Han, S. M. 2010. Hydrochemical characteristics and hydrogeochemical modeling of groundwater in the Jiaozuo mining district. Geoscienc, 24, 369-375 (in Chinese).

Ingebritsen, S.E., Sanford, W.E. and Neuzil, C.E. 2006. Groundwater in Geologic Processes, second ed. Cambridge University Press.

Jacobus, J. and Simmers, I. 2006. Groundwater recharge: an overview of processes and challenges. Hydrogeol. J. 10, 5–17.

Jiang, J., Zhang, Y., Wegehenkel, M., Yu, Q. and Xia, J. 2008. Estimation of soil water content and evapotranspiration from irrigated cropland on the North China Plain. J. Plant Nutr. Soil Sci. 171, 751–761

Jiao, H. J. and Duan, Y. H. 2005. Sustainable utilization of groundwater resource in the Yubei plain. Hydrogeology & Engineering Geology, 32(1), 61-66 (in Chinese).

Kendal, C., and J.J. McDonell. 1998. Isotope Tracers in Catchment Hydrology. Amsterdam; Elsevier.

Li, F., Pan, G., Tang, C., Zhang, Q. and Yu, J. 2008. Recharge source and hydrogeochemical evolution of shallow groundwater in a complex alluvial fan system, southwest of North China Plain. Environmental Geology, 55(5), 1109-1122.

Liu, C., Zhang, X. and Zhang, Y. 2002. Determination of daily evaporation and evapotranspiration of winter wheat and maize by large-scale weighing lysimeter and micro-lysimeter. Agric. Forest Meteorol. 111, 109–120.

Lu, Y., Tang, C., Chen, J., Song, X., Li, F. and Sakura, Y. 2008. Spatial characteristics of water quality, stable isotopes and tritium associated with groundwater flow in the

Hutuo River alluvial fan plain of the North China Plain. Hydrogeology Journal, 16(5), 1003-1015.

Ma, J., Ding, Z., Edmunds, W. M., Gates, J. B. and Huang, T. 2009. Limits to recharge of groundwater from Tibetan plateau to the Gobi desert, implications for water management in the mountain front. Journal of Hydrology, 364(1), 128-141.

Mahlknecht, J., Schneider, J.F., Merkel, B.J., Navarro, de Leon I. and Bernasconi, S.M. 2004. Groundwater recharge in a sedimentary basin in semi-arid Mexico. Hydrogeology Journal 12, 511–530.

McCarthy, K.A., W.D. McFarland, J.M. Wilkinson, and L.D. White. 1992. The dynamic relationship between groundwater and the Columbia River: using deuterium and oxygen-18 as tracers. Journal of Hydrology, Vol. 135, pp. 1-12.

Miao, J. X. 2010. Formation of the shallow groundwater in the Northern Henan Plain based on isotope analyses. Hydrogeology & Engineering Geology, 4: 004 (in Chinese).

Miao, J. X. 2011. Application of Isotope Techniques in the Groundwater Source Planning of the Yubei Plain in Henan Province. Ground Water, 4: 002 (in Chinese).

Nakaya, S., Uesugi, K., Motodate, Y., Ohmiya, I., Komiya, H., Masuda, H. and Kusakabe, M. 2007. Spatial separation of groundwater flow paths from a multi-flow system by a simple mixing model using stable isotopes of oxygen and hydrogen as natural tracers. Water Resour. Res. 43 (9), W09404. http://dx.doi.org/10.1029/2006WR005059.

Pan, G. Y. 1996. The Influence of Man-made Feature on Hydrogeologic of Jiaozuo Area. Journal of Jiaozuo Institute of Technology, 5 (in Chinese).

Pan, G. Y., Liu, Y. L. and Gan, R. 2009. Characters and Evolution Rule of the Hydrochemistry of Surface Water and Groundwater in Dashahe River Basin. Journal of Water Resources and Water Engineering, 3: 013 (in Chinese).

Pei, J. G., Tao, Y. L. and Tong, C. S. 1993. Environmental isotope of natural water and its application in karst hydrogeology in Jiaozuo area. Carsologica Sinica, 1, 005 (in Chinese).

Peng, T. R., Lu, W. C., Chen, K. Y., Zhan, W. J. and Liu, T. K. 2014. Groundwater-recharge connectivity between a hills-and-plains' area of western Taiwan using water isotopes and electrical conductivity. Journal of Hydrology, 517, 226-235.

Peterson, B. J. and Fry, B. 1987. Stable isotopes in ecosystem studies. Annual review of ecology and systematics, 293-320.

Piper, A.M. 1944. A graphic procedure in the geochemical interpretations of water analyses. Trans. Am. Geophys. Union 25, 914–923

Praamsma, T., Novakowski, K., Kyser, K. and Hall, K. 2009. Using stable isotopes and hydraulic head data to investigate groundwater recharge and discharge in a fractured rock aquifer. Journal of Hydrology, 366(1), 35-45.

Qian, Y., Qin, D., Pang, Z. and Wang, L. 2006. A discussion of recharge sources of deep groundwater in the Ejin Basin in the lower reaches of Heihe River. Hydrogeol. Eng. Geol. 3, 25–29 (in Chinese).

Rohden, C., Kreuzer, A., Chen, Z., Kipfer, R. and Aeschbach-Hertig, W. 2010. Characterizing the recharge regime of the strongly exploited aquifers of the North China Plain by environmental tracers. Water Resour. Res. 46, W05511. doi:10.1029/2008WR007660.

Scanlon, B. R., Healy, R.W. and Cook, P.G. 2002. Choosing appropriate techniques for quantifying groundwater recharge. Hydrogeology Journal 10, 18–39.

Scanlon, B. R., Keese, K. E., Flint, A. L., Flint, L. E., Gaye, C. B., Edmunds, W. M. and Simmers, I. 2006. Global synthesis of groundwater recharge in semiarid and arid regions. Hydrological processes, 20(15), 3335-3370.

Schu ¨rch M and Vuataz FD. 2000. Groundwater components in the alluvial aquifer of the alpine Rhone River valley, Bois de Finges area, Wallis Canton, Switzerland. Hydrogeol J 8: 549–563

Seiler, K. P. and Lindner, W. 1995. Near-surface and deep groundwaters. Journal of hydrology, 165(1), 33-44.

Stiff HAJ. 1951. The interpretation of chemical water analysis by means of patterns. J Pet Technol 3:15–17

Subrahmanyam, K. and Yadaiah, P. 2001. Assessment of the impact of industrial effluents on water quality in Patancheru and environs, Medak district, Andhra Pradesh, India. Hydrogeol. J. 9 (3), 297–312.

Tsujimura, M., Abe, Y., Tanaka, T., Shimada, J., Higuchi, S., Yamanaka, T., Davaa, G. and Oyunbaatar, D. 2007. Stable isotopic and geochemical characteristics of groundwater in Kherlen River basin, a semi-arid region in eastern Mongolia. Journal of hydrology, 333(1), 47-57.

UNESCO. 1979. Map of the world distribution of arid regions. Man and Biosphere Tech Notes, no. 7, UNESCO: Paris; 54.

Vanderzalm, J.L., Jeuken, B.M., Wischusen, J.D.H., Pavelic, P., Le Gal La Salle, C., Knapton A. and Dillon, P.J. 2011. Recharge sources and hydrogeochemical evolution of groundwater in alluvial basins in arid central Australia. Journal of Hydrology. 397, 71–82.

Wang, B., Jin, M., Nimmo, J.R., Yang, L. and Wang, W. 2008. Estimating groundwater recharge in Hebei Plain, China under varying land use practices using tritium and bromide tracers. Journal of Hydrology 356, 209–222.

Wang, P., Yu, J., Zhang, Y. and Liu, C. 2010. Groundwater recharge and hydrogeochemical evolution in the Ejina Basin, northwest China. Journal of Hydrology, 476, 72-86.

Wilson, J. L. and Guan, H. 2004. Mountain‐Block Hydrology and Mountain- Front Recharge. Groundwater recharge in a desert environment: The Southwestern United States, 113-137.

Yamanaka, T., Shimada, J., Hamada, Y., Tanaka, T., Yang, Y., Zhang, W. and Hu, C. 2004. Hydrogen and oxygen isotopes in precipitation in the northern part of the North China Plain: climatology and inter‐storm variability. Hydrological Processes, 18(12), 2211-2222.

Yuan, R., Song, X., Han, D., Zhang, L. and Wang, S. 2013. Upward recharge through groundwater depression cone in piedmont plain of North China Plain. Journal of Hydrology, 500, 1-11.

Yuan, R., Song, X., Zhang, Y., Han, D., Wang, S. and Tang, C. 2011. Using major ions and stable isotopes to characterize recharge regime of a fault-influenced aquifer in Beiyishui River Watershed, North China Plain. Journal of Hydrology, 405(3), 512-521.

Zhang, D., Liu, C. Q. and Yin, G. X. 2010. Study on Inland Groundwater Salinization Based on Stable Isotope and Hydrochemistry: A Case Study in Jiaozuo City, China. Earth and Environment, 2: 010 (in Chinese).

Zheng, J. D., Li, D. Y., Hu, B. and Xu, Z. F. 2003. The characteristics and origins of shallow groundwater pollution in Jiaozuo coal mining area. Energy Environmental Protection, 3, 008 (in Chinese).

Zhu, C., Winterle, J.R. and Love, E.I. 2003. Late Pleistocene and Holocene

groundwater recharge from the chloride mass balance method and chlorine-36 data. Water Resource Research 39 (7), 1182–1201

Zhu, G. F., Li, Z. Z., Su, Y. H., Ma, J. Z. and Zhang, Y. Y. 2007. Hydrogeochemical and isotope evidence of groundwater evolution and recharge in Minqin Basin, Northwest China. Journal of Hydrology, 333(2), 239-251.

Appendix

Table 1 Water sample ID, well depth, locations, elevation and groundwater table.

ID	Type	Well depth (m)	North latitude	East longitude	Elevation (m)	Water table (m)	
						2013-Nov	2014-Aug
SW1	S		35.265	113.100	347		
SW2	S		35.264	113.060	490		
SW3	S		35.251	113.029	430		
MG1	M		35.243	113.108	193		
MG2	M	4	35.241	113.069	246	244.58	244.3
MG3	M		35.241	113.070	245	242.68	
MG5	M	350	35.235	113.039	382		
MG6	M	329	35.235	113.039	329	357.66	
MG2-2	M	7	35.242	113.070	245		242
MG2-1	M		35.260	113.063	246		
MG2-3	M	300	35.260	113.063	464		
MG42	M		35.280	113.030	570		
MG43	M	300	35.256	112.995	319		
MG45	M		35.211	113.004	168		
MG46	M	60	35.286	113.053	535		
MG49	M	200-300	35.256	113.147	287		
SG4	SG	20	35.211	113.068	154	146	145.1
SG12	SG	27	35.183	113.032	131	119.07	119.4
SG15	SG	45	35.152	113.094	108	106.16	
SG19	SG	40	35.127	113.146	100	89.23	89.95
SG22	SG	40	35.107	113.126	101	93.68	91.1
SG25	SG	35	35.085	113.108	98	89.07	
SG28	SG	40	35.083	113.171	93	88.97	
SG31	SG	40	35.140	113.180	91	80.39	77
SG34	SG	30	35.058	113.088	107	96.4	94.2
SG39	SG	17	35.130	113.033	128		
SG14	SG	70	35.146	113.066	116	112.26	
SG18	SG	50	35.182	113.165	111		101.4
SG24	SG	49	35.090	113.139	109	96	97.4
SG32	SG	70	35.116	113.210	91	71	
SG36	SG	50	35.103	113.092	101	92.89	91.5
SG37	SG	50	35.107	113.061	105	98.45	
SG41	SG	50	35.074	113.024	117	104.81	102.6
SG55	SG	29	35.169	112.972	148		133.1
SG52	SG	15	35.200	113.051	145		142.6
SG51	SG	28	35.203	113.041	176		

S = spring water, M = mountain groundwater, SG = shallow groundwater, DG = deep groundwater, R = river water

Table 1 (continued)

SG58	SG	13	35.188	113.078	131		125
SG37-2	SG		35.109	113.049	116		
SG38-2	SG	17	35.130	113.033	128		
SG15-1	SG	20	35.154	113.095	130		
SG28-1	SG	40	35.088	113.179	93		
DG7	DG	75	35.197	113.196	104	97.06	96.9
DG8	DG	80	35.196	113.143	124	91.21	94.54
DG9	DG	150	35.199	113.103	136	90.95	86
DG10	DG	150	35.199	113.098	136	86	86
DG11	DG	85	35.200	113.093	137	92.02	91.7
DG13	DG	150	35.161	113.020	130	120	119.3
DG16	DG	120	35.173	113.123	114	86	
DG17	DG	164	35.172	113.151	114	97.9	97
DG20	DG	160	35.123	113.148	103	93.5	90.6
DG21	DG	120	35.109	113.160	100	91.65	91.8
DG23	DG	160	35.106	113.119	102	99.74	97.92
DG26	DG	160	35.057	113.124	97	82.39	79.26
DG27	DG	180	35.067	113.175	92	84.22	80.8
DG29	DG	200	35.076	113.205	93	87.77	78.5
DG33	DG	160	35.058	113.088	107	95.82	93.5
DG35	DG	160	35.080	113.070	111	102.43	98.5
DG38	DG	160	35.130	113.033	128	124.27	124
DG40	DG	160	35.076	113.022	113	103.75	
DG56	DG	60	35.186	112.993	154	127.7	
DG57	DG	100	35.166	112.994	131	114.9	
DG50	DG	100	35.201	113.017	160	130	
DG12-2	DG	168	35.182	113.036	133	115.75	
DG59	DG	70	35.188	113.077	120		
DG53	DG	410	35.201	113.125	140	95	
DG60	DG	100	35.169	113.095	131		
DG61	DG	140	35.187	113.136	124	95.68	
DG54	DG	100	35.208	113.161	144	94	
DG14-1	DG	130	35.152	113.064	116	114.8	
DG18-2	DG	130	35.184	113.166	111	97	
DG37-1	DG	165	35.110	113.052	116	113.5	
DG25-1	DG	100	35.083	113.116	98		
DG31-1	DG	180	35.142	113.181	91	76.55	
RW1	R		35.044	113.088	105		
RW2	R		35.054	113.023	104		
DRW-1	R		35.279	112.999	254		
DRW-2	R		35.183	112.983	128		

Table 2 Water sample ID, measurements of physicochemical parameters and results of isotopic analyses

ID	Type	pH		EC (μS/cm)		ORP (mV)	$\delta^{18}O$ (‰)		δD (‰)	
		2013-Nov	2014-Aug	2013-Nov	2014-Aug	2014-Aug	2013-Nov	2014-Aug	2013-Nov	2014-Aug
SW1	S	8.01	8.05	460	420	222	-8.94	-8.52	-61.7	-60.8
SW2	S	8.12		710			-9.59		-69.9	
SW3	S	7.30	7.18	1740	1640	133	-8.77	-8.74	-61.8	-61.5
MG1	M	7.80	7.55	840	830	165	-9.12	-9.14	-64.6	-64.8
MG2	M		6.9	1240	1630	156	-8.86	-8.73	-63.3	-63.5
MG3	M	6.95		1860			-9.01		-62	
MG5	M	7.62	7.81	1120	860	156	-9.05	-9.02	-65.9	-65.1
MG6	M	6.95		1240			-9.1		-64.2	
MG2-2	M		6.95		1630	165		-8.87		-62.3
MG2-1	M		6.90		1630	156		-8.73		-63.5
MG2-3	M		7.93		560	149		-9.34		-67.3
MG42	M		7.96		770	157		-8.38		-59.1
MG43	M		7.74		880	115		-9.05		-68.3
MG45	M		7.73		1140	103		-8.74		-64.9
MG46	M		7.58		980	195		-8.51		-63.1
MG49	M		7.57		760	164		-9.28		-68.1
SG4	SG	7.12	7.17	1680	1690	130	-8.85	-8.74	-64.8	-64.9
SG12	SG	7.55	7.2	1070	1140	155	-8.93	-8.79	-64.2	-65.2
SG15	SG	7.33		1180			-8.77		-64	
SG19	SG	7.76	7.2	1030	1320	159	-9.43	-9.11	-71.4	-68.3
SG22	SG	7.30	7.44	960	2500	-33	-9.28	-8.55	-70.1	-60.5
SG25	SG	7.28		1630			-8.39		-64.6	
SG28	SG	7.08		2300			-8.37		-61.4	
SG31	SG	7.28	7.61	1550	710	33	-8.99	-10.05	-65.9	-76
SG34	SG	6.85	6.92	1340	1830	-33	-7.31	-8.5	-47.6	-61.8
SG39	SG	7.46		1020			-8.6		-63.1	
SG14	SG	7.19		1790			-8.56		-62.3	
SG18	SG	7.48	7.13	2400	3600	111	-8.65	-8.31	-65.5	-63.4
SG24	SG	7.85	7.2	610	2500	-34	-10.68	-8.48	-81	-63.8
SG32	SG	7.50	7.44	1060	950	11	-9.55	-9.69	-68.8	-70.7
SG36	SG	7.30	7.3	1810	2300	1	-8.96	-8.3	-64.4	-63.1
SG37	SG	7.58	7.44	1060	950	11	-9.34		-69.3	
SG41	SG	7.30	7.5	1880	2200	-60	-8.9	-8.97	-64.5	-66.3
SG55	SG		7.38		1290	146		-8.86		-65.5
SG52	SG		7.48		1100	149		-8.3		-58.4
SG51	SG		7.41		1080	131		-8.86		-68.7

S = spring water, M = mountain groundwater, SG = shallow groundwater, DG = deep groundwater, R = river water

Table 2 (continued)

SG58	SG		7.15		1420	160		-8.63		-64.2
SG37-2	SG		7.27		1360	-31		-8.54		-63.2
SG38-2	SG		7.4		980	-80		-8.51		-65.3
SG15-1	SG		7.23		1810	125		-8.66		-63.4
SG28-1	SG		7.16		2000	-38		-10.48		-76
DG7	DG	7.44	7.44	950	900	-30	-9.35	-9.24	-70.5	-71.2
DG8	DG	7.38	7.32	1140	1580	113	-9.34	-9.31	-71.4	-67.6
DG9	DG	7.50	7.44	830	830	186	-9.57	-9.53	-70.8	-70
DG10	DG	7.39	7.13	980	980	166	-9.15	-9.22	-67.1	-67.2
DG11	DG	7.39	7.34	1100	1100	130	-9.09	-9.04	-66.3	-66.2
DG13	DG	7.53	7.41	930	910	150	-9.09	-9.12	-68.1	-66.9
DG16	DG	7.81	7.73	760	750	177	-10.49	-10.24	-76.4	-76
DG17	DG	7.41	7.6	740	740	189	-10.01	-9.97	-74.9	-72.5
DG20	DG	8.21	7.41	740	800	167	-9.91	-9.63	-73.8	-71.3
DG21	DG	7.50	7.59	1880	700	196	-9.12	-9.69	-67.5	-71.2
DG23	DG	7.35	7.33	780	760	44	-9.61	-9.59	-69.1	-70.6
DG26	DG	7.62	7.73	820	780	5	-9.63	-9.74	-73	-71.4
DG27	DG	7.40	7.62	800	690	44	-9.57	-9.55	-71.4	-70.8
DG29	DG	7.70	7.75	1490	1530	-41	-9.48	-9.4	-70.6	-69
DG33	DG	7.50	7.63	640	630	45	-9.63	-9.73	-72.6	-71.1
DG35	DG	7.72	7.61	590	580	53	-9.8	-9.94	-72.5	-72.2
DG38	DG	7.43	7.37	820	830	-7	-9.33	-9.23	-68.5	-68.1
DG40	DG	7.94	7.41	670	660	33	-9.64	-9.7	-73.8	-70.9
DG56	DG		7.47		1190	129		-9		-68.7
DG57	DG		7.41		840	148		-9.17		-66.5
DG50	DG		7.36		1020	143		-8.95		-64.5
DG12-2	DG		7.25		940	189		-9.31		-68.3
DG59	DG		7.12		1240	165		-8.97		-68.8
DG53	DG		7.48		1060	116		-10.57		-79.1
DG60	DG		7.3		990	179		-9.16		-68.3
DG61	DG		7.23		1280	130		-9.2		-68
DG54	DG		7.34		930	152		-9.25		-67.9
DG14-1	DG		7.54		720	207		-9.64		-71.1
DG18-2	DG		7.5		800	169		-9.73		-70.1
DG37-1	DG		7.25		760	26		-9.45		-71.8
DG25-1	DG		7.58		540	60		-10		-72.3
DG31-1	DG		7.54		720	10		-10.26		-75.6
RW1	R	7.96	8.25	1220	840	-18	-7.13	-7.9	-57.1	-58.6
RW2	R	8.06	8.24	1250	850	-46	-7.13	-7.81	-56.2	-57.9
DRW-1	R		7.92		940	140		-8.9		-65.8
DRW-2	R		7.9		970	121		-8.85		-64.3

Table 3 Water sample ID, results of chemical composition analyses

ID	Type	Na^+ (meq/L)		K^+ (meq/L)		Mg^{2+} (meq/L)		Ca^{2+} (meq/L)		Cl^- (meq/L)		NO_3^- (meq/L)		SO_4^{2-} (meq/L)		HCO_3^- (meq/L)	
		2013-Nov	2014-Aug	2013-Nov	2014-Aug	2013-Nov	2014-Aug	2013-Nov	2014-Aug	2013-Nov	2014-Aug	2013-Nov	2014-Aug	2013-Nov	2014-Aug	2013-Nov	2014-Aug
SW1	S	0.33	0.12	0.05	0.03	1.76	1.65	2.97	2.68	0.19	0.17	0.26	0.18	1.36	0.98	2.83	2.74
SW2	S	0.66		0.07		0.56		6.36		0.88		0.33		3.28		2.47	
SW3	S	1.70	0.91	0.06	0.00	3.41	3.32	15.93	15.90	1.65	2.06	1.90	1.87	12.12	9.96	4.19	4.41
MG1	M	1.49	1.05	0.13	0.05	2.88	2.65	4.95	5.19	0.86	0.89	0.52	0.47	3.45	2.73	3.73	4.00
MG2	M	1.85	1.25	0.04	0.01	4.01	5.50	8.80	13.82	0.78	1.56	0.42	1.07	8.20	10.82	4.48	5.25
MG3	M	2.47		0.08		5.94		15.58		1.58		1.27		13.67		5.96	
MG5	M	1.87	1.36	0.13	0.05	3.67	2.73	6.72	5.35	1.53	1.16	1.40	0.42	5.53	3.10	3.00	3.92
MG6	M	1.46		0.07		2.81		10.21		1.05		0.87		8.83		2.97	
MG2-2	M		1.33		0.01		5.41		13.79		1.64		1.17		10.50		5.35
MG2-1	M		1.25		0.01		5.50		13.82		1.56		1.07		10.82		5.25
MG2-3	M		0.25		0.04		1.91		3.81		0.34		0.00		1.81		3.29
MG42	M		0.83		0.20		0.73		6.24		0.77		0.73		3.06		2.69
MG43	M		1.40		0.05		2.73		5.50		1.19		0.57		2.93		4.11
MG45	M		2.30		0.05		3.32		6.45		3.22		0.51		3.44		3.82
MG46	M		0.42		0.01		1.11		8.92		0.81		0.79		3.96		3.94
MG49	M		0.69		0.04		2.55		5.02		0.74		0.60		1.66		4.52
SG4	SG	3.55	2.62	0.07	0.01	4.86	4.81	11.07	11.32	3.00	4.66	1.23	2.07	6.48	3.39	7.01	6.88
SG12	SG	1.26	0.93	0.05	0.01	2.57	3.27	8.30	9.08	0.99	1.43	1.21	1.37	2.91	2.74	5.99	6.56
SG15	SG	2.75	3.08	0.09	0.01	3.64	7.32	6.87	10.66	1.68	4.40	0.30	2.61	4.47	5.97	5.64	6.13
SG19	SG	2.47	2.36	0.05	0.02	5.05	6.03	4.48	7.09	1.19	1.82	1.23	1.41	2.46	3.43	6.01	7.39

S = spring water, M = mountain groundwater, SG = shallow groundwater, DG = deep groundwater, R = river water

Table 3 (continued)

SG22	SG	1.38	11.57	0.06	0.12	3.99	10.97	5.55	8.17	0.97	4.59	0.37	3.36	2.41	10.13	6.19	9.93
SG25	SG	4.75	1.19	0.06	0.03	8.64	1.99	6.43	2.62	2.78	0.17	1.15	0.11	5.05	0.62	9.03	4.57
SG28	SG	8.18	8.85	0.07	0.10	10.28	9.10	11.08	6.15	3.65	3.55	1.42	0.61	12.69	10.89	9.05	6.89
SG31	SG	3.82	2.18	0.09	0.00	7.45	3.36	7.19	2.40	2.41	0.41	1.04	0.04	2.86	1.01	10.49	5.79
SG34	SG	3.88	8.03	0.30	0.07	3.76	6.99	8.42	6.77	1.15	2.35	0.08	1.22	2.58	3.54	11.02	12.69
SG39	SG	1.59	0.65	0.03	0.03	4.02	3.53	6.36	5.16	1.00	0.62	0.02	0.47	3.71	1.55	6.25	5.85
SG14	SG	4.37		0.09		7.12		9.30		2.65		1.99		6.25		8.09	
SG18	SG	8.22	15.47	0.11	0.11	6.61	7.63	11.96	18.73	8.77	15.75	0.86	1.06	9.65	17.31	5.08	3.89
SG24	SG	2.74	8.07	0.04	0.03	2.08	12.70	2.31	10.03	0.16	5.76	0.02	3.06	1.42	10.02	5.17	9.15
SG32	SG	3.92	3.28	0.05	0.02	3.77	3.44	4.42	3.96	1.27	1.16	0.42	0.31	3.45	2.50	5.90	5.73
SG36	SG	5.50	6.47	0.07	0.07	7.55	11.47	7.52	10.46	2.81	6.33	1.87	1.75	7.00	10.40	7.51	7.32
SG37	SG	2.57		0.05		5.08		4.82		1.04		0.11		3.45		6.87	
SG41	SG	6.24	6.02	0.07	0.02	10.03	13.80	6.89	8.85	3.06	5.83	2.01	0.95	7.10	10.93	8.94	8.29
SG55	SG		1.49		0.11		4.15		9.23		2.05		1.69		4.09		5.77
SG52	SG		1.13		0.91		2.76		7.08		1.25		0.74		2.92		6.10
SG51	SG		1.16		0.01		3.51		7.60		1.36		1.03		2.95		5.80
SG58	SG		1.53		0.00		4.51		10.67		2.44		2.05		4.71		5.95
SG37-2	SG		2.71		0.09		6.73		6.82		1.89		1.56		5.03		6.36
SG38-2	SG		1.12		0.00		4.13		6.46		1.33		0.20		3.34		5.73
SG15-1	SG		3.08		0.01		7.32		10.66		4.40		2.61		5.97		6.13
SG28-1	SG		8.85		0.10		9.10		6.15		3.55		0.61		10.89		6.89
DG7	DG	2.11	1.74	0.06	0.02	3.46	3.55	10.21	4.80	1.28	0.54	0.36	0.20	2.35	1.54	5.37	5.30
DG8	DG	2.50	4.19	0.06	0.03	4.55	5.20	5.52	7.37	2.74	5.41	0.41	0.50	2.72	4.40	5.59	5.10
DG9	DG	1.66	1.26	0.06	0.03	3.45	3.60	4.20	4.37	0.60	0.71	0.32	0.30	2.01	1.82	5.56	5.58
DG10	DG	1.45	1.06	0.05	0.02	4.50	4.60	5.46	5.63	0.80	0.92	0.67	0.77	2.86	2.37	6.05	6.19

Table 3 (continued)

DG11	DG	1.74	1.33	0.05	0.02	4.62	4.66	6.23	6.72	1.02	1.31	0.93	1.07	3.24	3.04	6.26	6.10
DG13	DG	1.26	0.86	0.06	0.03	3.43	3.61	5.72	5.93	0.85	0.93	0.80	0.82	2.67	2.31	5.28	5.39
DG16	DG	2.61	2.12	0.08	0.03	2.57	2.70	3.21	3.18	0.66	0.73	0.15	0.16	2.01	1.73	4.84	4.66
DG17	DG	2.12	1.61	0.05	0.02	3.01	3.06	3.43	3.52	0.41	0.54	0.19	0.20	1.74	1.54	5.49	5.30
DG20	DG	2.02	1.02	0.05	0.03	2.97	3.43	3.26	4.55	0.48	0.51	0.32	0.25	1.58	1.51	5.14	5.92
DG21	DG	6.27	1.10	0.06	0.02	8.84	2.95	7.46	3.78	4.08	0.36	1.47	0.18	7.30	1.29	7.64	5.30
DG23	DG	0.98	0.62	0.06	0.03	3.60	3.56	4.61	4.58	0.37	0.34	0.23	0.20	1.68	1.37	6.09	6.09
DG26	DG	3.18	2.64	0.04	0.01	3.41	3.32	2.88	2.68	0.60	0.50	0.18	0.14	1.74	1.41	6.19	5.80
DG27	DG	0.98	0.66	0.06	0.03	3.50	3.38	4.40	3.74	0.38	0.33	0.20	0.16	1.50	1.28	6.06	5.31
DG29	DG	10.20	9.89	0.06	0.01	5.30	5.51	2.60	2.41	1.42	1.88	0.12	0.30	7.07	6.71	7.88	7.32
DG33	DG	1.24	0.85	0.05	0.02	2.75	2.67	3.53	3.49	0.27	0.23	0.15	0.13	1.12	0.94	5.32	5.29
DG35	DG	1.66	1.19	0.05	0.02	2.17	2.13	3.02	2.97	0.24	0.20	0.13	0.13	1.00	0.80	4.88	4.60
DG38	DG	1.02	0.65	0.06	0.03	3.51	3.53	4.91	5.16	0.58	0.62	0.46	0.47	1.87	1.55	5.69	5.85
DG40	DG	1.13	0.84	0.05	0.03	2.86	2.93	3.37	3.78	0.30	0.27	0.17	0.17	1.23	1.04	5.32	5.42
DG56	DG		1.68		0.03		3.40		1.00		1.73		1.16		3.66		5.50
DG57	DG		0.74		0.03		3.31		5.33		0.86		0.65		2.13		4.96
DG50	DG		1.69		0.01		3.06		7.29		1.45		0.84		3.32		5.34
DG12-2	DG		1.08		0.03		3.53		6.00		0.96		0.72		2.10		5.87
DG59	DG		1.50		0.01		3.95		8.60		1.45		1.07		3.60		6.63
DG53	DG		3.20		0.05		3.51		4.45		3.46		0.17		2.21		4.34
DG60	DG		1.51		0.02		4.50		4.97		1.25		0.91		1.94		5.88
DG61	DG		2.40		0.02		5.23		6.84		4.04		0.66		3.26		5.19
DG54	DG		1.47		0.03		3.36		5.34		1.43		0.43		1.64		5.73
DG14-1	DG		0.66		0.03		3.23		4.09		0.32		0.19		1.29		5.49

S = spring water, M = mountain groundwater, SG = shallow groundwater, DG = deep groundwater, R = river water

Table 3 (continued)

DG18-2	DG		1.57		0.03		3.17		4.09		0.86		0.23		1.81		5.15
DG37-1	DG		0.59		0.03		3.59		4.51		0.35		0.22		1.37		5.97
DG25-1	DG		1.19		0.03		1.99		2.62		0.17		0.11		0.62		4.57
DG31-1	DG		2.47		0.02		2.55		3.15		0.52		0.09		1.41		5.39
RW1	R	2.78	1.43	0.14	0.08	4.25	2.98	6.94	4.63	2.31	0.99	0.36	0.26	6.20	3.64	3.93	3.39
RW2	R	2.72	1.43	0.14	0.08	4.25	3.03	7.22	4.64	2.37	1.11	0.37	0.37	6.02	3.78	4.36	3.08
DRW-1	R		2.15		0.12		2.51		5.49		1.46		0.45		3.64		3.75
DRW-2	R		2.36		0.14		2.57		5.45		1.58		0.42		3.53		4.02